ABSTRACT

Title of Thesis:	HYDRAULIC AND ENVIRONMENTAL BEHAVIOR OF RECYCLED ASPHALT PAVEMENT IN HIGHWAY SHOULDER APPLICATIONS
	Zorana Mijic, Master of Science, 2017
Thesis directed by:	Professor Ahmet H. Aydilek, Department of Civil and Environmental Engineering

Hydraulic conductivity of seven recycled asphalt pavement materials was evaluated through a series of constant head tests, while their leaching potential was determined through batch water leach tests and column leach tests. The contaminant transport in surface waters as a function of distance was numerically simulated. Laboratory test results indicated that the hydraulic conductivity of recycled asphalt pavement is comparable to that of the natural aggregate with the gradation of clean sand-gravel mixture as it ranged from 6.89×10^{-3} cm/s to 1.14×10^{-2} cm/s. The amounts of all metals released during the water leach tests were below the water quality limits, except for Cu. Column leach tests yielded generally low or non-detectable metal concentrations. The deviation from this trend occurred for Cu and Zn concentrations, but they fell below the regulatory limits at 4 and 0.5 pore volumes of flow, respectively. Finally, concentrations of metals conformed to the water quality standards in surface waters after passing through the natural formation.

HYDRAULIC AND ENVIRONMENTAL BEHAVIOR OF RECYCLED ASPHALT PAVEMENT IN HIGHWAY SHOULDER APPLICATIONS

by

Zorana Mijic

Thesis submitted to the Faculty of the Graduate School of the
University of Maryland, College Park, in partial fulfillment
of the requirements for the degree of
Master of Science
2017

Advisory Committee:
Dr. Ahmet H. Aydilek, Chair
Dr. Mohamed S. Aggour, Committee Member
Dr. Natasha A. Andrade, Committee Member

To my mom and dad, eternally thankful for your love, support, and advice …

Acknowledgements

First and foremost, I would like to thank my advisor, Dr. Ahmet H. Aydilek, for giving me the opportunity to conduct the research. Dr. Aydilek introduced me to geotechnical engineering and laboratory, which had the crucial impact on the choice of my career path. I will always appreciate his advice and patience. I am also greatly thankful to my committee members, Dr. Mohamed Sherif Aggour and Dr. Natasha N. Andrade, for their guidance throughout my studies. I took many courses with Dr. Aggour, I stopped keeping a count, and I enjoyed all of them without exception. I have learned so much from him, and I loved his geotechnical sense of humor. Dr. Andrade's class made me think every day about my carbon footprint and how to practice civil engineering sustainably. I cannot thank enough to all my professors of civil engineering and geophysics at the University of Maryland for knowledge I have gained. My Teacher Miladin Mijatovic, Professor Mira Gredo, and Professor Jovan Prodanov in my native Serbia had left a big print in my life. Because of them, I love nature, mathematics, physics, and engineering.

I extend my thanks to Maryland State Highway Administration that made this research project possible and to Dr. Intikhab Haider who helped me tremendously. Big thanks go to amazing Marya Orf Anderson, who was very patient and answered all my numerous questions. Stela Barbosa, Rafael Campolina, and Alexander Koontz were extraordinary research assistants and I will always be thankful for their help, as well as Atul Kumar's. Thanks to my friends Emre Odabasi and Ousmane Insa, who were always there for me and who made me laugh every day. Dr. Asli Yalcin

Dayioglu, my friend, my “big sister,” thank you for everything. Dr. Mustafa Hatipoglu, many thanks for sharing your knowledge with me so selflessly.

Finally, my thanks go to the best parents one could ask for; to the most unique sister in the world who makes me complete; and to my extraordinary grandma for loving me so dearly. Special thanks go to my fiancé, Farzin Nabili, without whom none of this would mean so much. Thank you for your love, support, and for being so understanding; you rock my world. Thank you for all the rice you made while I was writing this thesis.

And last but not least, I am grateful to the United States Navy and my dad’s service to the country; had it not been for them, I would not have been where I am today. I give a promise to strive continually to make this world a better place for everyone.

Table of Contents

List of Tables

List of Figures

1 INTRODUCTION

According to the National Asphalt Pavement Association (NAPA), it is estimated that 74.2 million tons of reclaimed asphalt pavement were used in asphalt mixes across the United States in 2015, which reduced the need for approximately 3.7 million tons of asphalt binder and 70.5 million tons of aggregate. This, in turn, saved the amount of landfill space by roughly 50 million cubic yards and taxpayers more than $2.4 billion.

Recycled asphalt pavement (also referred to as roadway millings herein, RAP) is produced by removing and processing of existing asphalt pavement materials and, therefore, consists of aggregate, asphalt binder, and some impurities. It has been identified as “America's No. 1 recycled product” by the Environmental Protection Agency (EPA) and Federal Highway Administration (FHWA) ever since 1993 (NAPA, 2017). RAP can be used as a substitute for natural aggregate and virgin asphalt binder in asphalt paving practices, as a granular base or subbase, stabilized base aggregate, embankment or fill material, and for other construction applications (Copeland, 2011).

The use of RAP preserves nonrenewable natural resources such as virgin aggregate, which is harvested mostly from crushing of natural rock, and asphalt binder, which is produced by refining crude oil, and neutralizes the negative consequences these processes have on the environment – erosion, air and water pollution, contamination of soil, and biodiversity loss. It reduces the amount of construction debris going into landfills and costs associated with transportation of

quality virgin aggregate from remote quarries to construction sites (FHWA, 2010). Overall, the RAP usage has a great potential to perform well, be cost-effective, and environmentally sound.

To allow for more massive use of RAP in roadway maintenance and construction practices, the support from State Highway Administrations is required. Maryland State Highway Administration expressed concern over the limited guidance on the use of pure RAP in highway shoulder applications and the lack of information on its performance when used as a highway shoulder backup material. In particular, due to relation of pavement with chemicals generated from the "vehicle exhaust, gasoline, lubricating oils, and metals from [automobile tires] and break lining wear" (Legret et al., 2005) and the high fines content frequently found in many RAP stockpiles, there is a need for a thorough assessment of environmental suitability and hydraulic conductivity of RAP.

A laboratory testing program was undertaken as a part of the current project in order to define the hydraulic and environmental behavior of Maryland RAPs for their possible use in construction of highway shoulder backups. Graded aggregate base, stone No. 57, and topsoil were included as reference materials in the testing program as they are commonly used in highway shoulder applications. The research consisted of the following tasks:

1) Determining the physical properties of recycled asphalt pavement, topsoil, graded aggregate base, and stone No. 57.
2) Evaluating the coefficient of hydraulic conductivity through a laboratory constant head test for granular materials (recycled asphalt pavement, graded

aggregate base, and stone No. 57) and a laboratory falling head test for fine-grained materials (topsoil).

3) Conducting batch water leach tests for a quick estimate of metal leaching behavior.
4) Performing column leach tests to understand the long-term leaching potential and controlling mechanisms for trace metals from recycled asphalt pavement, graded aggregate base, stone No. 57, and topsoil.
5) Simulating the transport of effluents in surface waters as a function of distance via numerical model to study fate of chemicals in highway systems.

Section 2 of this study contains physical properties and hydraulic behavior of reclaimed asphalt pavement, graded aggregate base, stone No. 57, and topsoil. Section 3 evaluates metal leaching potential of recycled asphalt pavement, graded aggregate base, stone No. 57, and topsoil as determined through batch water and column leaching tests and the numerical model. Section 4 provides a summary of research findings and recommendations for future studies.

2 HYDRAULIC BEHAVIOR OF RECYCLED ASPHALT PAVEMENT

2.1 INTRODUCTION

Maryland State Highway Administration (SHA) desires to evaluate the hydraulic behavior of roadway millings (also called recycled asphalt pavement, RAP) to be placed in highway shoulder backups (i.e., the compacted areas adjacent to the highway shoulders). RAP is obtained by removing and reprocessing the existing asphalt pavement and is commonly reused in highway construction (FHWA, 2012). RAP is typically produced through milling operations, which involves the grinding and collection of the existing hot mix asphalt. Keller (2013) defines roadway millings as "the fine particles (generally from dust to less than an inch or so) of bitumen and inorganic material that are produced by the mechanical grinding of bituminous concrete surfaces."

FHWA Recycled Asphalt Pavement Expert Task Group conducted a national survey in 2011 to evaluate the use of RAP in highway systems (Copeland, 2011). In total, 18 out of 52 division offices responded, and 17 of them stated that the use of RAP depended on the contractor as well as the cost and availability. RAP material can be used as a construction material for compacted shoulder backup applications in Pennsylvania in accordance with the 25 Pa Code, Chapter 287.9, and WMGR 090. Furthermore, New York DOT allows use of roadway millings in shoulder backup applications and considers it as pervious (NYDOT, 2002). A special provision that allows RAP for shoulder dressing exists in Indiana (McDaniel et al., 2012).

RAP is nonplastic, is generally classified as well-graded material with less than 1% fines (Koch et al., 2011), provides free drainage (Rathje et al., 2006; FHWA, 2012), and is not frost susceptible (FHWA, 2012). In order to evaluate the drainage behavior of RAP-amended shoulder backups, hydraulic conductivity measurements are essential. Hydraulic conductivity of pure or blended RAP can be classified as similar to that of conventional granular material or soil-aggregate blends with similar gradation; however, hydraulic conductivity is significantly influenced by the size distribution of RAP particles.

Several studies were undertaken to investigate the hydraulic behavior of RAP and virgin aggregates. Trzebiatowski and Benson (2005) conducted hydraulic conductivity tests on three RAP materials compacted with standard Proctor effort (ASTM D 698) and modified Proctor effort (ASTM D 1557). Hydraulic conductivity of RAP varied from $2.4x10^{-3}$ to $9.0x10^{-3}$ cm/s (standard Proctor effort) and from $4.5x10^{-6}$ to $1.7x10^{-4}$ cm/s (modified Proctor effort). The same tests performed on Lodi gravel, a crushed rock aggregate used for base course in Wisconsin, showed that Lodi gravel was less permeable than RAP ($5.8x10^{-5}$ cm/s for standard Proctor effort and $2.4x10^{-7}$ cm/s for modified Proctor effort).

Mokwa and Peebles (2005) compacted RAP blended with granular cohesionless materials at 92-97% of maximum dry unit weight per modified Proctor test (ASTM D1557) and performed a series of constant-head tests in a 10-in diameter permeameter equipped with a Marriotte tube (ASTM D 2434 and AASHTO T 215). The addition of RAP to the blend improved the overall hydraulic conductivity because it decreased the amount of fines and increased the amount of coarse particles

within the mixture. The greater hydraulic conductivity could also be explained by RAP's natural aversion to water due to bitumen coating.

Viyanant (2006) investigates the hydraulic conductivity of RAP as a function of effective confining pressure using the falling head-rising tail flexible wall testing procedure (ASTM D 5804). Hydraulic conductivity decreases with an increase in effective confining pressure, and ranges from $3.84x10^{-3}$ to $5.5x10^{-4}$ cm/s for an effective confining pressure range of 5 to 50 psi, respectively.

Locander (2009) reports the hydraulic conductivity of twelve pure RAP samples tested in accordance with the United States Bureau Reclamation of (USBR) Test Method 5606 to range between $7.3x10^{-3}$ cm/s to $1.5x10^{-1}$ cm/s, with an average of $6.9x10^{-2}$ cm/s, and defines the quality of drainage provided by RAP "good to excellent".

Shedivy et al. (2012) compacted five RAP samples collected from different regions in the United States using the modified Proctor effort (ASTM D1557). The samples had an asphalt binder content range of 4.65-6.2% and were subjected to laboratory hydraulic conductivity testing. The measured hydraulic conductivity values stayed within a range of $2.19x10^{-3}$ – $3.69x10^{-2}$ cm/s and generally increased with the increasing asphalt content.

Nokkaew (2014) subjected six RAP materials compacted at 95% of maximum dry unit weight of modified Proctor effort (ASTM D 1557) to constant-head testing in a rigid-wall permeameter (ASTM D 5856) and reported hydraulic conductivity to vary between $3.69x10^{-2}$ and $1.1x10^{-4}$ cm/s. The variation in hydraulic conductivity was explained by changes in gravel and fines contents.

Most of the previous studies suggest that RAP is an excellent material for use as a base/subbase course aggregate or hot mix asphalt aggregate; however, limited information exists on use of RAP as a highway shoulder backup material. Properties of RAP depend on asphalt content and aggregate properties, and may differ from one region to another. No study has been conducted on hydraulic properties of Maryland RAP materials.

The existing information on RAP indicates that it is a coarse-grained material and has the hydraulic conductivity comparable to that of Maryland graded aggregate base (GAB) materials ($6x10^{-4}$-$2.6x10^{-2}$ cm/s, Aydilek et al., 2015) and fine to medium coarse sands (10^{-3} to 10^{-1} cm/s, Holtz et al., 2011). To more adequately investigate the hydraulic suitability of RAP in highway shoulder backups, a battery of hydraulic conductivity tests was conducted on seven Maryland RAP samples. Control tests were performed on GAB, stone No. 57, and topsoil, which are commonly used by SHA in Maryland highway applications. The effects of grain size distribution, fines content, bitumen content, and free lime content on hydraulic conductivity were investigated. The validity of Hazen's empirical equation in predicting the laboratory-measured hydraulic conductivities was studied.

2.2 MATERIALS

Seven different RAP samples originating from different highways around Maryland and covering a wide range of characteristics were investigated in this study (Figure 2.1). The asphalt was prepared following the same specifications in all of these regions, but the amount of salt added for thawing purposes varied and may have affected the environmental behavior of RAP. Each RAP sample was numbered based

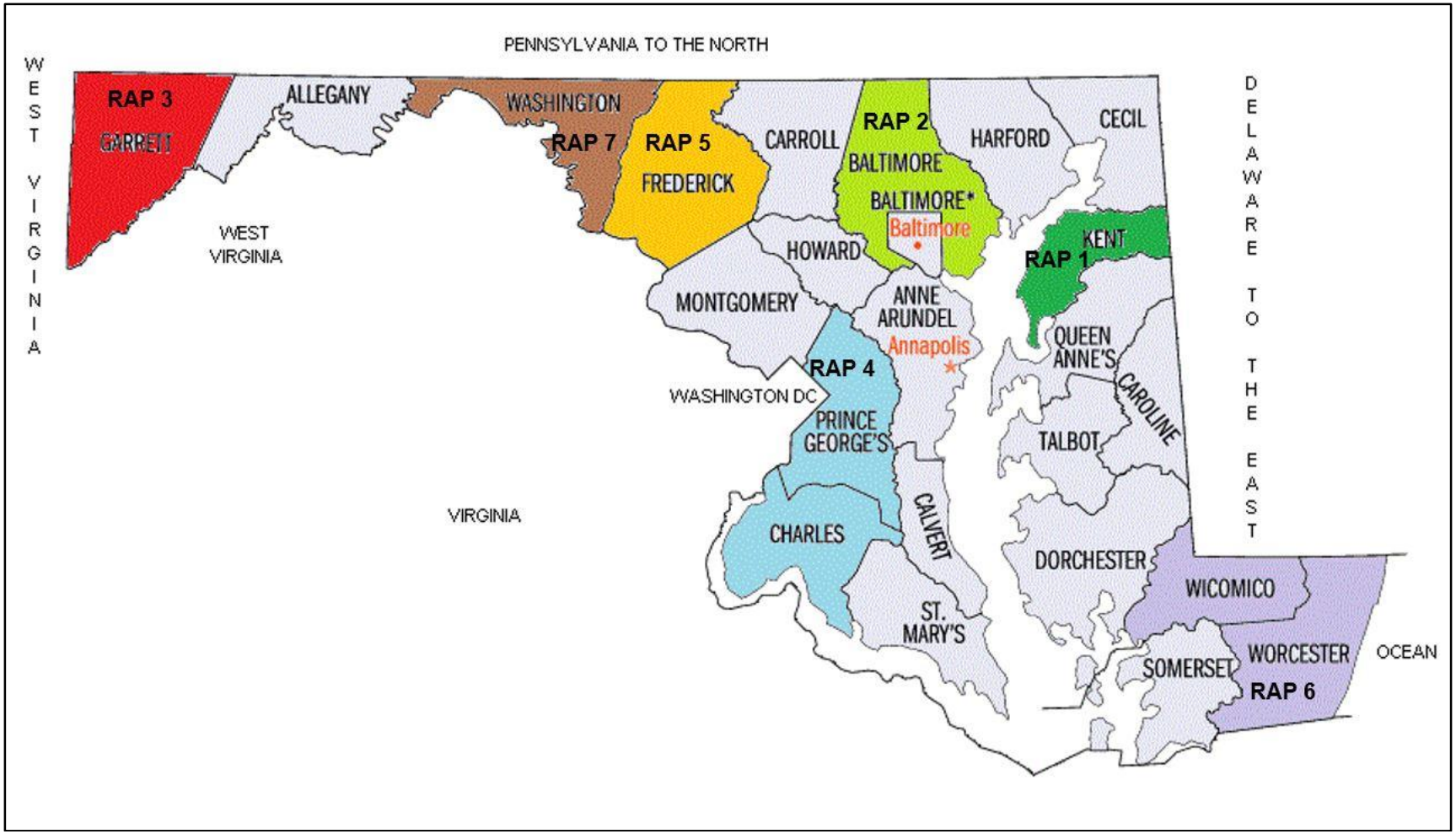

Figure 2.1. Seven RAP materials and their origin locations.

on the order of reception at the University of Maryland Geotechnical Laboratories. Approximately 50 kg [110 lbs] of a RAP material originating from the same location were thoroughly mixed, quartered, and stored in buckets. A representative sample of the stored material was obtained prior to every laboratory testing procedure by utilizing a mechanical splitter (ASTM C 702). Debris and foreign materials within the RAP samples were removed by hand before sieving. According to the Unified Soil Classification System (USCS), all RAP samples were classified as well-graded sand with gravel (SW), except RAP3, which was classified as poorly-graded sand with gravel (SP). According to the American Association of State Highway and Transportation Officials (AASHTO) Classification System, all RAP samples were labeled as A-1-a (0). The RAP materials did not exhibit any plasticity per ASTM D 4318 and their as-received fines content ranged from 0.1% to 1.8% by mass. Table 2.1 summarizes their physical properties.

Graded aggregate base (GAB), stone No. 57, and two topsoils (referred to as Topsoil 1 and Topsoil 2 herein after) were also subjected to the same experiments in this research study. They served as control materials due to their common application in State highway shoulder practices. Impurities within the materials were removed by hand prior to sieving. According to the USCS, GAB, stone No. 57, Topsoil 1, and Topsoil 2 were classified as poorly-graded gravel with sand (GP), poorly-graded gravel (GP), silty sand (SM), and poorly-graded sand with c (SP-SM), respectively. According to the AASHTO Classification System, GAB, stone No. 57, Topsoil 1, and Topsoil 2 were termed as A-1-a (0), A-1-a (0), A-2-4 (0), and A-2-5 (0), respectively. Topsoil 1 and Topsoil 2 contained 2.5% and 2.8% of organic matter, respectively.

Table 2.1. Physical properties of RAP, GAB, stone No. 57, and topsoil.

Material	Fines (%)	Sand (%)	Gravel (%)	C_c	C_u	I_p	G_s			ω_{opt} (%)	$\gamma_{dry, max}$ (pcf) (kN/m^3))
							F	C	Avg		
RAP 1	1.83	51.8	46.3	1.79	14.0	NP	2.25	2.24	2.25	5.7	124.9 (19.6)
RAP 2	0.93	61.3	37.8	1.26	10.6	NP	2.33	2.42	2.36	6.8	118.1 (18.5)
RAP 3	0.13	54.1	45.7	1.03	5.60	NP	2.23	2.28	2.25	6.3	109.7 (17.2)
RAP 4	0.33	59.0	40.7	1.58	8.28	NP	2.33	2.59	2.44	6.8	119.1 (18.7)
RAP 5	1.19	54.8	44	1.36	11.7	NP	2.16	2.46	2.29	7.5	122.4 (19.2)
RAP 6	0.47	54.2	45.3	1.32	11.2	NP	2.44	2.52	2.48	6.4	121.7 (19.1)
RAP 7	0.39	52.0	47.6	1.26	6.87	NP	2.34	2.47	2.40	8.2	117.5 (18.5)
GAB	3.18	32.5	64.3	2.80	58.7	5	2.80	2.84	2.83	4.2	152.1 (23.4)
Stone No. 57	0.21	1.7	98.1	0.89	1.52	NP	2.60	2.58	2.58	--	--
Topsoil 1	12.4	73.3	14.3	2.39	17.6	8	1.59	--	1.59	11.6	116.2 (18.3)
Topsoil 2	5.97	86.2	7.8	0.77	7.50	9	1.26	--	1.26	13.8	108.9 (17.1)

C_c: coefficient of curvature, C_u: coefficient of uniformity, I_p: plasticity index, NP: non-plastic, G_s: specific gravity, F: fine fraction, C: coarse fraction, Avg: weighted average, ω_{opt}: optimum moisture content, $\gamma_{dry, max}$: maximum dry unit weight.

The physical properties of GAB, stone No. 57, and topsoil are shown in Table 2.1.

2.3 METHODS

2.3.1 Moisture-Unit Weight Relationship Test

Standard Proctor test was performed on reclaimed asphalt pavement (RAP) and topsoil. To determine the maximum unit weight and the optimum moisture content, Topsoil 1 and Topsoil 2 were tested according to ASTM D 698, while all RAP samples were analyzed according to ASTM D 698 and MSMT (Maryland Standard Method of Tests) 321. MSMT 321 applies to materials (like RAP) that do not experience a decrease or change in the wet weight per cubic foot during compaction by increasing the moisture content, but rather free water around the bottom of the mold and the base plate. Once this point was observed, the moisture-density test was stopped. One-half of the difference between the moisture content where free water was observed and the preceding point was taken and added to the moisture content value prior to where free water was noticed. The maximum dry unit weight corresponding to this "optimum moisture content" was then read from the plot. The obtained values are shown in Table 2.1. The maximum dry unit weight and the optimum moisture content of GAB were determined following ASTM D 1557 (Haider, 2013).

2.3.2 Asphalt Binder Content

To determine the asphalt binder content of a RAP sample, the extraction method (AASHTO T 164) was preferred over the ignition method (AASHTO T 308).

AASHTO T 308 involves the determination of asphalt binder content by ignition of a loose RAP sample in a furnace at 1000°F [538°C]. The asphalt binder content is calculated as the difference between the mass of RAP prior to the ignition and the mass of RAP after the ignition, with adjustments for the correction factor and the moisture content. The correction factor must be used because a certain amount of aggregate fines may be burned off during the ignition process. Typically, the correction factor is determined by placing a sample of known asphalt binder content in the furnace and by comparing the test result with the known asphalt binder content. Since the initial binder content of RAP was not known, the extraction test method was used to evaluate the percent of asphalt binder coating RAP aggregate as it would provide more accurate results.

The extraction method was performed following the procedures in AASHTO T 164 Method A using Technical Grade of Trichloroethylene. The solvent was used to remove the asphalt binder from the aggregate. It was added to a loose, representative RAP sample to disintegrate it and was then centrifuged to separate the asphalt binder/solvent and aggregate. The initial and final masses of RAP were compared and the difference was calculated as the asphalt binder percent. The results are presented in Table 2.2.

2.3.3 Chemical Analysis

Hydraulic conductivity of RAP, GAB, stone No. 57, and topsoil may be influenced by their chemical properties. Specifically, calcium-based compounds such as free lime (CaO) and portlandite [$Ca(OH)_2$] may leach and precipitate in the presence of carbon-dioxide thus reduce hydraulic conductivity (Snyder and Brunisma, 1996).

Table 2.2. Effect of fines, sand-to-gravel ratio, D_{10}, bitumen content, and free lime on hydraulic conductivity.

Material	**Fines (%)**	**S/G**	**D_{10} (mm)**	**BC (%)**	**CaO (mg/L)**	**$k_{predicted}$ (cm/s)**	**$k_{experimental}$ (cm/s)**	**Standard Deviation**
RAP1	1.83	1.12	0.40	3.77	6,000	1.60×10^{-1}	9.83×10^{-3}	2.61×10^{-3}
RAP2	0.93	1.62	0.43	4.87	151,200	1.81×10^{-1}	5.66×10^{-2}	6.31×10^{-3}
RAP3	0.13	1.18	1.0	5.31	172,500	1.00×10^{0}	1.14×10^{-1}	3.20×10^{-3}
RAP4	0.33	1.45	0.58	5.07	70,500	3.36×10^{-1}	2.51×10^{-2}	4.94×10^{-3}
RAP5	1.19	1.25	0.45	4.18	33,824	2.03×10^{-1}	6.89×10^{-3}	2.95×10^{-3}
RAP6	0.47	1.20	0.48	4.78	9,752	2.30×10^{-1}	2.01×10^{-2}	1.61×10^{-3}
RAP7	0.39	1.09	0.83	3.97	45,701	6.89×10^{-1}	5.27×10^{-2}	1.60×10^{-2}
GAB	3.18	0.51	0.23	--	45,195	5.29×10^{-2}	6.57×10^{-3}	--
Stone No. 57	0.21	0.02	10.4	--	<40	1.08×10^{2}	2.40×10^{0}	1.10×10^{-1}
Topsoil 1	12.4	5.13	0.047	--	384	2.21×10^{-3}	7.16×10^{-5}	7.29×10^{-6}
Topsoil 2	5.97	11.05	0.10	--	2,622	1.00×10^{-2}	6.23×10^{-4}	5.36×10^{-5}

S/G: sand-to-gravel ratio, D_{10}: effective size, BC: bitumen content, F: fine portion, C: coarse portion, k: hydraulic conductivity coefficient.

Total elemental analyses (TEA) were employed to determine the amount of free lime within all of the aforementioned materials. RAPs 1, 2, 3, and 4 were sent to the University of Wisconsin-Madison Soil and Forage Analysis Laboratory, while RAPs 5, 6, and 7, GAB, stone No. 57, Topsoil 1, and Topsoil 2 were analyzed by Bureau Veritas Commodities Canada Ltd.

The TEA method consisted of a digestion process and analysis of pure pulp samples for major and minor element contents. First, the sample was weighed in a 50-ml glass digestion tube and 5ml of concentrated HNO_3 (trace element grade) was added into the tube. The tube was loosely capped and placed on a digestion block heated to 1200°C [2192°F]. The digestion of the sample lasted for 15-16 hours, after which the sample was removed from the block and allowed to cool down. Then, 1mL of H_2O_2 was added to the tube and placed back on the block for 30 minutes. This step was repeated twice. The sample was finally removed from the block to cool down. The volume of the sample was brought to 50 mL, mixed, and after three hours analyzed for the concentrations of metals using a Varian Vista-MPX CCD Simultaneous Inductively Coupled Plasma Optical Emission Spectrometer (ICP-OES). The CaO amounts within RAP, GAB, stone No. 57, and topsoil are presented in Table 2.2.

2.3.4 Laboratory Hydraulic Conductivity Test

2.3.4.1 Constant-Head Test

A bubble-tube constant-head permeameter specifically developed for testing of asphalt and GAB specimens was used to evaluate the hydraulic conductivity coefficient of RAP, GAB, and stone No. 57. The samples were compacted in the

mold having dimensions of 8.0 in. [203 mm] in diameter and 8.0 in. [203 mm] in height. The seven RAP samples were compacted in four layers at 2% dry of optimum moisture content, while stone No. 57 was compacted by a vibratory compactor to a unit weight of 110 pcf [17.3 kN/m^3]. GAB was compacted to a maximum dry unit weight of 152.1 pcf [23.9 kN/m^3] corresponding to the modified Proctor compactive effort (ASTM D 1557).

The test set-up accommodates high flow rates associated with testing of permeable specimens and significantly minimizes sidewall leakage. The unique design also eliminates the use of valves, fittings and smaller diameter tubing, all of which contribute to head losses that interfere with the test measurements, yet follows all recommendations in ASTM D 2434 (Figure 2.2).

The permeameter was placed in a bath to maintain constant tail water elevation. The tub rim was located a few millimeters above the specimen top. As the water flew out of the reservoir tube through the specimen, air bubbles emerged from the bottom of the bubble tube. The height difference between the bottom of the bubble tube and the top of the water bath, i.e., the total head loss through the specimen, was kept constant throughout the test to achieve the hydraulic gradient of one. The total flow rate through the specimen was determined by noting the water elevation drop in the reservoir tube and multiplying it with the inner area of the reservoir tube. Finally, the vertical hydraulic conductivity coefficients (k) were calculated using Darcy's law.

The test was repeated three to four times on every specimen. Initially, the specimen was prepared and the permeameter was filled up with tap water. The

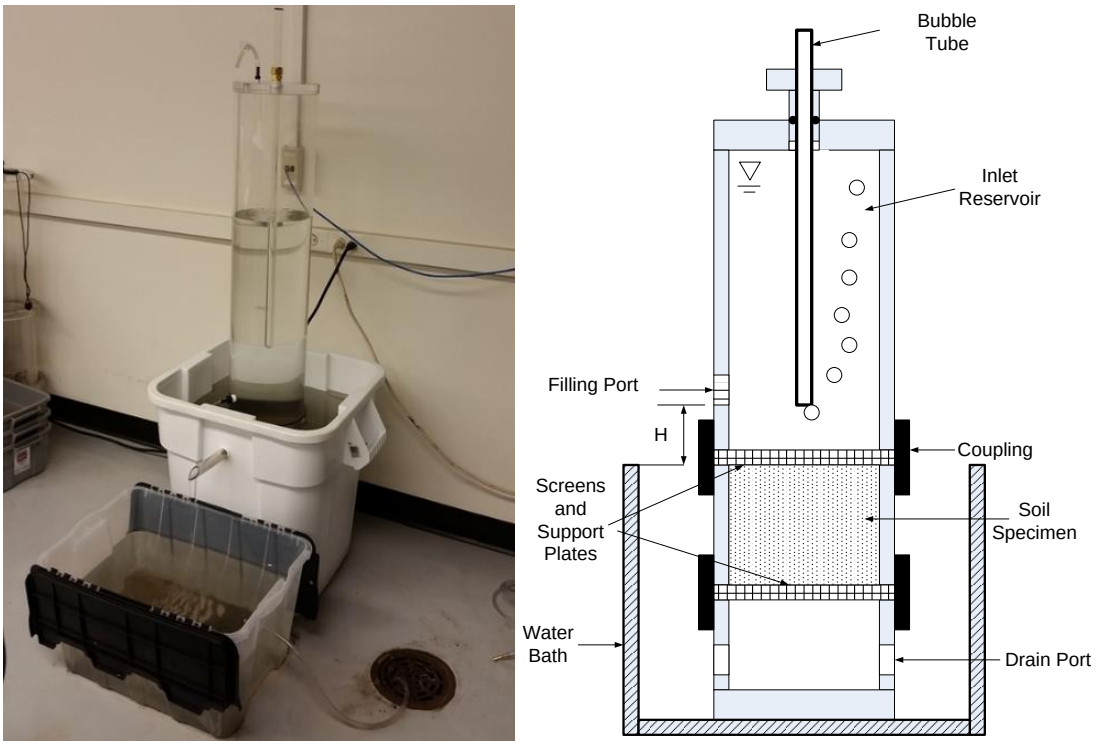

Figure 2.2. Image and schematic diagram of the bubble-tube permeameter.

specimen was left for 24 hours to saturate, and, thereafter, the first test was conducted. No vacuum was applied. After completion of the first test, the upper chamber of the permeameter was filled with tap water once again and vacuum was applied to remove any trapped air within the specimen. The amount of vacuum applied was quantified by the increase in water level in the upper chamber of the permeameter. For the second test, the vacuum was applied to increase the level of water by 5cm, from 82 to 87cm, as the maximum total height of water in the upper chamber was 87cm. In the third test, the vacuum was implemented to raise the water level by 15 cm, from 72 to 87cm. Finally, the fourth test involved applying vacuum by which the water level in the upper chamber of the permeameter increased by 25cm, from 62 to 87cm. The average hydraulic conductivity coefficients (k_m) corresponding to the four replicate tests performed were computed as geometric means of the last few stabilized k values. The arithmetic mean of k_m values of each material was reported as the hydraulic conductivity of that material.

Furthermore, to study the effect of fines content and sand-to-gravel ratio on hydraulic conductivity, adjustments in the gradations of RAP 1 and RAP 2 were made to achieve 0% to 8% fines content (Figure 2.3). Following the suggestions of Cote and Konrad (2003), the equivalent weight of fine material was added or removed to achieve the desired fines content, and RAP material was removed or added, respectively, equally by mass between the 9.5-12.7 mm and 12.7-19 mm sieves. The prepared specimens were tested in the bubble-tube constant-head permeameter according to the same procedure explained above.

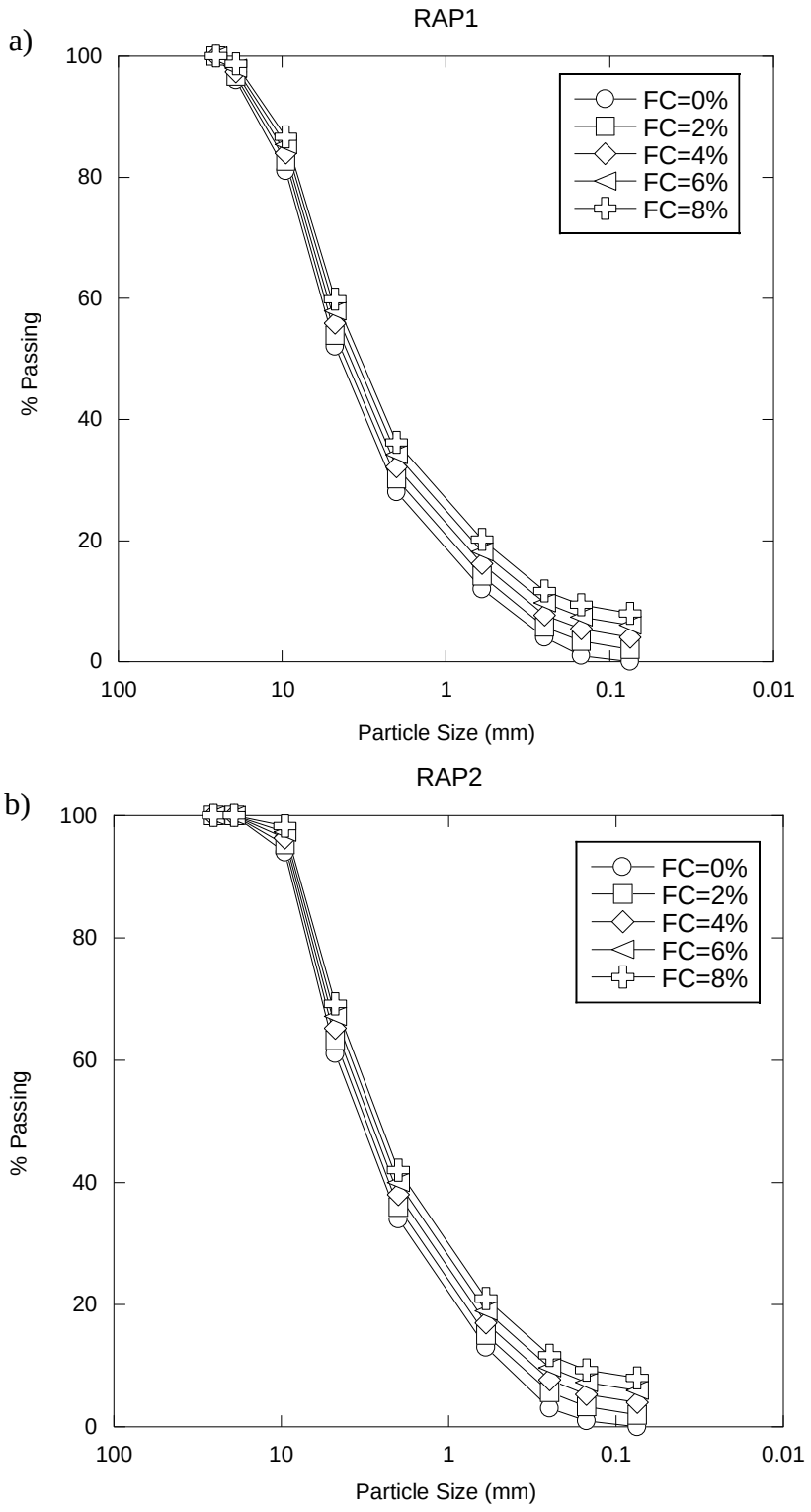

Figure 2.3. Controlled gradation curves for a) RAP1 and b) RAP2.

2.3.4.2 Falling-Head Test

Topsoil 1 and Topsoil 2 were subjected to a series of falling-head tests due to their low hydraulic conductivity. The specimens were compacted to 85% of maximum dry unit weight using the standard Proctor effort (ASTM D 698) in a PVC mold with an inner diameter of 4 in. [102 mm] and a height of 4.6 in. [116 mm]. The maximum hydraulic gradient of two was applied to avoid channeling along the sidewall, consolidation, washing of fine particles downstream and plugging of the effluent end of the specimen, which would increase or decrease the hydraulic conductivity (ASTM D 5856). The length (L) of the specimen was measured after completion of permeation.

2.4 RESULTS

2.4.1 Particle Size Distribution

Figure 2.4 shows the grain size distribution curves for seven recycled asphalt pavement (RAP) materials and control materials, i.e., graded aggregate base (GAB), Stone No. 57, Topsoil 1, and Topsoil 2. All gradation curves pertaining to RAP are packed closely together and are between those corresponding to the topsoil, on the upper side, and Stone No. 57, on the lower side. Unlike RAPs, Stone No. 57 is uniformly-graded, and GAB, Topsoil 1, and Topsoil 2 contain significantly higher amounts of fine particles, 3.18, 12.4, and 5.97%, respectively. The lowest percent of fines, 0.13%, is contained within RAP3, while RAP1 has the highest amount of fine particles, 1.83%. Furthermore, both topsoils contain almost no gravel, while Stone No. 57 is mainly composed of gravel-size particles.

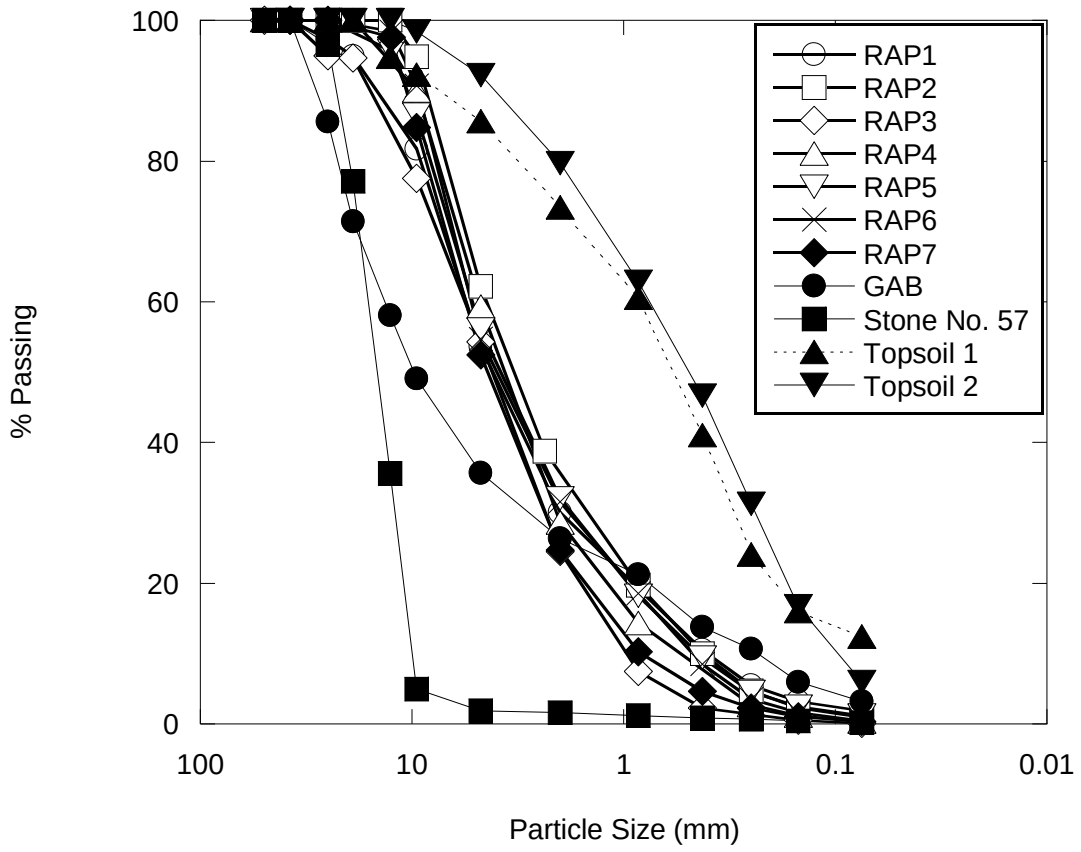

Figure 2.4. Grain size distribution of RAP, GAB, Stone No. 57, and topsoil.

2.4.2 Specific Gravity

The values of specific gravity, G_s, for seven recycled asphalt pavement (RAP) materials and control materials, i.e., graded aggregate base (GAB), Stone No. 57, Topsoil 1, and Topsoil 2, are presented in Table 2.1. RAP has an average G_s of 2.35 with the values ranging from 2.24 for RAP 1 to 2.48 for RAP 6. As compared to GAB (G_s = 2.83) and Stone No. 57 (G_s = 2.54), specific gravity values of RAP are significantly lower. Such behavior is most likely due to the bitumen coating of RAP aggregate and was observed by other researchers as well (Rathje et al., 2006; Okafor, 2010; Nokkaew et al., 2012; Shedivy et al., 2012; Rahman et al., 2015). Bitumen itself has a low specific gravity, typically 1.03 (Asphalt, 2012), which reduces the overall specific gravity of RAP (Okafor, 2010; Nokkaew et al., 2012; Rahman et al., 2015). Its hydrophobicity also contributes to the lower G_s as it increases the "impermeable volume of solids" (Rathje et al., 2006). No correlation between the percent of bitumen and specific gravity is observed for the seven RAPs tested, which may be explained by the variations in the percent of bitumen being small (3.77-5.31%, Table 2.2) and the specific gravities of pure RAP aggregates being unknown. Moreover, it is noticeable that the coarse fraction of RAP has higher G_s than the fine fraction probably due to a higher density of coarse particles (Rahman et al., 2015). Finally, the low specific gravity of the topsoil can be attributed to the organic content (2.5-2.8%) present in the material (Rahman et al., 2015).

2.4.3 Maximum Dry Unit Weight and Optimum Moisture Content

Table 2.1 shows the optimum moisture content and the maximum dry unit weight

of RAP, while Figure 2.5a contains moisture-unit weight curves corresponding to RAP. Clearly, RAP does not exhibit a typical moisture-unit weight curve like the natural topsoil (Figure 2.5b). The curve does not reach a peak, a point where water begins to replace soil particles and the dry unit weight starts to decrease due to much lower density of water as compared to density of solid particles (Holtz et al., 2011). Instead, the water quickly escapes through the base of the compaction mold because of good drainage properties and low adsorption associated with hydrophobicity of bitumen (Viyanant, 2006). The same shape of the compaction curve was reported for 100% RAP by Gupta et al. (2009).

The optimum moisture contents for RAP are in the range of 5.78.2%, and are much lower than those for the natural topsoil (11.6-13.8%), which may be attributed to coating of RAP aggregate with bitumen and to a significantly lower percent of non-plastic fine particles within the RAP matrix. Fine particles have a higher surface area than coarse particles, which allows them to absorb more water (Kang et al., 2011; Rahman et al., 2015).

The dry unit weight of RAP varies from 109.7 pcf [17.2 kN/m^3] for RAP3 to 124.9 pcf [19.6 kN/m^3] for RAP1. These two extreme values may be related to the gradation and the amount of fine particles. RAP3 is poorly-graded and contains only 0.13% fines, while RAP 1 is well-graded and contains slightly higher amount of fines (1.83%). Poorly-graded geomaterials generally have a more porous matrix than well-graded ones due to absence of finer grains that would otherwise fill the voids between the larger grains (Onur, 2014). Therefore, RAP 1 has a better packing arrangement of particles than RAP 3 and, thus, has a higher dry unit weight. However, the variations

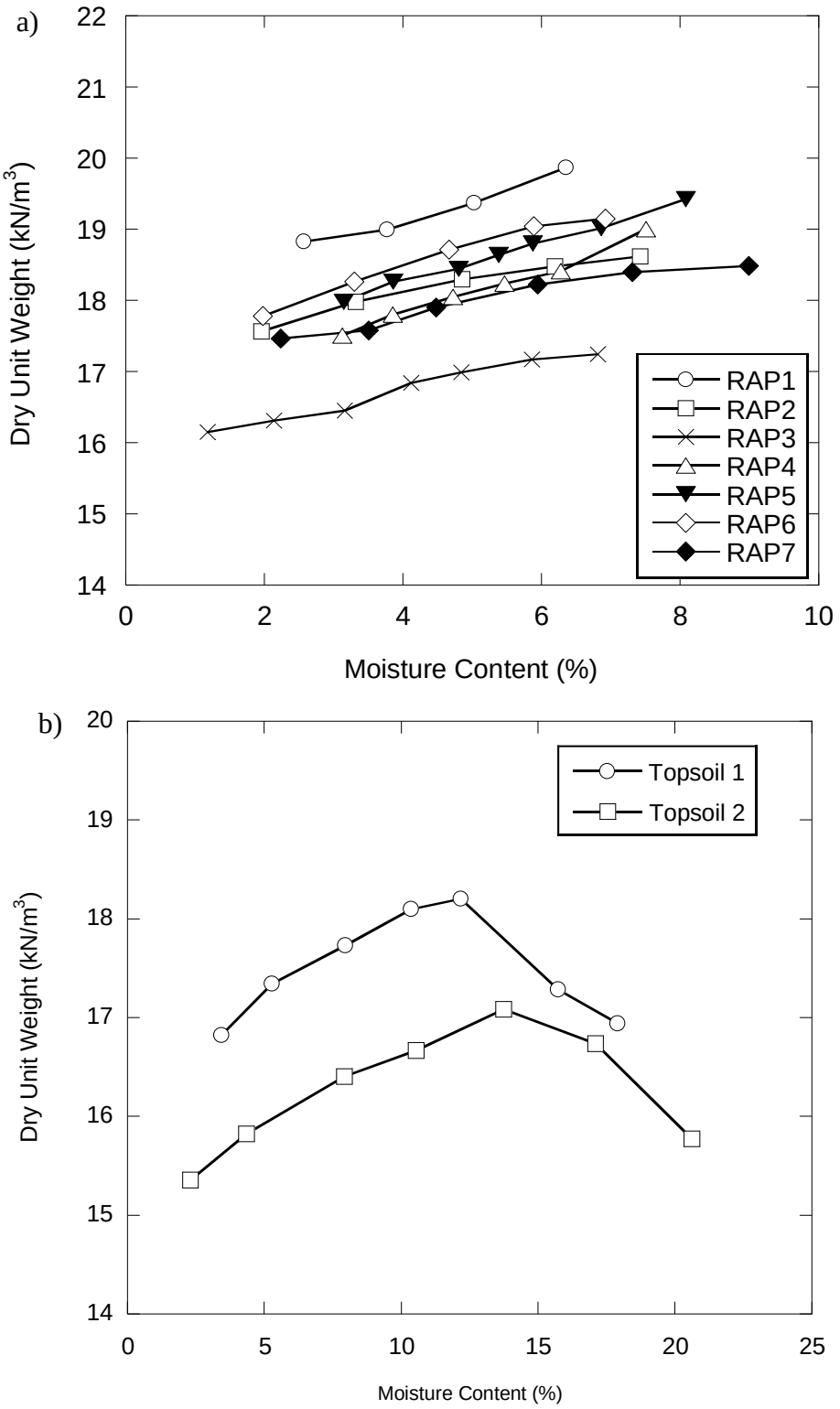

Figure 2.5. Moisture-dry unit weight relationship for a) RAP and b) topsoil.

in the maximum dry unit weight of the other RAPs cannot be explained by the differences in the percent of fines. The amount of fines may increase by impact compaction due to crushing of coarse particles, which, in turn, would result in better packing and a higher dry unit weight. Rathje et al. (2006) noted a 0.6-% increase in the fines content in RAP after impact compaction. In this research study, the consistency of the RAP gradation was not verified upon compaction.

The data in Figure 2.6a show that there is a good linear relationship between the free lime (CaO) content and the maximum dry unit weight of RAP. The maximum dry unit weight of RAP is inversely proportional to the concentration of CaO. This reduction in the maximum dry unit weight of geomaterials is consistent with the observations made by other researchers (Townsend and Kylm, 1966; Little, 1999; Mallela et al., 2004; Bin et al., 2007; Cuisinier et al., 2011). The presence of lime induces the flocculation and aggregation, primarily of fine particles, which leads to the formation of small pores and, thereby, reduces the densification potential of RAP under impact compaction.

The maximum dry unit weights of RAPs are slightly higher than those of topsoils (110-128.2 pcf [17.3-20.1 kN/m3] versus 108.9-116.2 pcf [17.1-18.3 kN/m3], Table 2.1). Lower values of the topsoils may be related to the low specific gravity associated with the organic matter in the materials (Rahman et al., 2015). Subsequently, Topsoil 1 has a lower percent of organic matter than Topsoil 2 (2.5% versus 2.8%) and, thus, has a higher maximum dry unit weight than Topsoil 2 (116.2 pcf [18.3 kN/m^3] versus 108.9 pcf [17.1 kN/m^3]).

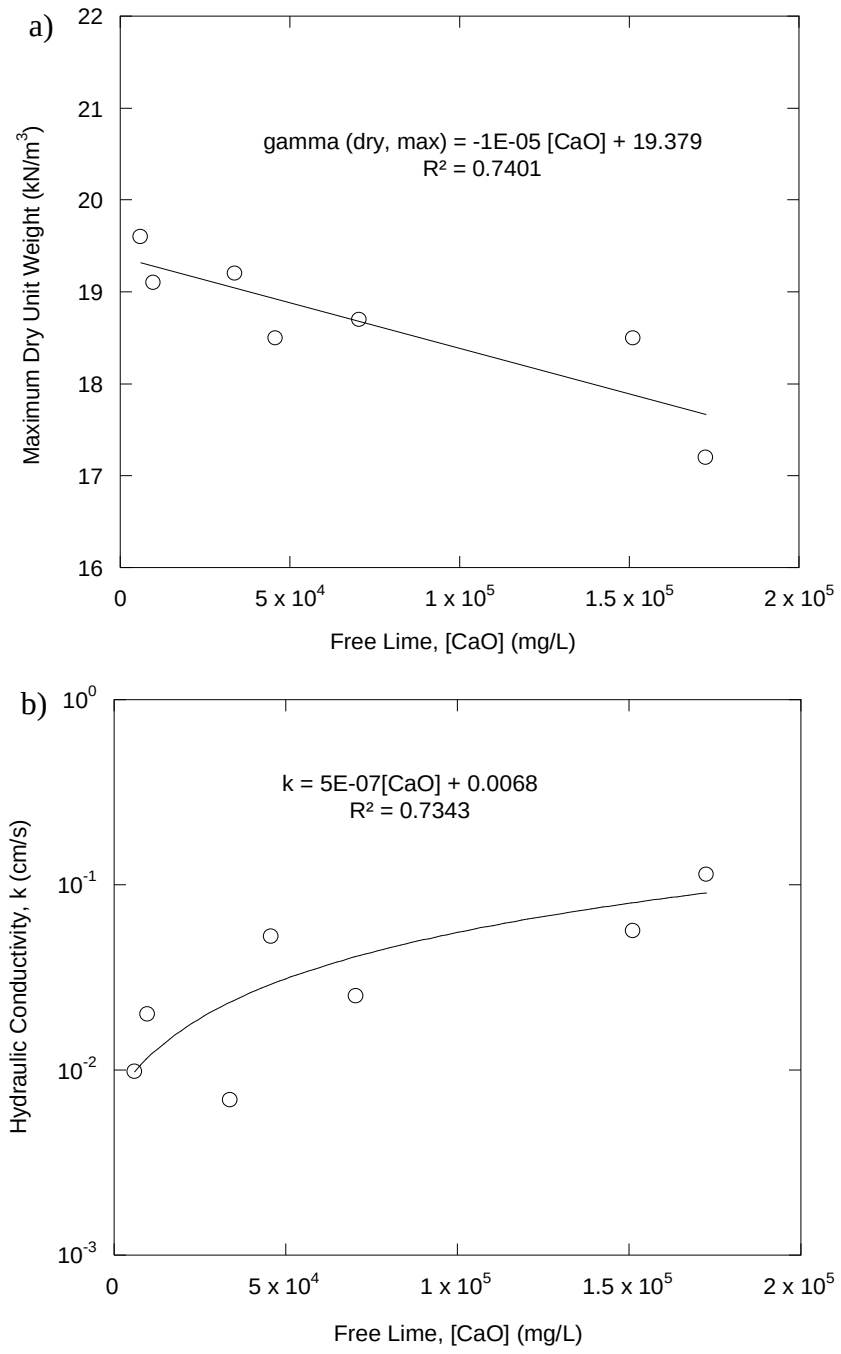

Figure 2.6. Effect of free lime content on a) maximum dry unit weight of RAP and b) hydraulic conductivity of RAP.

2.4.4 Hydraulic Conductivity

The hydraulic conductivity of RAP varies from 6.89×10^{-3} cm/s (RAP5) to 1.14×10^{-1} cm/s (RAP3) with an average of 4.08×10^{-2} cm/s (see Table 2.2 and Figures A.1 through A.7), and compares well to the range of hydraulic conductivities for clean sand and gravel mixtures reported by Holtz et al. (2011). According to Casagrande and Fadum (1940), who proposed hydraulic conductivity of 10^{-4} cm/s as a boundary between free-draining and poor-draining materials under low gradients, Maryland RAPs can be classified as free-draining materials.

Hydraulic conductivity of RAP is higher than that of the natural topsoil (6.89×10^{-3}-1.14×10^{-1} cm/s versus 7.16×10^{-5}-6.23×10^{-4} cm/s, Table 2.2). RAP is mainly composed of sand and gravel with little fines, whereas the topsoil generally consists of sand and fines. Such dissimilarity in the gradation may explain the different coefficients of hydraulic conductivity between RAP and the topsoil. By contrast, the hydraulic conductivity of RAP is lower than that of Stone No.57 ($k = 2.40 \times 10^{0}$ cm/s), a material commonly used as a free-draining material in Maryland highway applications. Unlike RAP which is generally classified as well-graded sand with gravel and has up to 2% of fines, Stone No. 57 is a uniformly-graded gravel with almost zero percent fine particles, meaning that its matrix is more porous and allows water to flow more freely. Therefore, the difference in the hydraulic conductivity of RAP and Stone No. 57 is not unusual. Finally, the hydraulic conductivity of RAP tested for highway shoulder backup applications in Maryland is comparable to that of GAB used in Maryland road base and subbase coarse layers. It should also be noted that RAP was compacted at more than 97% of maximum dry unit weight as per

standard Proctor, while GAB was compacted at 100% of the maximum dry unit weight as per modified Proctor. Figures A.8 through A.10 illustrate hydraulic conductivity of control materials as a function of time.

2.4.4.1 Effect of fines and sand-to-gravel ratio on hydraulic conductivity

A RAP matrix consists of fine-, sand-, and gravel-sized particles and voids that these particles enclose. Theoretically, a wider range of particle sizes results in a better packing configuration (lower void ratio), which, in turn, yields a lower coefficient of hydraulic conductivity (Holtz et al., 2011). In other words, an increase in the fines content and/or sand-to-gravel ratio generates a less porous medium and, thereby, reduces the hydraulic conductivity coefficient.

Figure 2.7 illustrates the hydraulic conductivity of RAP and control materials as a function of fines percent. In regard to the hydraulic conductivity of RAP materials, it generally decreases with increasing fines content. Topsoils yield the lowest hydraulic conductivity due to their large fines content, followed by RAP5 and RAP1. Although one might assume that RAP1 would have a lower hydraulic conductivity coefficient than RAP5 due its higher fines content (1.83% versus 1.19%, Table 2.2), their sand-to-gravel ratios (1.12 versus 1.18, Table 2.2) should also be taken into consideration. It is clear from Figures 2.7 and 2.8 that both fines content and sand-to-gravel ratios influence hydraulic conductivity values of RAP and control materials.

2.4.4.2 Effect of coefficient of uniformity on hydraulic conductivity

A lower coefficient of uniformity (C_u) reflects materials with a narrower range of

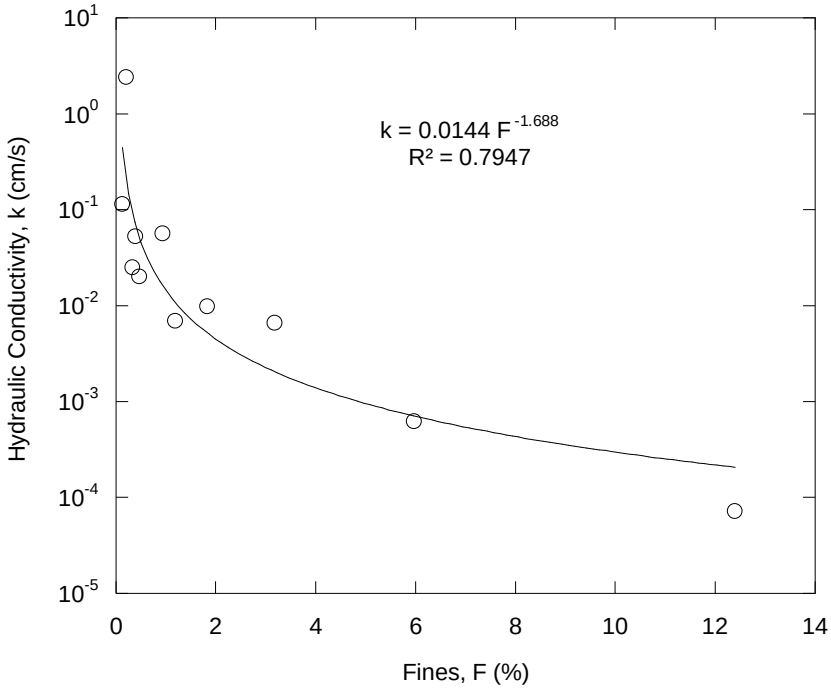

Figure 2.7. Effect of fines content on the hydraulic conductivity of RAP, Stone No. 57, GAB, and topsoil.

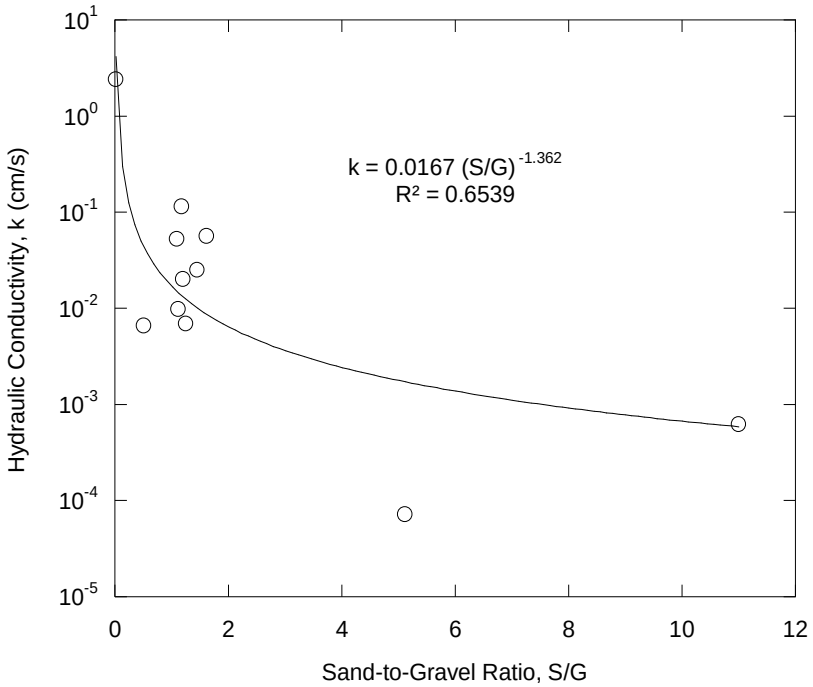

Figure 2.8. Effect of sand-to-gravel ratio on the hydraulic conductivity of RAP, Stone No. 57, GAB, and topsoil.

particle sizes thus a more porous matrix, while materials with tightly-packed particles have higher C_u values. Consequently, the hydraulic conductivity is expected to decrease with an increase in C_u. Figure 2.9 shows that RAP and control materials altogether follow this trend well. Stone No. 57 has the lowest C_u (1.52) and the highest hydraulic conductivity ($2.40x10^0$ cm/s), whereas GAB has the highest C_u (58.7) and the lowest hydraulic conductivity ($6.57x10^{-3}$ cm/s). The seven RAP materials have similar C_u values that are in between those corresponding to Stone No. 57 and GAB. Likewise, the coefficients of hydraulic conductivity of the RAPs are alike and fall within the range of the hydraulic conductivity coefficients pertaining to the two control materials.

2.4.4.3 Effect of maximum dry unit weight on hydraulic conductivity

Figure 2.10 shows that the hydraulic conductivity of RAP decreases with an increase in the maximum dry unit weight. It is believed that different gradations, packing arrangements of particles, and the fines content of the RAP materials resulted in differences between maximum dry unit weights. The void ratio hence the hydraulic conductivity is lower at a greater maximum dry unit weight, which is constant with the findings of Trzebiatowski and Benson (2005) and Rahman et al. (2015). RAP3 has the lowest maximum dry unit weight (17.2 kN/m^3 [109.7 pcf]) and the highest coefficient of hydraulic conductivity ($1.14x10^{-3}$ cm/s), while RAP5 and RAP1 have the greatest maximum dry unit weights (19.1 kN/m^3 [122.4 pcf] and 19.6 kN/m^3 [124.9 pcf], respectively) and the lowest hydraulic conductivity values ($6.89x10^{-3}$ and $9.83x10^{-3}$ cm/s, respectively).

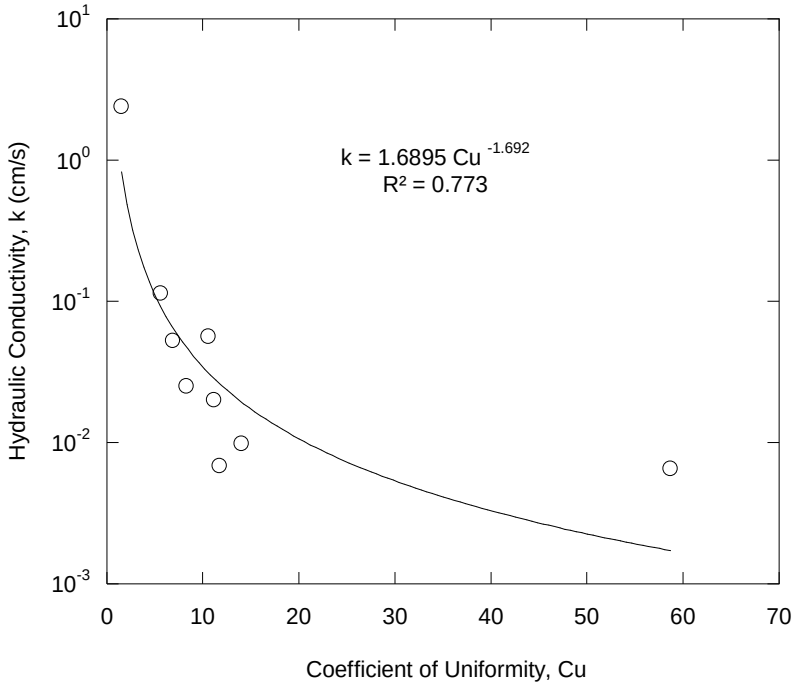

Figure 2.9. Effect of coefficient of uniformity on the hydraulic conductivity of RAP, GAB, and Stone No. 57.

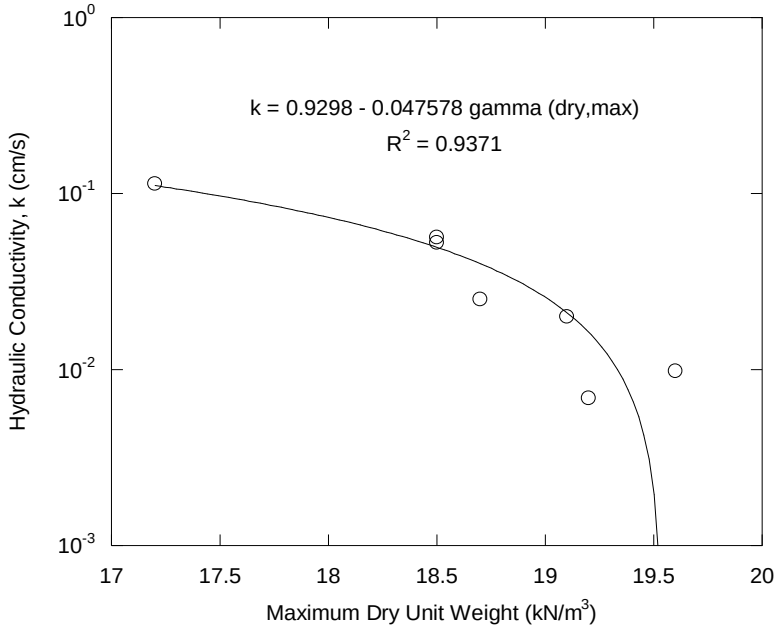

Figure 2.10. Effect of maximum dry unit weight on the hydraulic conductivity of RAP.

2.4.4.4 Effect of D_{10} on hydraulic conductivity and Hazen's empirical correlation between D_{10} and hydraulic conductivity

D_{10} is the grain size (in mm) that corresponds to 10% of material passing by mass. As a rule, the lower the effective particle size (D_{10}) is, the lower the hydraulic conductivity of a material is. Table 2.2 summarizes D_{10} and coefficients of hydraulic conductivity predicted by Hazen's empirical formula. Figure 2.11 compares the hydraulic conductivity coefficients of RAP determined experimentally as a function of D_{10} to those estimated using Hazen's equation. Evidently, the hydraulic conductivity of RAP is fairly proportional to D_{10} and Hazen's equation overpredicts the hydraulic conductivity of RAP by approximately one order of magnitude. Nokkaew et al. (2012) noticed the same behavior and concluded that Hazen's equation does not apply to RAP. Hazen developed the correlation between D_{10} and hydraulic conductivity for loose, poorly-graded aggregates. However, RAP has a wide range of particle sizes and is compacted. The exception is RAP3, which is poorly-graded sand with gravel and has the lowest maximum dry unit weight of the seven RAPs. It has the highest D_{10} and the highest coefficient of hydraulic conductivity.

2.4.4.5 Effect of grain size on hydraulic conductivity

Based on the coefficients of determination (R^2) presented in Figure 2.12, the hydraulic conductivity of RAP, GAB, Stone No. 57, Topsoil 1, and Topsoil 2 is highly sensitive to the smaller effective particle sizes, D_{10} and D_{30}, as compared to the larger ones, D_{50} and D_{60}. This is constant with the findings of Alyamani and Sen (1993), Carrier (2003), Haider (2013), and Svensson (2014), who concluded that the

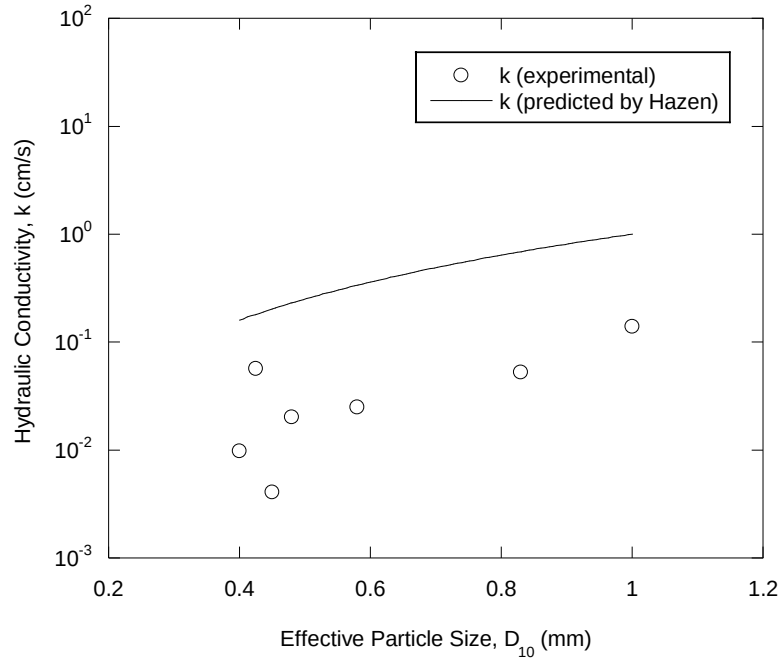

Figure 2.11. Effect of D_{10} on the hydraulic conductivity of RAP.

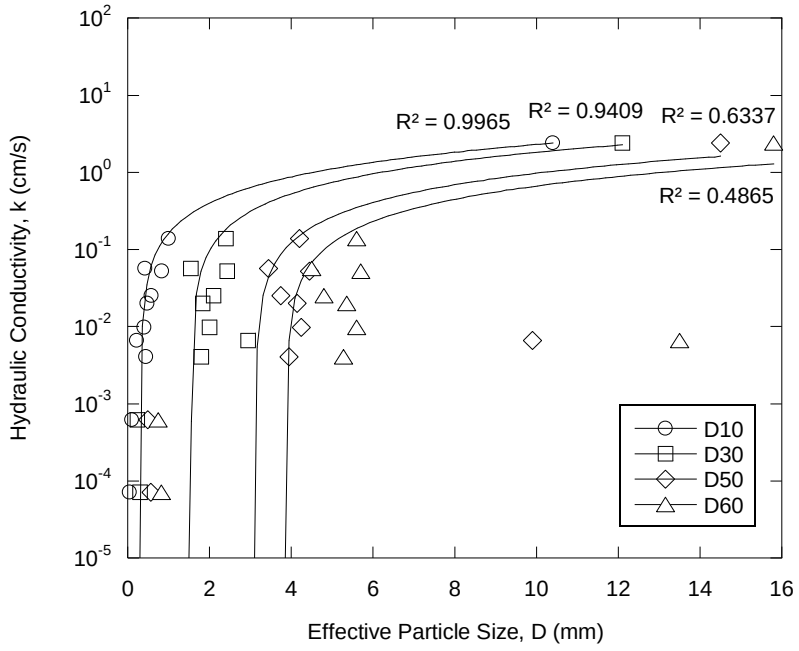

Figure 2.12. Effect of grain size on the hydraulic conductivity of RAP, GAB, Stone No. 57, and topsoil.

hydraulic conductivity of geomaterials are affected by finer grain sizes such as D_{10} and D_{30}.

2.4.4.6 Effect of free lime content on hydraulic conductivity

Figure 2.6b illustrates a correlation between the free lime (CaO) content and the hydraulic conductivity of RAP; the hydraulic conductivity of RAP increases with an increase in the concentration of CaO. The same behavior was observed for different types of soil by numerous researchers, and was attributed to the formation of a more porous fabric due to flocculation/aggregation processes that increase the resistance to compaction and enable a better vertical flow of water (Townsend and Kylm, 1966; Broms and Boman, 1979b; Brandl, 1981; Nalbantoglu and Tuncer, 2001). McCallister (1990) and Cuisinier et al. (2011), on the other hand, could not draw a correlation between free lime content and hydraulic conductivity, and indicated that hydraulic conductivity was mainly influenced by large pore volumes and the effect of the small pores was minimal.

2.4.4.7 Effect of bitumen content on hydraulic conductivity

The effect of bitumen content on hydraulic conductivity of RAP is illustrated in Figure 2.12. There is a general increase in the hydraulic conductivity with an increase in the amount of bitumen. RAP3 has the highest percent of asphalt binder (5.31%) and yields the highest hydraulic conductivity ($1.14x10^{-1}$ cm/s) among all RAPs tested. Bitumen is hydrophobic, i.e., it does not attract or absorb water, which allows water to flow through voids more easily, as stated by Viyanant (2006) and Shedivy et al. (2012). In spite of an increasing trend presented in Figure 2.13, the difference in the

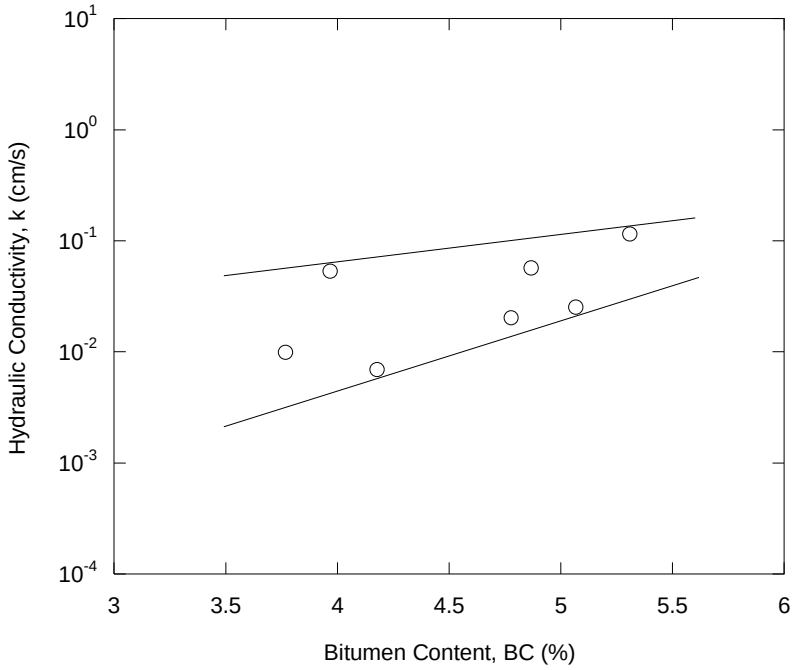

Figure 2.13. Effect of bitumen content the hydraulic conductivity of RAP.

percentages of bitumen coating of RAP aggregates is small. In order to better assess the influence of bitumen on hydraulic conductivity of RAP, samples with a wider range of asphalt binder content should be subjected to hydraulic conductivity testing.

2.4.4.8 Effect of fines, sand-to-gravel ratio, coefficient of uniformity, and effective particle size on hydraulic conductivity under controlled gradation

To better understand the effect of fines, sand-to-gravel ratio, coefficient of uniformity, and effective particle size on the hydraulic conductivity of RAP, two RAP materials, RAP1 and RAP2, were selected for testing under controlled gradation. The corresponding relationships are shown in Figures 2.14 through 2.18.

It is evident from Figure 2.14 that the hydraulic conductivity of both RAPs is highly dependent on the percent of fines. As the percent of fines increases by 8%, the coefficient of hydraulic conductivity decreases by more than one order of magnitude. When tested with 0% of fine particles, RAP1 and RAP2 have hydraulic conductivity values of $2x10^{-2}$ cm/s and $2.68x10^{-3}$ cm/s, respectively. At 8% of fines, the coefficients of hydraulic conductivity for RAP1 and RAP2 are $2.00x10^{-3}$ cm/s and $7.55x10^{-3}$ cm/s. As the presence of fines leads to better packing and tends to increase dry unit weight, which, in turn, decreases a coefficient of hydraulic conductivity. Similar observations were made by Bouchedid and Humphrey (2005), Berthelot et al. (2009), and Aydilek et al. (2015).

Figure 2.15 depicts the impact of sand-to-gravel ratio on the hydraulic conductivity of RAP1 and RAP2; higher sand-to-gravel ratio yields lower hydraulic conductivities. Gravel particles generate the void space that finer sand particles fill in, while fines occupy the voids formed by sand (Xiao et al., 2012). The porosity as well

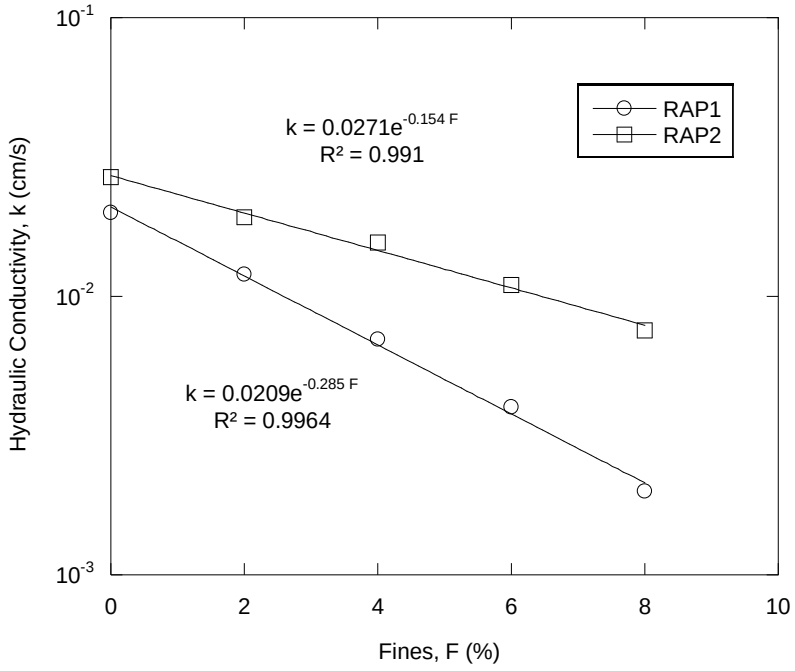

Figure 2.14. Effect of fines on the hydraulic conductivity of RAP under controlled gradation conditions.

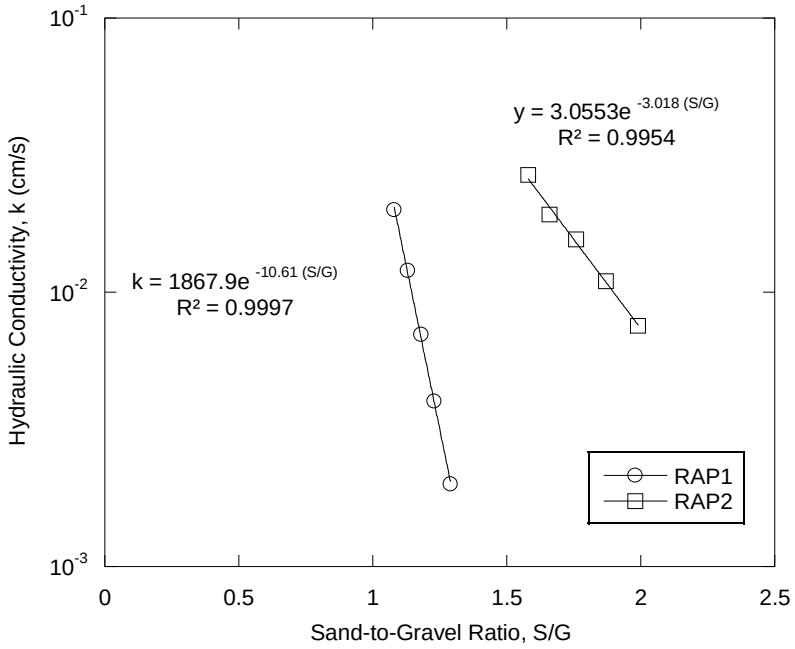

Figure 2.15. Effect of sand-to-gravel ratio on the hydraulic conductivity of RAP under controlled gradation conditions.

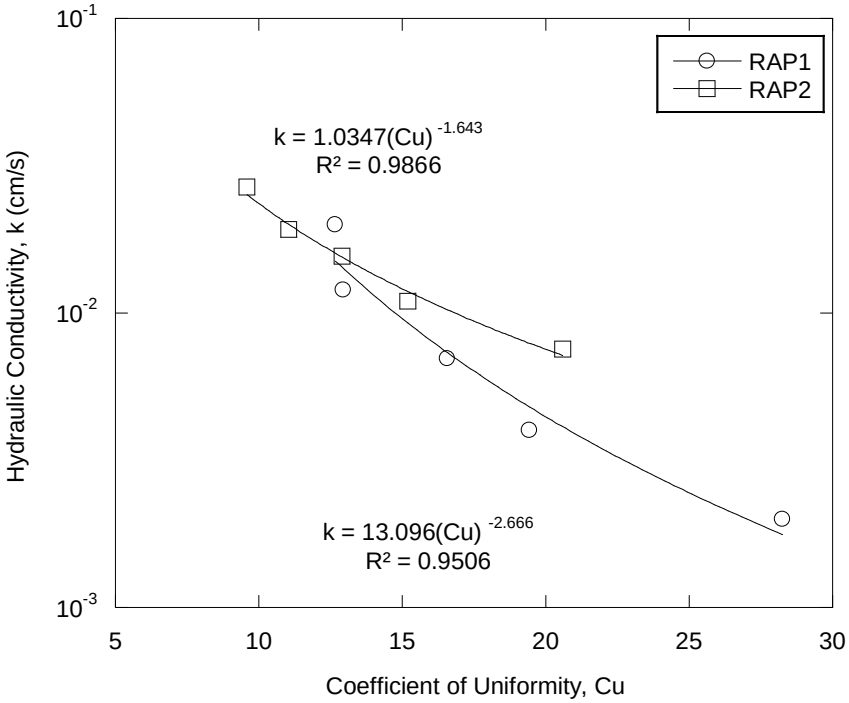

Figure 2.16. Effect of coefficient of uniformity on the hydraulic conductivity of RAP under controlled gradation.

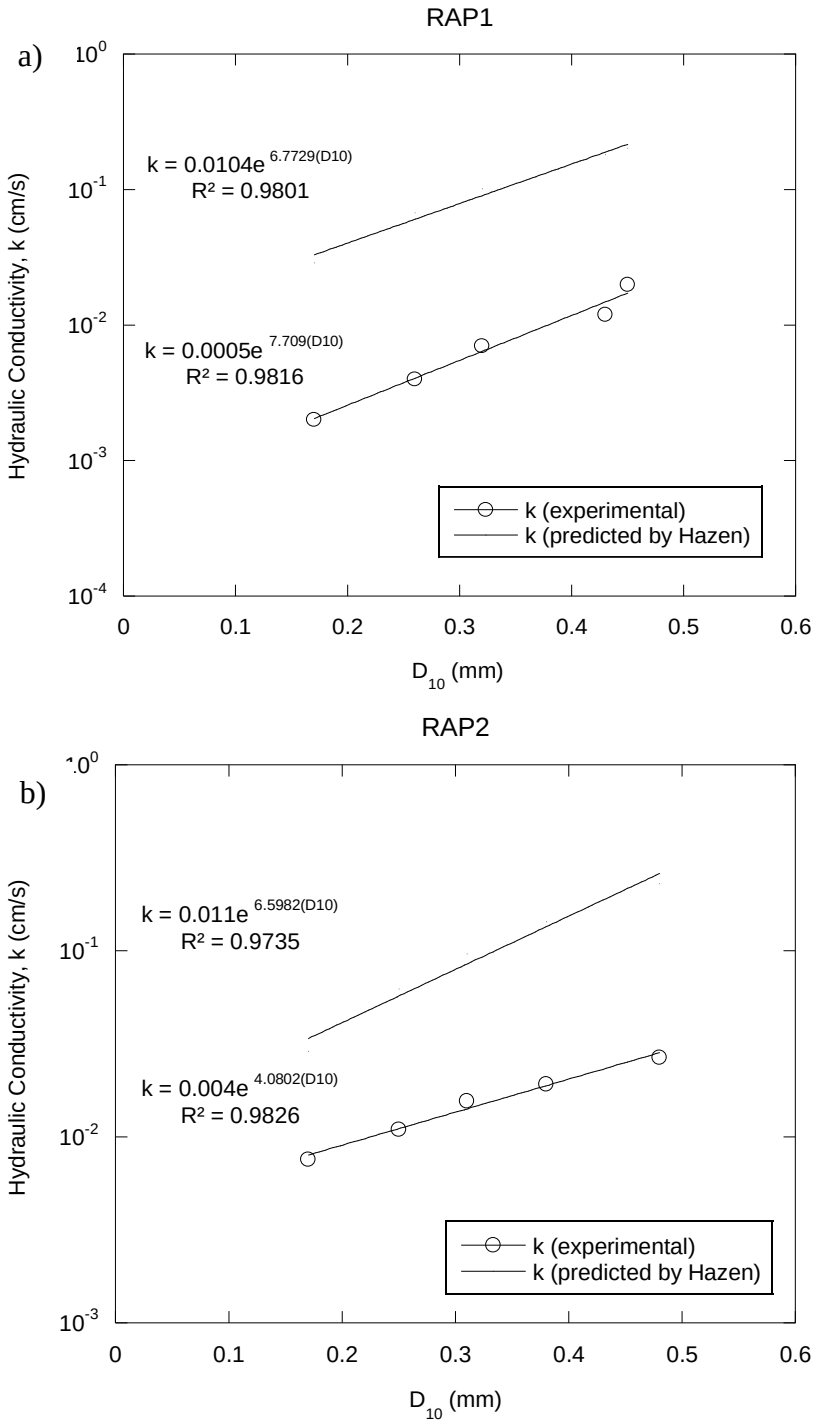

Figure 2.17. Effect of D10 on the hydraulic conductivity of a) RAP1 and b) RAP2.

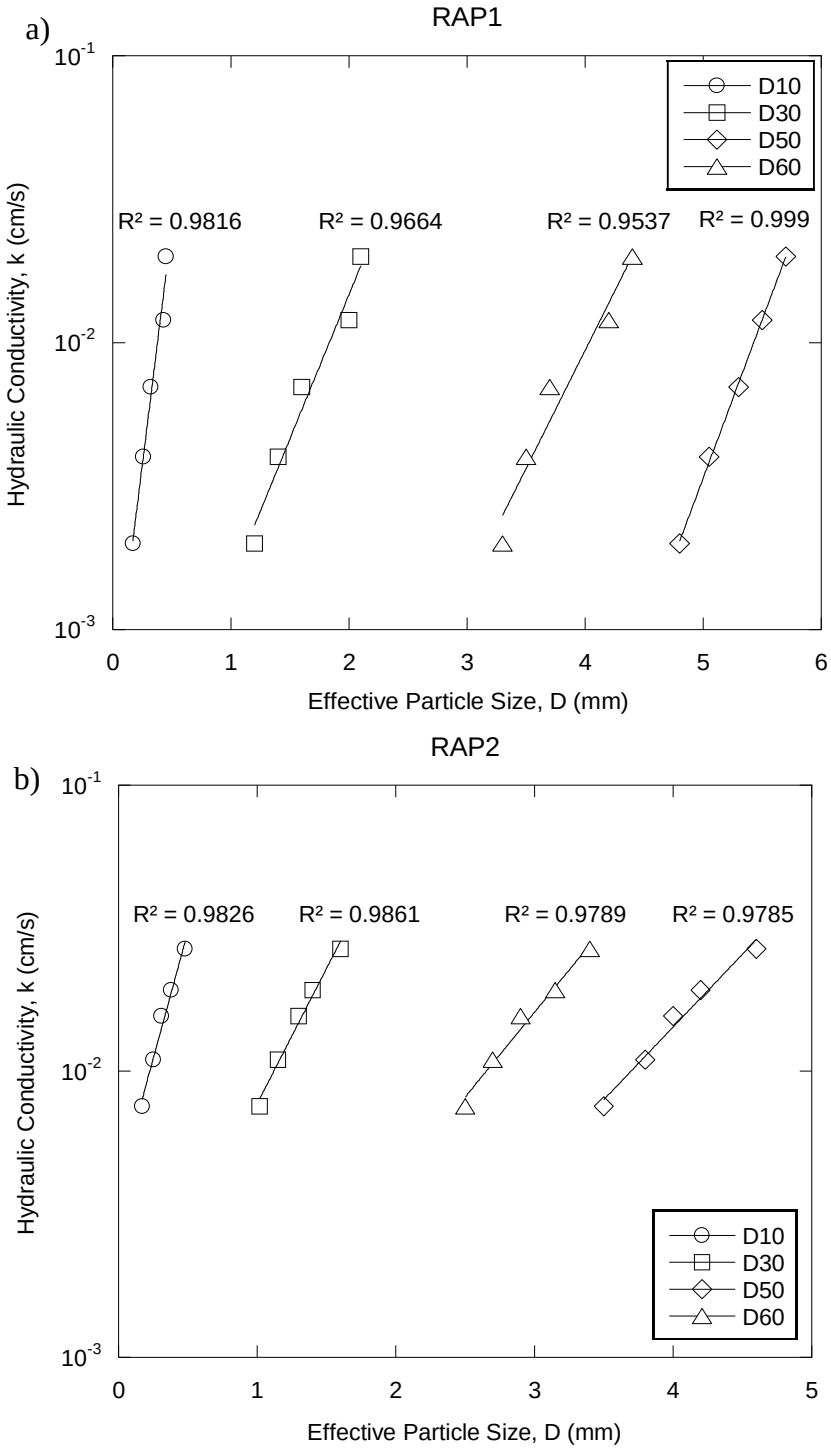

Figure 2.18. Effect of particle size on the hydraulic conductivity of a) RAP1 and b) RAP2.

as the hydraulic conductivity of RAP decrease as the amount of sand-to-gravel increases. The hydraulic conductivity of RAP1 decreases 10 times as its sand-to-gravel ratio is varied from 1.08 to 1.29, whereas the reduction in sand-to-gravel ratio of RAP2 from 1.58 to 1.99 causes a 28-fold decrease in hydraulic conductivity.

The hydraulic conductivity of RAP1 and RAP2 is affected by the coefficient of uniformity (Cu). As aforementioned, higher values of Cu mean a less porous medium hence the lower hydraulic conductivity. Both RAPs follow the same pattern; their conductivities are larger by roughly one order of magnitude with a raise of 2.2 times in Cu (Figure 2.16).

The data in Figure 2.17 show that higher coefficients of hydraulic conductivity are obtained for materials with a larger D_{10}. A reduction in D_{10} of RAP1 from 0.45 to 0.17 mm is followed by a 10-time decrease in the coefficient of hydraulic conductivity. As for RAP2, the coefficient of hydraulic conductivity for D_{10} = 0.48 mm is 26 times higher than that for D_{10} = 0.17 mm. The figure also contains the hydraulic conductivity coefficients as predicted by Hazen's formula. Even though the experimentally-determined hydraulic conductivity coefficients follow the trendline of the predicted coefficients well, these values are underestimated by nearly one order of magnitude. This again confirms the statement of Nokkaew et al. (2012) that Hazen's empirical formula is not a good predictor of RAP hydraulic conductivity. Furthermore, Figure 2.18 shows the effect of particle size on the hydraulic conductivity of RAP. In contrast to the as-received RAP and control materials, the impact of each, D_{10}, D_{30}, D_{50}, and D_{60}, on the hydraulic conductivity of RAP1 and RAP2 is comparable due to the controlled gradation.

2.5 CONCLUSIONS

A series of laboratory hydraulic conductivity tests were conducted on seven recycled asphalt pavement materials from Maryland using the bubble-tube constant-head permeameter. Graded aggregate base, Stone No. 57, and two topsoils served as control materials. The following conclusions are developed:

1) The hydraulic conductivity of recycled asphalt pavement ranges from $6.89x10^{-3}$ cm/s to $1.14x10^{-1}$ cm/s, with an average of $4.08x10^{-2}$ cm/s. The measured hydraulic conductivity values of the recycled asphalt pavement are significantly higher than those determined for the topsoils, $7.16x10^{-5}$ cm/s and $6.23x10^{-4}$ cm/s, and lower than that of Stone No. 57, $2.4x10^{0}$ cm/s. In other words, the hydraulic conductivity of recycled asphalt pavement is comparable to the hydraulic conductivity of the natural aggregate with the gradation of clean sand and gravel mixture. It is also in agreement with the hydraulic conductivities of recycled asphalt pavement reported in the literature.
2) Maryland RAPs are free-draining since their hydraulic conductivity values are above 10^{-4} cm/s, a boundary between poor-draining and free-draining materials proposed by Casagrande and Fadum (1940) for geomaterials tested under low gradients.
3) Although the hydraulic conductivity of as-received recycled asphalt pavement is not dependent solely on one parameter, there is a general increase in its hydraulic conductivity with an increase in the fines content and sand-to-gravel ratio and a decrease in the coefficient of uniformity. The grain size

distribution, packing arrangement of particles, and the content of fines altogether affect the void ratio and hydraulic conductivity of RAP.

4) There is an overall positive relationship between the effective particle size, D_{10}, and hydraulic conductivity of as-received recycled asphalt pavement; however, Hazen's empirical equation is not deemed a good predictor of its hydraulic conductivity because it overestimates it by approximately one order of magnitude. As-received recycled asphalt pavement also showed a greater sensitivity to finer grain sizes such as D_{10} and D_{30} than to the larger ones, D_{50} and D_{60}.
5) In general, a higher free lime content (CaO) and bitumen content within a RAP yield lower dry unit weight and higher hydraulic conductivity.
6) Under the controlled-gradation conditions, the hydraulic conductivity of recycled asphalt pavements decreases by more than one order of magnitude when the amount of fines is varied from 0 to 8% by mass. Similarly, an increase in the sand-to-gravel ratio and the coefficient of uniformity and a decrease in the grain size, D10, all reduce the hydraulic conductivity of recycled asphalt pavement.

3 ENVIRONMENTAL BEHAVIOR OF RECYCLED ASPHALT PAVEMENT

3.1 INTRODUCTION

Concerns over possible leaching of pollutants such as metals and polycyclic aromatic hydrocarbons (PAHs) from RAP stem from chemical composition of asphalt and contamination of asphalt by vehicle traffic (Lindgren, 1996; Brantley and Townsend, 1999; Legret et al., 2005). Asphalt is composed of mineral aggregate (~95%), bitumen (~5%), and fills such as adhesives and polymers (Lindgren, 1996). Bitumen is derived from crude oil and it commonly contains trace quantities of metals such as vanadium, nickel, iron, and calcium. The exact composition of bitumen varies with different sources of crude oil and the manufacturing processes (Whiteoak, 1990). The most common assumption is that bitumen is the main source of vanadium and nickel. Nonetheless, the mineral aggregate (stone material) itself is considered to be the major source of heavy metals depending on its natural composition (Lindgren, 1996). Other sources of pollutants that might leach from RAP originate from brake lining (Cu), tire wear and corrosion of galvanized steel crash barriers (Zn and Cd), gasoline (Pb and Ni), and lubricating oils (Ni) (Muschack, 1990; Hewitt and Rashed, 1990; Bjelkas and Lindmark, 1994; Legret and Pagotto, 2003). Due to use of leaded gasoline in the past, the greatest concentrations of lead have been observed within the oldest RAP samples (Keller, 2013).

RAP is generally recognized as a construction and debris waste material that does not pose a significant threat to human health and the environment (Keller, 2013). However, the amount and type of chemicals leached from RAP into the environment

must be better characterized (Keller, 2013). A few research studies on leaching of metals from RAP have been reported in the literature.

Brantley and Townsend (1999) conducted a series of batch tests and column (lysimeter) experiments on six RAP samples from Florida to evaluate their leaching characteristics when used as a fill material. Leachate concentrations of selected heavy metals (Ba, Ca, Cr, Cu, Ni, Pb, and Zn) were below detection limits and regulatory levels for groundwater. The exception was Pb that leached from one column with a RAP sample originating from an older roadway section, but it decreased over time. It was concluded that the source of Pb was not the aggregate or bitumen, but likely longer exposure of the roadway to vehicle traffic and emissions. The presence of Pb in the leachate derived from the column test and its absence from the batch leachate could be explained by lower dilution. Overall, the investigated RAP samples did not constitute hazardous waste and the leached heavy metal concentrations posed minimal threat to groundwater.

Morse et al. (2001) conducted batch leach tests on two RAP samples from Texas. The average concentrations of Ba and Pb exceeded the regulatory limits employed by Texas Department of Transportation. Elevated antimony concentration was detected in only one RAP sample.

Legret et al. (2005) investigated the leaching potential of RAP procured from France's RN76 highway through batch and column experiments. Leachates derived from batch tests were analyzed for eight heavy metals (Cu, Cr, Cd, Ni, Zn, Pb, Hg, and Mo). The concentrations were below European Commission limits for drinking water, except for Zn and Hg in the first stage of the test. On the other hand, column

leachates showed the greatest concentration of metals being leached in the initial stages of the test. All metals (Cu, Pb, Hg, and Mo) but Zn concentrations were noticeably below detection limits. Zn followed a typical leaching curve, i.e., its concentration within the leachate was high at first, but then dropped rapidly below the detection limit. It was concluded that the grain size and the percolation flow rate had the main influence on the results.

Kang et al. (2011) analyzed the potential of pure RAP and virgin aggregate to leach heavy metals. Inductively coupled plasma atomic emission spectrophotometry (ICP-AES) and atomic absorption spectrophotometer were utilized to detect metals within batch leachates. Cr, Cd, Mo, Ni, Pb, Sr, V, and Zn were not detectable in RAP filtrates. If detectable, all metal concentrations except for As were higher in virgin aggregate leachates than in RAP leachates. The concentration of Al in both RAP and virgin aggregate leachates exceeded the secondary drinking water standard. However, the U.S. EPA does not enforce the secondary maximum contaminant levels. Leachate pH values for the batch mode were reported for RAP and virgin aggregate as 9.67 and 9.19, respectively.

Shedivy et al. (2012) reported on the leaching characteristics of heavy metals from five different RAP samples collected from Ohio, Wisconsin, California, New Jersey, and Colorado. To assess chemical leaching potential from RAP, batch leaching tests with deionized water as the leaching fluid were performed. The measured pH values were in the range between 8.59 and 9.58. Electrical conductivity was low, indicating limited mineralization of leachates due to bitumen coating. Heavy metals in the leachates were detected using the inductively coupled plasma optical

emission spectrometry (ICP-OES) technique. All metal concentrations except Mn and As were below Maximum Contamination Level concentrations for drinking water. Concentrations of Cr and Cd were below detection limits.

The aforementioned studies provide limited information on the leaching behavior of recycled asphalt pavement. There are no data reported on the potential of Maryland RAPs to leach heavy metals. Furthermore, no research study was conducted to assess the pollutant characteristics in surface water bodies due to a lateral flow of RAP leachate from highway shoulder backups. Therefore, to address environmental concerns related to the possible leaching of heavy metals from Maryland RAPs used in highway shoulder backups, a series of batch water leach tests (WLT) and long-term column leach tests (CLT) were performed in this research study. A numerical model, UMDSurf, was also implemented in the testing program to simulate the contaminant transport in surface waters like rivers and streams as a function of distance.

3.2 MATERIALS

Reclaimed asphalt pavement (RAP) samples listed above were used in leach tests. Table 3.1 provides a summary of the chemical properties of the materials used in this study.

3.3 METHODS

3.3.1 Batch Water Leach Test (WLT)

Batch water leach tests (WLT) were conducted on pure RAP samples, GAB, Topsoil 1, and Topsoil 2 in accordance with slightly modified ASTM D 3987. The specimens

Table 3.1. Elemental composition of RAP, GAB, stone No. 57, and topsoil.

Analyte (mg/L)	RAP1	RAP2	RAP3	RAP4	RAP5	RAP6	RAP7	GAB	Stone No. 57	Topsoil 1	Topsoil 2
Al	12138	5942	5660	6948	5096	7383	2783	3013	720	6648	19665
As	<3	11.2	14.8	6.56	<5	<5	<5	<5	<5	<5	<5
B	2.32	8.14	16.8	9.48	--	--	--	--	--	--	--
Ba	36.5	26.9	204	30.7	109	311	154	115	23	365	1183
Cd	<0.4	<0.4	<0.4	<0.4	0.5	<0.4	0.6	0.4	<0.4	<0.4	<0.4
Ca	6000	151200	172500	70500	33824	9752	45701	45195	<40	384	2622
Co	5.20	7.07	5.05	4.78	14	7	3	<2	<2	4	20
Cr	15.2	53.0	9.11	27.9	239	38	20	11	8	23	49
Cu	11.3	9.43	11.7	23.5	14	26	8	4	4	9	32
Fe	9506	8280	7668	10326	5516	5681	1840	1495	4800	3744	11776
Li	5.97	6.87	15.5	4.47	--	--	--	--	--	--	--
Mg	2900	39100	10000	17700	8204	4209	12466	23368	<40	360	2438
Mn	181	207	450	153	296	525	155	134	86	303	619
Mo	--	--	--	--	<2	<2	<2	<2	<2	<2	<2
Ni	2.27	98.3	<0.3	5.93	187	22	17	5	3	10	31
Pb	32.6	13.1	8.82	6.23	8	8	46	6	<5	12	28
P	200	200	200	200	30.8	46	29.9	23	16	86.4	138
K	900	3000	2900	1100	2212	2208	1679	3059	200	2712	6371
Ag	--	--	--	--	<0.5	<0.5	<0.5	<0.5	<0.5	<0.5	<0.5
Se	<3	<3	<3	<3	--	--	--	--	--	--	--
Na	363	340	205	727	336	2461	276	92	40	648	1380
Sr	12.9	191	614	109	238	115	310	129	4	58	124
S	2200	5000	5200	4400	--	--	--	--	--	--	--
Ti	228	234	42.5	257	252	506	12	1428	40	816	1311
V	42.8	71.3	27.2	71.3	62	93	67	14	6	35	87
Zn	26.5	22.8	36.1	33.0	22	54	40	19	3	30	113

were prepared in a liquid-to-solid ratio (L:S) of 20:1. All materials were oven-dried and sieved through the No. 10 (2.0 mm) sieve before use. First, 2.5 grams of dry sample were added into the high-density polyethylene (HDPE) tube along with 50 ml of 0.02 M NaCl. The tubes with specimens were then set at 29 rotations per minute and rotated for 18 hours. The specimens were allowed to sit for five minutes and were centrifuged at 5800 rpm for 15 minutes. Finally, the specimens were filtered through the 0.2-µm pore size, 25-mm membrane disk filters fitted in a 25-mm Easy Pressure syringe filter holder by a 60-mL plastic syringe. The filtered effluents were subjected to the pH and electrical conductivity (EC) measurements, acidified to pH<2 with 2% HNO_3, and stored at 39°F [4°C] for metal concentration analyses using the inductively coupled plasma optical emission spectroscopy (ICP-OES) technique. Triplicate WLTs were performed on all materials. The WLT set-up is schematically given in Figure 3.1.

3.3.2 Column Leach Test (CLT)

Column leach tests (CLT) were conducted on seven RAP materials, GAB, stone No. 57, Topsoil 1, and Topsoil 2. The smooth fluid flow was established through the column set-up shown in Figure 3.2. The liquid-to-solid ratio (L:S) of 0.1:1 was achieved and it varied with time. RAP specimens were compacted at 2% dry of optimum moisture content in a polyvinyl chloride (PVC) mold having a diameter of 6.0 in. [152 mm] and a height of 6.1 in. [155 mm] using the standard Proctor compactive effort (ASTM D 698). The GAB specimen was compacted to the maximum unit weight as determined per ASTM D 1557, while stone No. 57 was compacted to a unit weight of 110 pcf [17.2 kN/m^3]. The columns were operated in

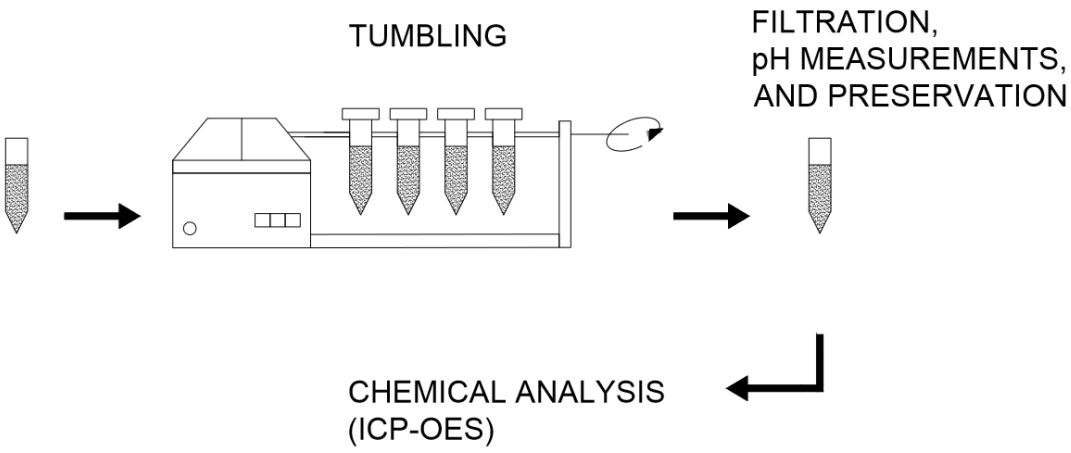

Figure 3.1. Schematics of batch water leach test set-up.

a)

b)

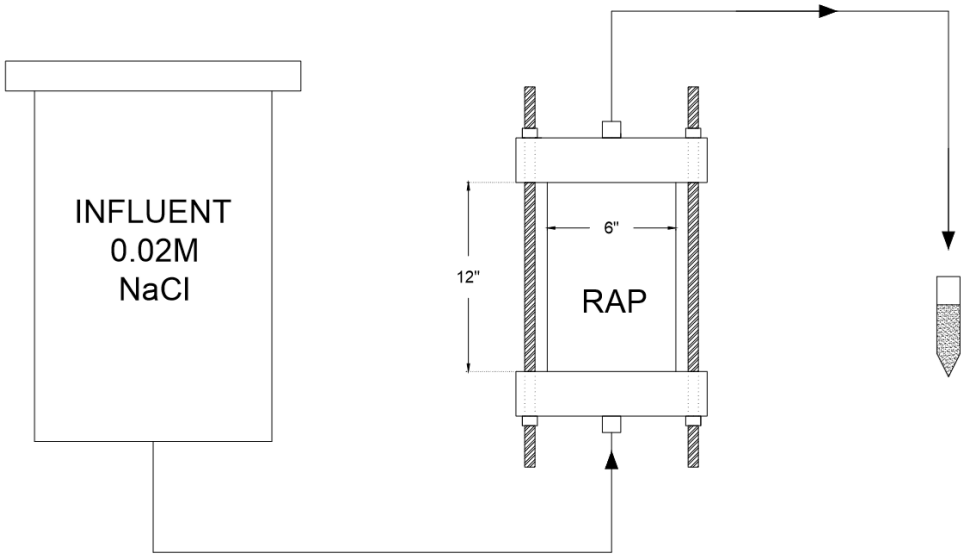

Figure 3.2. (a) Image and (b) sketch of the column leach test set-up.

an up-flow mode with an inflow rate of 60mL/hr, as recommended by Gelhar et al. (1992) and Morar (2008). The flow was provided by a peristaltic pump on the polypropylene (PP) influent lines having a 3.1-mm inner diameter and connected to a polyethylene reservoir filled with a 0.02M NaCl solution. The pH of the influent solution was kept between 6.0 and 6.5 to simulate typical field conditions in Maryland. The effluent solution was transferred from the column into a collection tube via polytetrafluoroethylene tubing. The pH and electrical conductivity (EC) measurements were recorded immediately after the sample collection on a daily basis. The samples were then filtered through a 0.2-μm membrane filter, acidified to pH<2 with 2% HNO3, and stored at 39ºF [4ºC] for inorganic component concentrations analyses using the ICP-OES procedure.

Topsoil specimens were compacted at 85% of maximum dry unit weight as per ASTM D 698 in a PVC mold with a 4-in. [101.6-mm] diameter and a 4.6-in. [116.4-mm] height. An inflow rate of 15 mL/hr was used due to their low hydraulic conductivity values, as suggested by Dayioglu (2016). The PVC molds were preferred because they minimize the outside effects on effluent metal concentrations.

3.3.3 Chemical Analysis

The concentrations of all metals in total elemental analyses (TEA), batch water leach test (WLT), and column leach test (CLT) leachates were determined using a Varian Vista-MPX CCD Simultaneous ICP-OES (Thermo Jarrell Ash IRIS Advantage Inductively Coupled Plasma Optical Emission Spectrometer). All equipment that came in contact with the leachate samples was acid-cleaned, rinsed with deionized (DI) water, dried, and stored in sealed, plastic bags. A reagent blank was tested every

20 samples and a spiked sample was analyzed every 12 samples for calibration. A set of calibration standards was prepared following the U.S. Code of Federal Regulations Title 40. A minimum detection limit (MDL) for ICP-OES was evaluated for every metal.

WLT and CLT leachates were analyzed for Al, As, B, Ba, Ca, Cd, Co, Cr, Cu, Fe, Hg, Li, Mn, Na, Ni, Pb, V, and Zn. The elements selected for further discussion were Al, B, Ba, Cu, Mn, Ni, and Zn due to their potential impact on the environment and human health and their mobility in surface waters.

Aluminum is one of the most abundant metals in the Earth's crust (Sparks, 2003) and is also one of the most widely used metals in the world industry (Periodic Table, 2017). It is considered as a non-toxic metal, but water-soluble forms of aluminum such as aluminum chlorine as well as long-lasting exposure to higher concentrations of aluminum can cause serious health problems (Periodic Table, 2017). Higher levels of aluminum intake through breathing, food or by skin contact can cause damage to the lung and central nervous system, bone and kidney disease, and Alzheimer's disease (Public Health Statement, 2017). High aluminum concentrations have also significant impact on the environment due to acidifying problems (Periodic Table, 2017). Accumulated aluminum in plants can cause health problems to animals that consume these plants. In addition, high levels of aluminum in acidifying lakes can have negative impact not only on aquatic organisms, but also on birds and other animals that consume contaminated fish (Periodic Table, 2017).

Boron occurs in the environment after natural weathering of soils and rocks, while smaller amounts are released from industrial plants or during pesticide usage

(Periodic Table, 2017). If animals absorb larger amounts of boron through drinking water or food over a longer period of time, male reproductive organs can be affected. Also, higher levels of boron have negative impact on pregnant animals and their offspring (Periodic Table, 2017). Humans can accumulate higher levels of boron in their bodies when consuming fruits, vegetables, or water containing boron (Public Health Statement, 2017). High levels of boron over shorter periods of time may affect stomach, intestines, liver, kidney, and brain, and can even cause death (Public Health Statement, 2017).

Barium can be found in higher concentrations in the environment due to extensive use in industry (Periodic Table, 2017). Barium often forms poisoning compounds with nonmetals, oxidizes in the air, and reacts intensively with water to form hydroxides. When aquatic organisms absorb the barium compounds, barium accumulates in their bodies (Periodic Table, 2017). Barium compounds that dissolve in water can also be harmful to human health (Public Health Statement, 2017). Smaller amounts of water-soluble barium can cause breathing difficulties, increased blood pressure, changes in hearth rhythm and nerve reflexes, kidney and hearth damage, while higher amounts may cause paralyses and in some cases even death (Public Health Statement, 2017).

Copper occurs naturally in water, soil, rocks and, in small amounts, air (Periodic Table, 2017). It can also occur in plants and animals and is an essential element for humans. Due to their properties, copper and copper compounds are intensively used in industry and agriculture and its production still rises. This means that amount of copper released in environment also rises. When it enters the

environment, it attaches to organic matters and minerals. It does not spread easily, but once it enters surface waters, it can travel long distances. Higher levels of copper in the soil have negative impact on plants and farmland production and also on animals that consume these plants (Periodic Table, 2017). Humans are exposed to copper through breathing, drinking water, eating food, or by skin contact with soil, water and other copper-containing substances (Public Health Statement, 2017). Higher levels of copper are toxic and can cause headache, nausea, diarrhea and irritation of nose, mouth and eyes. Excessive amounts of cooper can cause brain, liver and kidney damage, and even death (Public Health Statement, 2017).

Manganese naturally occurs in soil, water, air and food (Periodic Table, 2017). Additionally, it can be found in water, air, and soil after release from the manufacture and due to disposal of manganese-based products. Even though manganese is an essential element for all species, higher concentrations can be toxic and can cause lung, liver and vascular changes, lower blood pressure, and brain damage (Public Health Statement, 2017). High levels of manganese in humans can cause symptoms of dullness, weak muscles, headaches, and insomnia. Long-term exposure to manganese can affect central nervous system and cause permanent disability, Parkinson, lung embolism, and bronchitis (Public Health Statement, 2017).

Nickel can combine in nature with other metals (e.g., iron, copper, chromium, and zinc) to form compounds (Periodic Table, 2017). Nickel compounds are typically released into the environment during industrial production or by power plants. They enter the air and then settle down during the rain. Nickel is also released to surface waters as a part of wastewater streams. High concentrations of nickel in surface water

can decrease the rate of algae growth. It is also known that high concentrations of nickel can cause various types of cancer in different parts within a body of some animals (Periodic Table, 2017). Humans may be exposed to nickel by breathing air, drinking water, eating food, smoking cigarettes or by skin contact with nickel-contaminated soil or water (Public Health Statement, 2017). While in small quantities nickel is essential for human health, excessive amounts of nickel, on the other hand, can have a serious impact on human health. It can cause chronic bronchitis and reduced lung function (Public Health Statement, 2017).

Zinc is present in all foods (Periodic Table, 2017) and is often combined with elements such as chlorine, oxygen, and sulfur to form zinc compounds, which are widely used in industry (Public Health Statement, 2017). Zinc enters the environment during the natural processes and human actions such as burning of wastes. Waste streams from chemical industry, domestic waste water, and run-off from soil containing zinc enter waterways. Through contaminated water in rivers, zinc can enter a body of aquatic organisms. Higher concentrations of zinc are also found in soil and farmland. Animals that consume these plants become contaminated. Zinc has negative impact on microorganisms and earthworm, too (Periodic Table, 2017). Humans can be exposed to zinc while they are breathing air, drinking water, and through food (Public Health Statement, 2017). Higher concentrations of zinc in human body can cause a short-term disease called metal fume fever, stomach cramps, nausea, and vomiting. Taking too much zinc for longer periods of time can cause anemia, damage of kidney and pancreas, and decreased levels of high-density lipoprotein (Public Health Statement, 2017).

3.3.4 Modeling of Contaminant Transport in Surface Waters

The implementation of reclaimed asphalt pavement (RAP) in highway shoulder backups raises concerns about the contamination of surface waters like rivers and streams. In general, computer models developed to assess the flow of groundwater through multiple soil deposits do not account for surface water runoff, but rather assume that the entire amount of precipitates infiltrates through the soil vadose zone.

In order to simulate contaminant transport in surface waters, analytical solutions of the advective-dispersive equation (ADE) and related models are necessary. The ADE takes into consideration advective transport and dispersive/diffusive transport. Van Genuchten (2013) developed a one-dimensional solution to the ADE, which was utilized to develop UMDSurf, a numerical model that forecasts the distribution of metal concentrations in surface waters as a function of distance away from the edge of the RAP-amended highway shoulder backup (Figure 3.3).

The solute flux for one-dimensional transport, J_s, is expressed as follows,

$$J_S = uC - D_X \frac{\partial C}{\partial x} \tag{3.1}$$

where u is the longitudinal fluid flow velocity, C is the solute concentration given in mass per unit volume of water, D_x is the longitudinal dispersion coefficient that accounts for the combined effects of ionic or molecular diffusion and hydrodynamic dispersion, and x is the longitudinal coordinate.

Next, the mass balance equation is formulated based on the accumulation of solute in a control volume over time caused by the divergence of flux (i.e., net inflow or outflow),

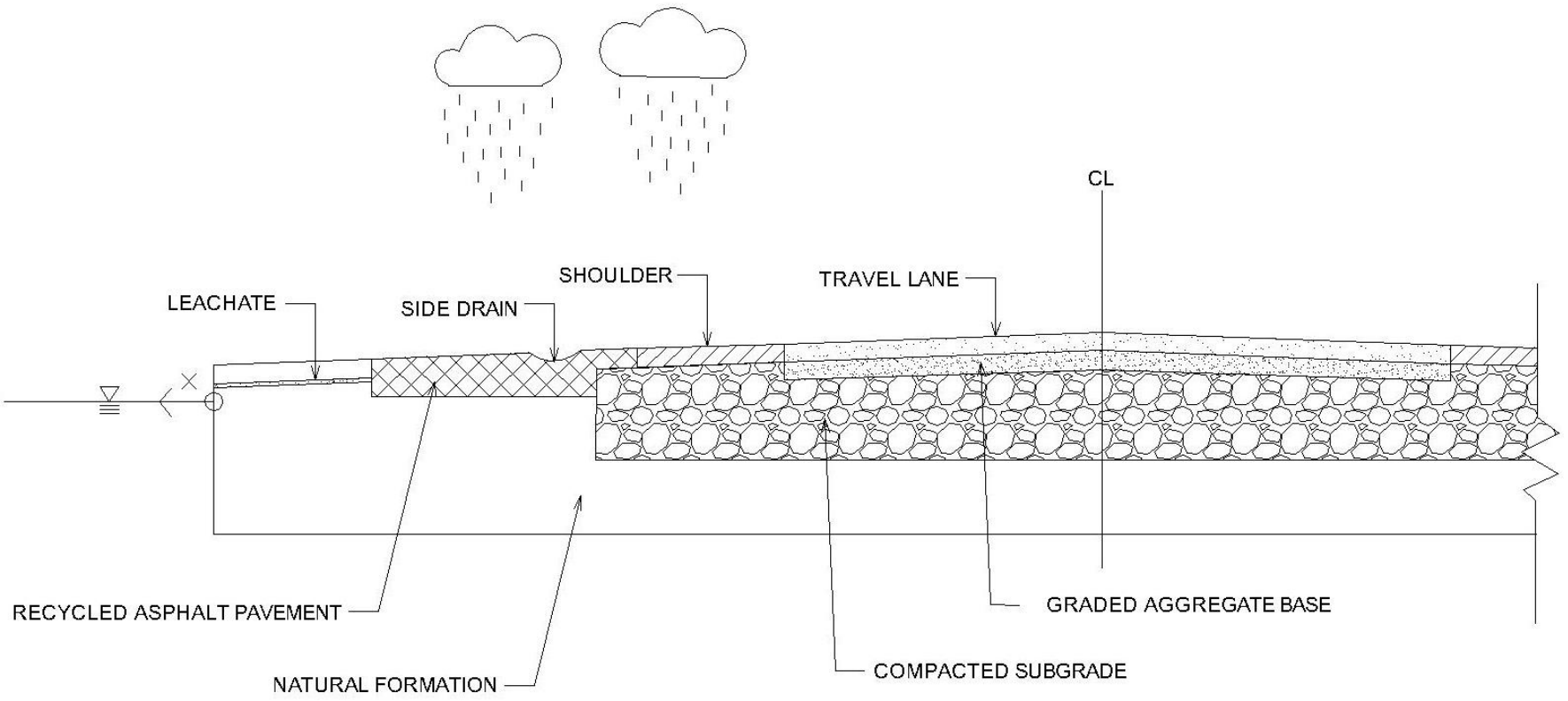

Figure 3.3. Conceptual model used to analyze the flow of recycled asphalt pavement leachate into surface waters.

$$\frac{\partial C}{\partial t} = -\nabla x J_S - R_S + R_w C_e \tag{3.2}$$

where t and R_s represent time and arbitrary sources or sinks of solute, respectively. $R_s<0$ stands for the consumption of solute, while $R_s>0$ means the feeding of solute. The last term in the equation denotes the injection (>0) or pumping (<0) of water with constituent concentration C_e at a rate R_w. A typical ADE equation, however, excludes the last two terms and is written as

$$\frac{\partial C}{\partial t} = D_x \frac{\partial^2 C}{\partial x^2} - \frac{\partial C}{\partial x} \tag{3.3}$$

In this study, a numerical one-dimensional solution of ADE with a third-type inlet (ω = 1) and the boundary conditions provided below was used.

$$C(x, 0) = f(x) \tag{3.4}$$

$$\left(uC - \omega D_x \frac{\partial C}{\partial x}\right)_{x=0^+} = ug(t) \tag{3.5}$$

$$\frac{\partial C}{\partial x}(\infty, t) = 0 \text{ or } \frac{\partial C}{\partial x}(L, t) = 0 \tag{3.6}$$

A semi-infinite domain with the uniform initial concentration, $f(x) = C_i$, and no production/decay were assumed to exist. The inlet concentration function of the pulse type, g(t), with the constant concentration C_0 is formulated as

$$g(t) = \begin{cases} C_0, & 0 < t \leq 0 \\ 0, & t \geq t_0 \end{cases} \tag{3.7}$$

Finally, the solution to Equation 3.3 is then given as

$$C(x, t) = \begin{cases} C_i + (C_0 - C_i)A(x, t), & 0 < t \leq t_0 \\ C_i + (C_0 - C_i)A(x, t) - C_0 A(x, t - t_0), & t \geq t_0 \end{cases} \tag{3.8}$$

where

$$A(x,t) = \frac{1}{2}\mathrm{erfc}\left[\frac{x-ut}{\sqrt{4D_x t}}\right] + \sqrt{\frac{tu^{\,2}}{\pi D_x}}\exp\left[-\frac{(x-tu)^2}{4D_x t}\right] - \frac{1}{2}\left(1+\frac{ux}{D_x}+\frac{tu^2}{D_x}\right)\exp\left(\frac{ux}{D_x}\right)\mathrm{erfc}\left[\frac{x+tu}{\sqrt{4D_x t}}\right] \quad (3.9)$$

Surface runoff and evaporation from the pavement surface, the shoulders, and the surrounding ground were not considered in the model. Infiltration of runoff along the edges of the pavement structure was ignored. The retardation factors for each metal were obtained by fitting van Genuchten (1981) analytical leaching model to the metal concentrations in the effluent of the Br-tracer column leaching tests (Dayioglu, 2016) and were incorporated into the model to simulate the retardation of the solute in natural soils (minimum of 0.6-m thick and 20-m long) located between the RAP and the surface waters. Two different natural formations were assumed to exist:

1) CL – similar to an embankment soil commonly used by SHA with the pH of 5.9 and retardation factors of 7 for Al, Cu, Ni, and Zn;
2) CL-ML – similar to a typical subgrade soil encountered in Maryland with the pH of 6.3 and retardation factors of 50, 44, 7, and 16 for Al, Cu, Ni, and Zn, respectively.

3.4 RESULTS

3.4.1 Batch Water Leach Test

Batch water leach tests (WLTs) with a liquid-to-solid ratio of 20: 1 (by mass) and 0.02M NaCl as the eluent were performed on seven recycled asphalt pavement (RAP) materials and control materials, i.e., graded aggregate base (GAB) and two topsoils (Topsoil 1 and Topsoil 2). Water soluble concentrations of inorganic elements (Al,

As, B, Ba, Cd, Co, Cr, Cu, Fe, Mn, Na, Ni, Pb, V, and Zn) in these materials, as analyzed by the inductively coupled plasma optical emission spectroscopy (ICP-OES) technique, are given in Table 3.2. The table also contains the U.S. EPA water quality limits for protection of aquatic life and human health in fresh water (WQL) and Maryland State aquatic toxicity limits for fresh water (MD ATL). As a note, RAPs 1 through 4 have different minimum detection limits (MDLs) for metals such as Ba, Cd, Cr, and Pb than RAPs 5 through 7, GAB, Topsoil 1, and Topsoil 2 because the two batches were not tested at the same time with the same standard solutions.

Of the aforementioned elements, B, Cd, Co, Cr, Mn, Ni, Pb, and V concentrations in the RAP filtrates are below the MDLs, as determined in accordance with the US Code of Federal Regulations Title 40. On the other hand, Al, As, Ba, Cu, Fe, Na, and Zn are detectable in the RAP leachates. Only aqueous concentrations of Cu from RAP1 and RAP2 exceed the EPA WQL; however, they are still well below the EPA maximum contaminant level for drinking water (MCL) of 1300 μg/L. Aquatic organisms and ecosystems are much more sensitive to the toxic effects of Cu than humans, thus resulting in the strikingly lower WQL as compared to the MCL. Cu is considered to be lethal to fish; for instance, toxic levels of Cu in fish disrupt the salt balance between the body of a fish and the surrounding water essential for the normal functioning of the cardiovascular and nervous systems and negatively affect the sense of smell in fish crucial for finding food and avoiding predators (Solomon, 2009). By comparison, elevated Cu concentrations in humans cause Cu to be bound to the low-molecular weight protein metallothionein, which render it water soluble and is excreted by kidneys (Solomon, 2009). Overall, the results are consistent with the

Table 3.2. Aqueous metal concentrations in WLTs.

Material	pH	Al (µg/L)	As (µg/L)	B (µg/L)	Ba (µg/L)	Cd (µg/L)	Co (µg/L)	Cr (µg/L)	Cu (µg/L)	Fe (µg/L)	Mn (µg/L)	Na (mg/L)	Ni (µg/L)	Pb (µg/L)	V (µg/L)	Zn (µg/L)
RAP1	8.30	272	<50	<5	<5	<2	<5	<25	**28.4**	10.2	<5	284	<5	<25	<5	6.95
RAP2	9.15	163	<50	<5	<5	<2	<5	<25	**19.2**	<5	<5	260	<5	<25	<5	<5
RAP3	9.31	154	<50	<5	<5	<2	<5	<25	11.5	<5	<5	267	<5	<25	<5	8.90
RAP4	9.24	236	<50	<5	<5	<2	<5	<25	11.3	<5	<5	267	<5	<25	<5	5.45
RAP5	9.20	<5	39.5	<5	12.4	<5	<5	<5	<5	<5	<5	477	<5	<5	<5	<5
RAP6	9.19	232	8.90	<5	13.0	<5	<5	<5	<5	<5	<5	472	<5	<5	<5	<5
RAP7	9.34	<5	31.7	<5	29.3	<5	<5	<5	<5	<5	<5	472	<5	<5	<5	<5
GAB	9.47	<5	33.8	<5	27.9	<5	<5	<5	<5	<5	<5	454	<5	<5	<5	<5
Topsoil 1	6.21	<5	17.1	<5	90.3	<5	<5	<5	<5	41.5	262	433	404	<5	<5	<5
Topsoil 2	7.67	<5	19.3	<5	126	<5	<5	<5	<5	<5	9.30	431	<5	<5	<5	<5
US EPA WQL		750	340	NA	NA	2	NA	570	13	NA	NA	NA	470	65	NA	120
MD ATL		50	10	5	10	2	3	1	5	NA	1	NA	10	5	10	120

Notes: WQL= water quality limit for protection of aquatic life and human health in fresh water; MD ATL= Maryland State aquatic toxicity limits for fresh water; NA= not available.

findings obtained by previous researchers in that no large quantities of EPA-regulated inorganic chemicals are found in the batch leachates from RAP (Brantley and Townsend, 1999; Kang et al., 2011; Shedivy et al., 2012).

By comparison, RAP1 has a higher concentration of Cu (28.4 μg/L) than RAP2 (19.2 μg/L), which may be attributed to a higher concentration of Cu based on the total elemental analyses (Table 3.1) and a lower bitumen content for RAP1 (3.77% versus 4.87%). Bitumen may prevent aggregate particles from coming into contact with the solution (Shedivy et al., 2012) therefore reduce the potential metal leaching.

The pH is reported as one of the controlling factors in the release of metals from geomaterials (Bin-Shafique et al., 2002; Edil et al., 2010; Dayioglu, 2016). Leaching of metals may follow different patterns such as amphoteric – concentrations increase at acidic and alkaline pH, cationic – concentrations decrease monotonically as pH increases, highly soluble, and oxyanionic (Kosson et al., 2002). However, neither of these leaching patterns is observed for any of the metals in the RAP leachates as their pH values do not differ significantly, i.e., they are in a narrow, alkaline range between 8.30 and 9.40. Similar pH values for batch leach tests conducted on RAP were found by Kang et al. (2011) and Shedivy et al. (2012).

Even though Gambrell et al. (1991) and McLaughlin and Tiller (1994) stated that salts can affect the release and solubilization of heavy metals into the solution, there is no obvious effect of Na on the metal leaching behavior. The overall variations in aqueous concentrations of analyzed metals for RAP do not follow a recognizably consistent pattern, which may be partially related to differences in their

concentrations based on the total elemental analyses (Table 3.1) and a complex interaction of metal dissolution/adsorption controlling mechanisms that was not examined in this study.

Furthermore, all metal concentrations leached from the control materials are either non-detectable or below the EPA WQLs. GAB effluent has a pH of 9.47, which is comparable to that of RAP. By contrast, Topsoil 1 and Topsoil 2 leachates have lower pH values than the RAP leachates (pH 6.21 and 7.67, respectively, versus pH 8.30-9.31, Table 3.2).

It is also worth mentioning that the elevated concentrations of Cu in the WLT leachates for two RAP materials do not necessarily indicate that RAP will release significant amounts of these metals into the environment as WLT does not fully simulate the flow conditions likely to exist in the field. A more realistic quantitative analysis of the leaching of contaminants in the environment is expected from the column leach tests (CLTs).

3.4.2 Column Leach Test

The column leach tests (CLTs) were conducted on seven recycled asphalt pavement (RAP) materials, graded aggregate base (GAB), Stone No. 57, Topsoil 1, and Topsoil 2, with the latter four serving as control materials. Figure 3.4 shows temporal characteristics of effluent pH for these materials. Leachates from RAP are neutral to moderately alkaline, which is within the regulatory limits set by the EPA. Of all RAP materials, RAP 1 has the lowest pH of 6.69, while RAP2 has the highest pH of 8.50. As a reference, pH of solution leached from both Stone No. 57 and Topsoil 1 does not conform to the EPA regulations. Topsoil 1 leachate reaches neutral pH values and

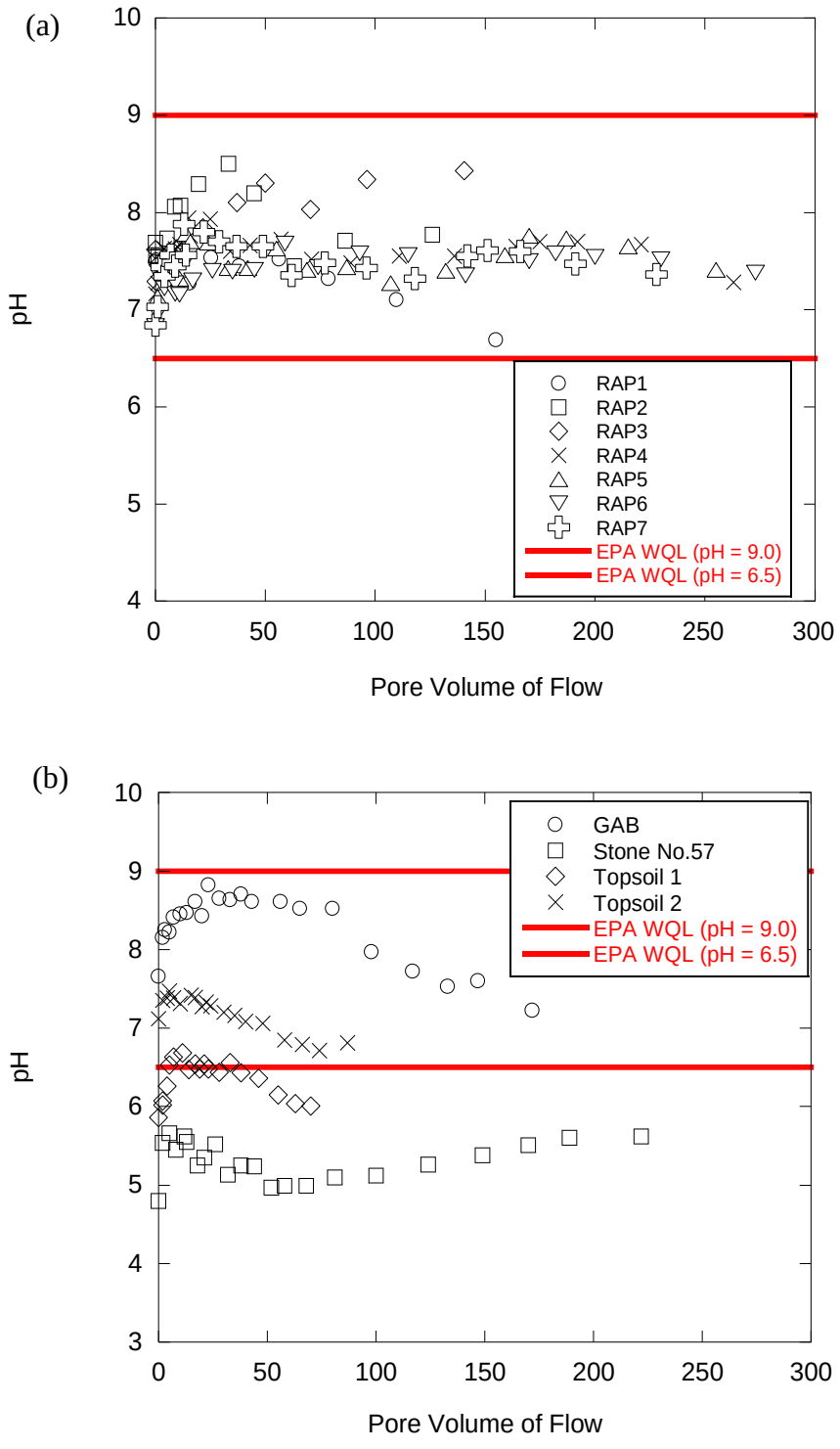

Figure 3.4. Effluent pH as a function of pore volumes of flow for a) RAP and b) control materials.

retains them for approximately 28 pore volumes of flow after which the pH drops to the levels of slight acidity; however, Stone No. 57 leachate endures only the acidic state until the test is terminated.

The elution curves for Ca given in Figure 3.5 usually indicate a change in pH (Dayioglu, 2016). The abundance of dissolved Ca is expected in alkaline effluent solutions. This correlation is not noticeable for RAP, but rather for Stone No. 57. Stone No. 57 has very negligible amounts of dissolved Ca, most likely due to a very low content of Ca as determined by the total elemental analyses. Its pH is, therefore, very low and varies between 4.80 and 5.66. On the contrary, Topsoil 2 has the greatest quantities of leached Ca, but does not have the highest pH. This indicates a good buffering capacity of Topsoil 2, which may be a result of colloidal material such as organic matter and clay that enable the cation exchange capacity (Sparks, 2003; Brady and Weil, 2010).

In addition to peak effluent pH values, Table 3.3 summarizes peak aqueous metal concentrations for RAP. Concentrations of As, Cd, Cr, Pb, and V are below the minimum detection limits (MDLs) for all RAP materials. Effluent concentration of Co is detected only for RAP1, but it falls below the MDL at 0.5 pore volumes of flow (PVFs). Similarly, Fe is detected in leachate of RAP5 initially, but the concentrations drop below the MDL after 24 PVF. Fe is also found in RAP1 leachate, however, its concentration fluctuates throughout the test.

Figures 3.6 through 3.12 illustrate a series of CLT elution curves for Al, B, Ba, Cu, Mn, Ni, and Zn. Leaching of B, Cu, Mn, Ni, and Zn for all RAP materials exhibits a first-flush pattern followed by stabilized concentrations. Peak

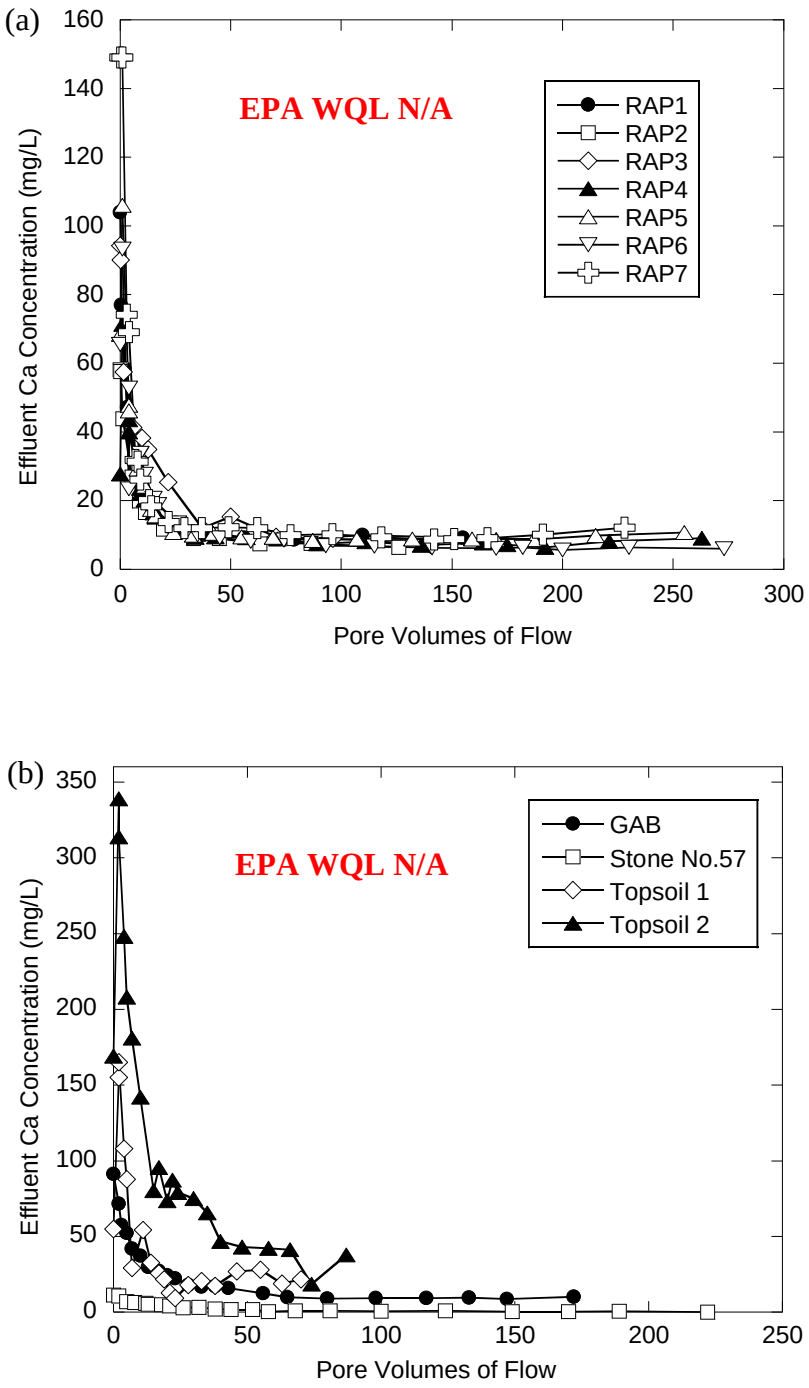

Figure 3.5. CLT elution curves for Ca pertaining to a) RAP and b) control materials.

Table 3.3. Peak effluent pH and metal concentrations in CLTs.

Material	pH	Al (µg/L)	As (µg/L)	B (µg/L)	Ba (µg/L)	Cd (µg/L)	Co (µg/L)	Cr (µg/L)	Cu (µg/L)	Fe (µg/L)	Mn (µg/L)	Na (mg/L)	Ni (µg/L)	Pb (µg/L)	V (µg/L)	Zn (µg/L)
RAP1	7.53	231	<25	608	172	<2	47.0	<5	11.8	224	426	790	61.9	<25	<5	**213**
RAP2	8.50	286	<25	31.6	14.2	<2	<5	<5	<5	<25	<5	385	<5	<25	<5	23.0
RAP3	8.43	320	<25	213	182	<2	<5	<5	<5	<25	32.6	352	<5	<25	<5	70.3
RAP4	7.94	<25	<25	151	40.2	<2	<5	<25	**16.1**	<25	93.6	483	21.2	<25	<5	53.7
RAP5	7.78	<25	<25	143	77.2	<2	<5	<25	<5	39.0	338	455	84.4	<25	<5	62.6
RAP6	7.68	<25	<25	111	80.9	<2	<5	<25	11.3	<25	328	453	108	<25	<5	74.2
RAP7	7.88	<25	<25	106	88.1	<2	<5	<25	6.84	<25	23	47	<5	<25	<5	65.6
GAB	8.82	<5	**348**	168	59.5	<5	<5	<25	<5	135	17.6	433	162	<5	<5	**470**
Stone No.57	5.66	<5	21.4	33.5	363	<5	21.0	162	**67.2**	21	70.2	451	22.9	<5	<5	**887**
Topsoil 1	6.68	<5	73.4	95.3	265	<5	<5	<5	<5	14,200	3,590	338	<5	<5	<5	116
Topsoil 2	7.47	<5	83.4	87.4	197	<5	<5	<5	<5	1,530	492	508	<5	<5	<5	41.9
US EPA WQL		750	340	NA	NA	2	NA	570	13	NA	NA	NA	470	65	NA	120
MD ATL		50	10	5	10	2	3	1	5	NA	1	NA	10	5	10	120

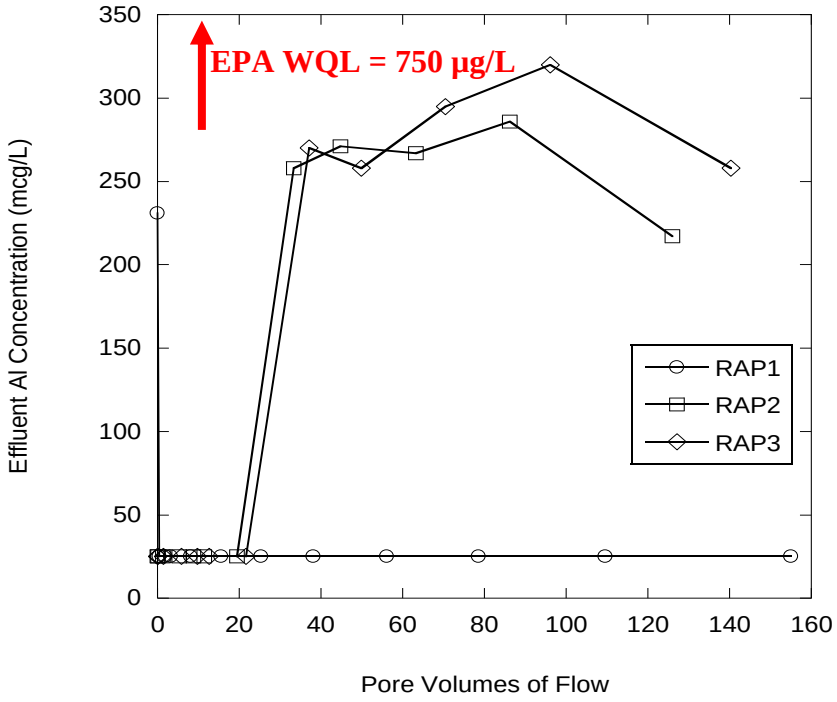

Figure 3.6. CLT elution curve for Al pertaining to RAP.

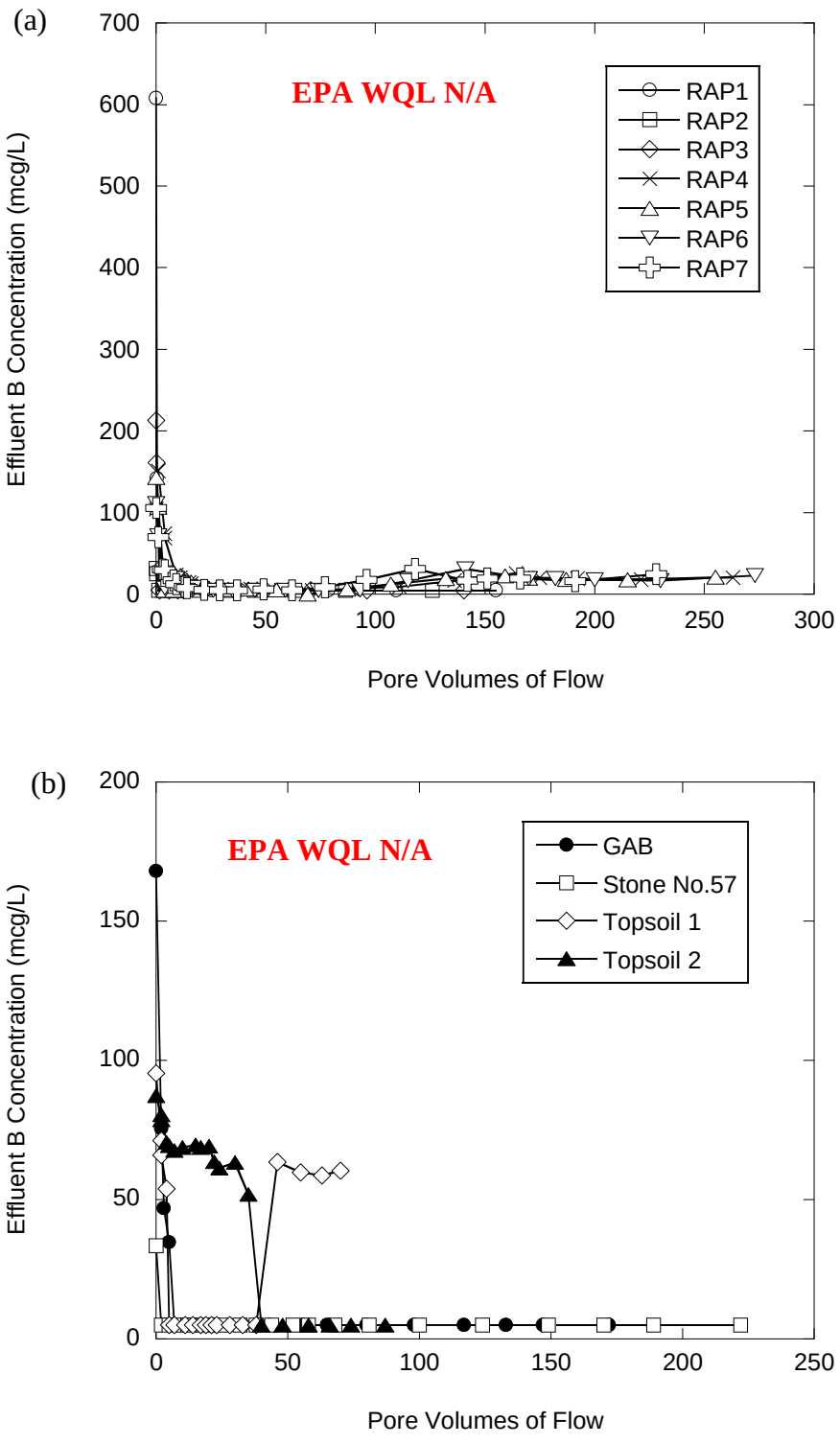

Figure 3.7. CLT elution curve for B pertaining to a) RAP and b) control materials.

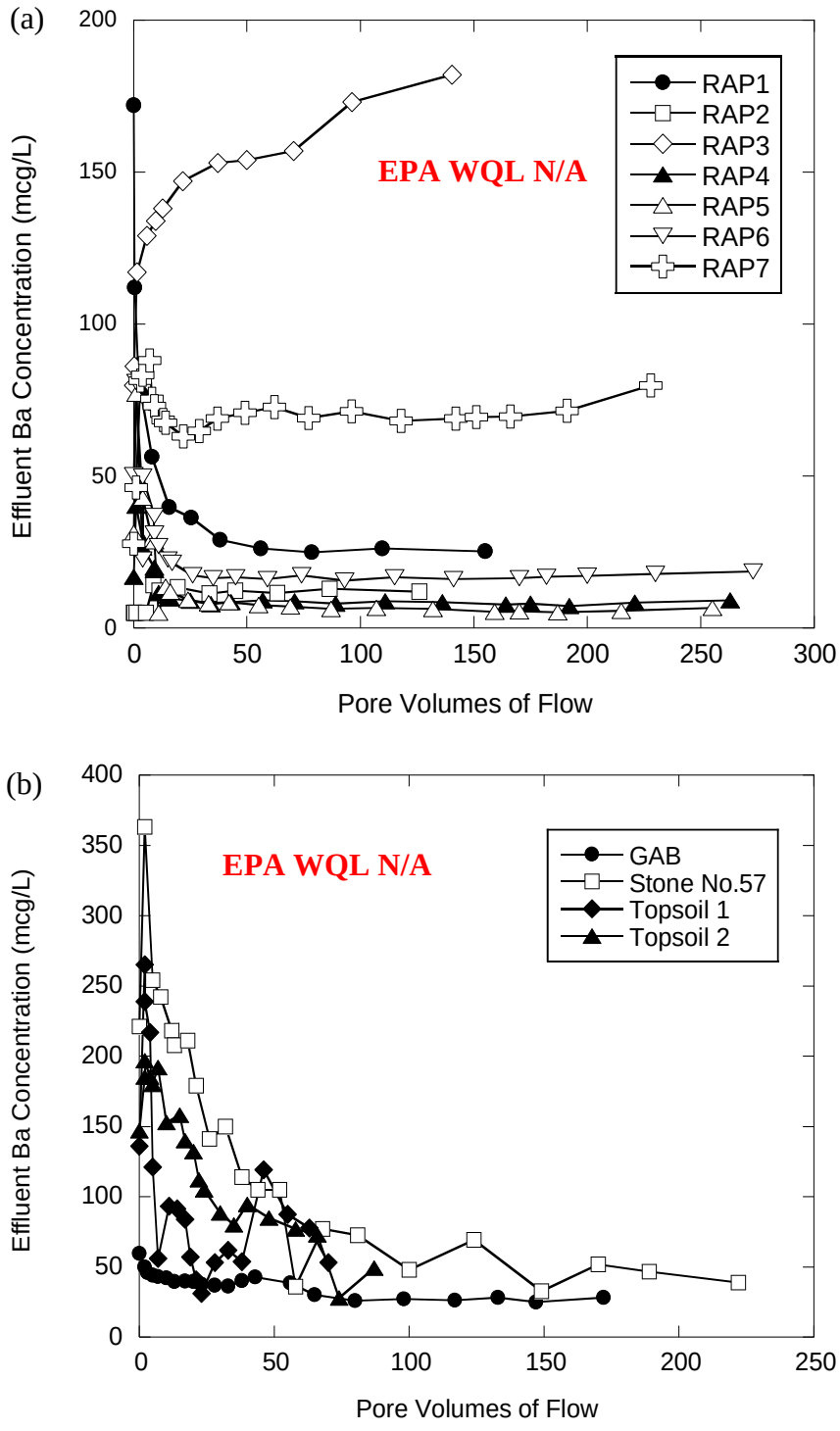

Figure 3.8. CLT elution curves for Ba pertaining to a) RAP and b) control materials.

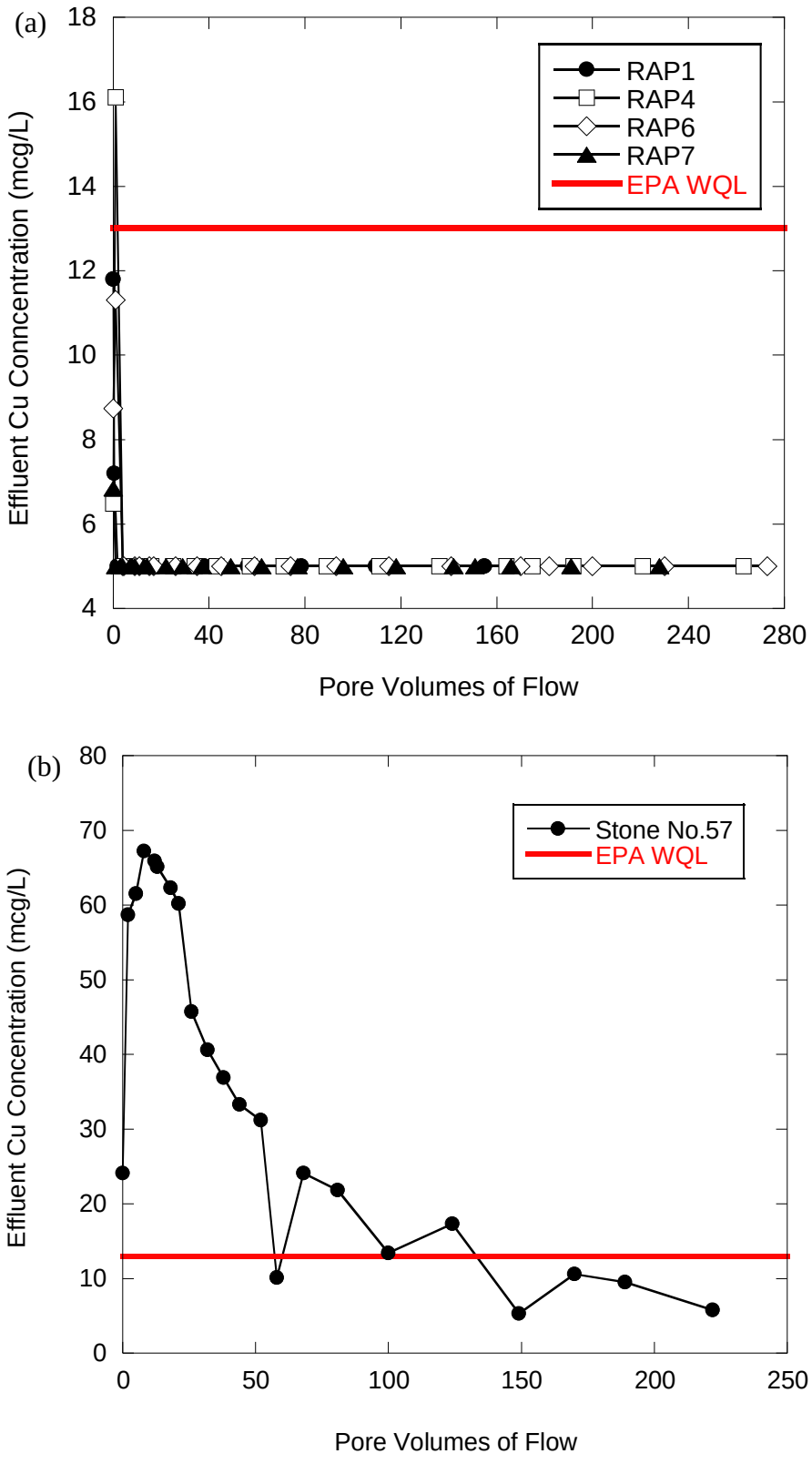

Figure 3.9. CLT elution curves for Cu pertaining to a) RAP and b) control materials.

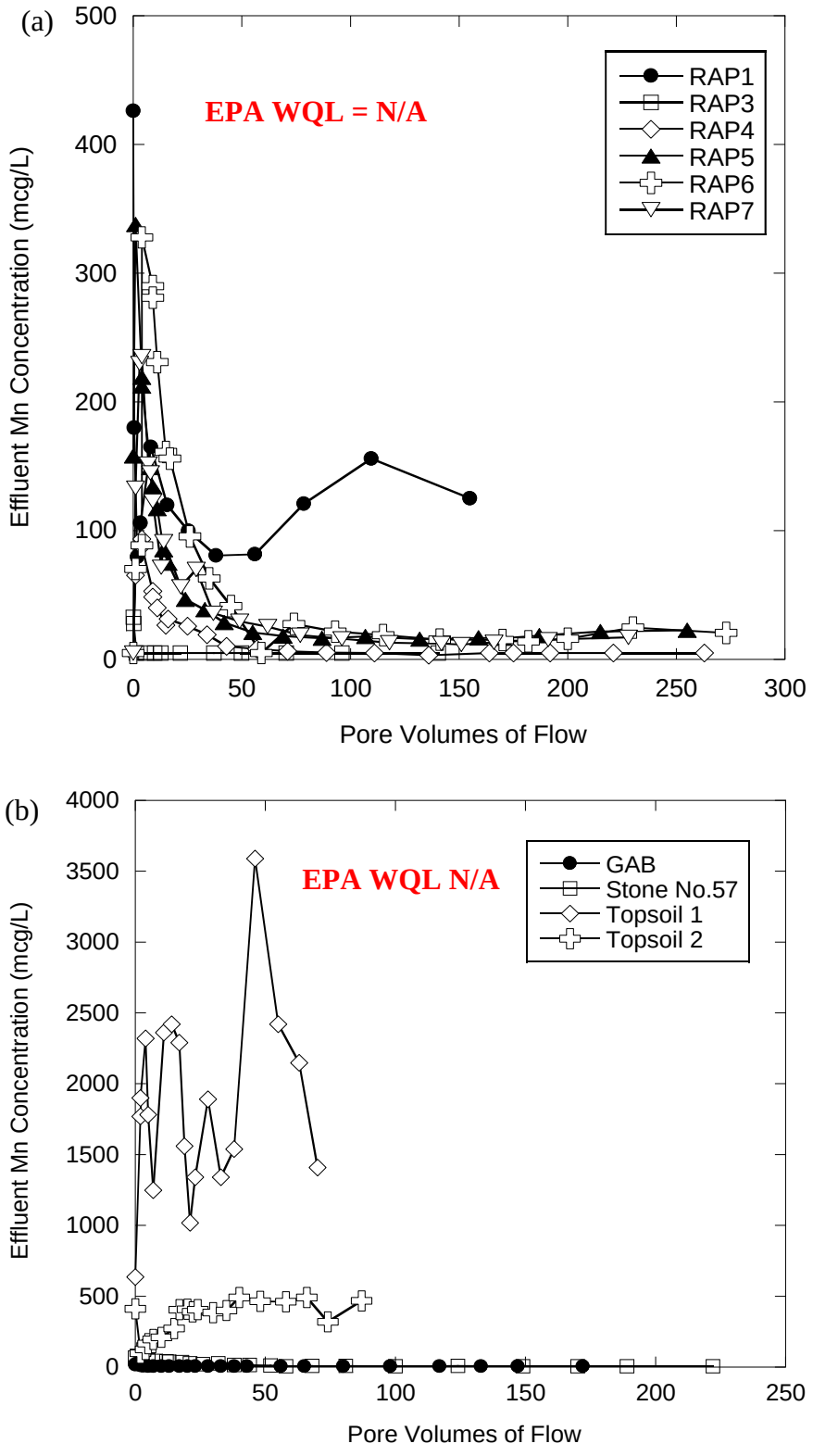

Figure 3.10. CLT elution curves for Mn pertaining to a) RAP and b) control materials.

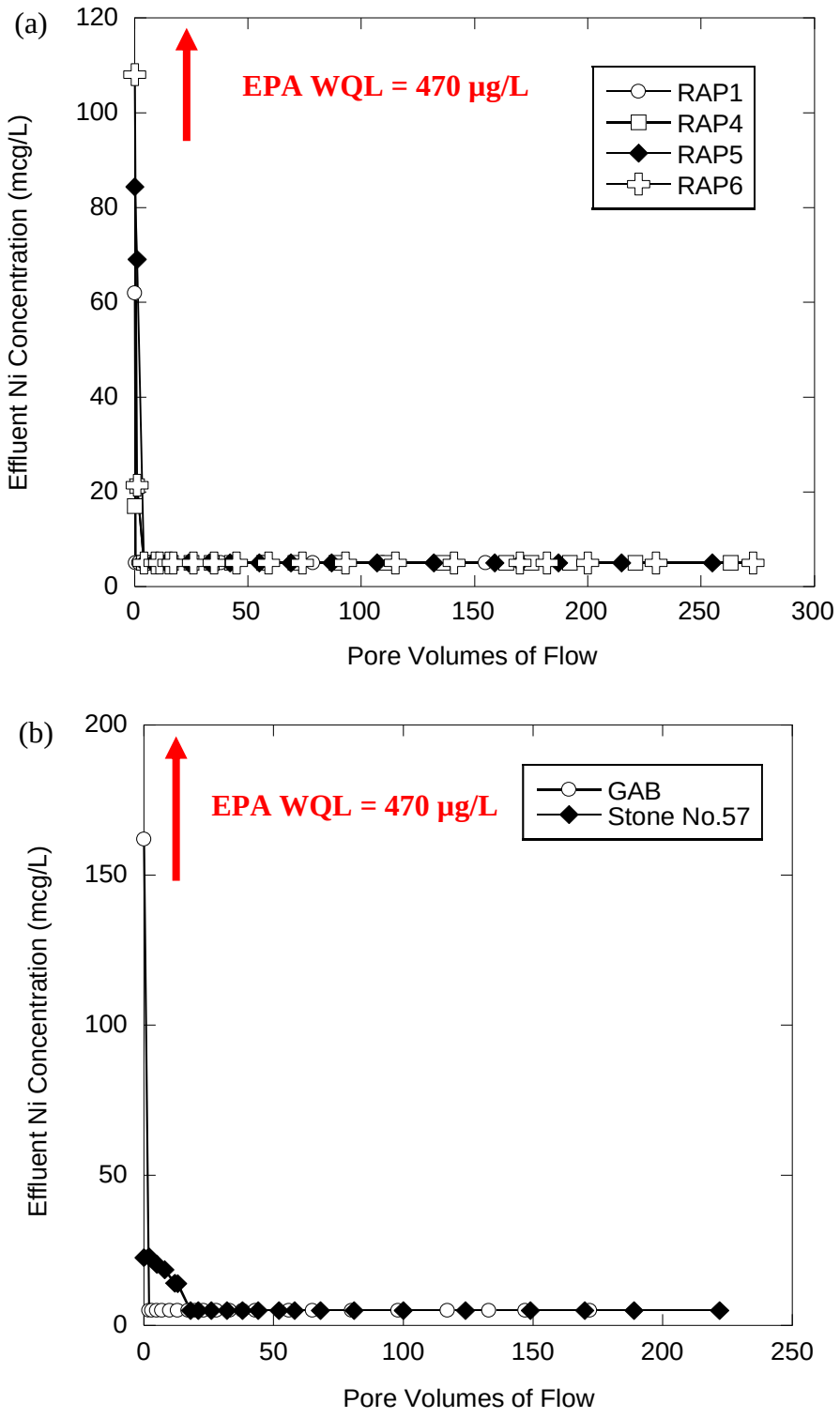

Figure 3.11. CLT elution curves for Ni pertaining to a) RAP and b) control materials.

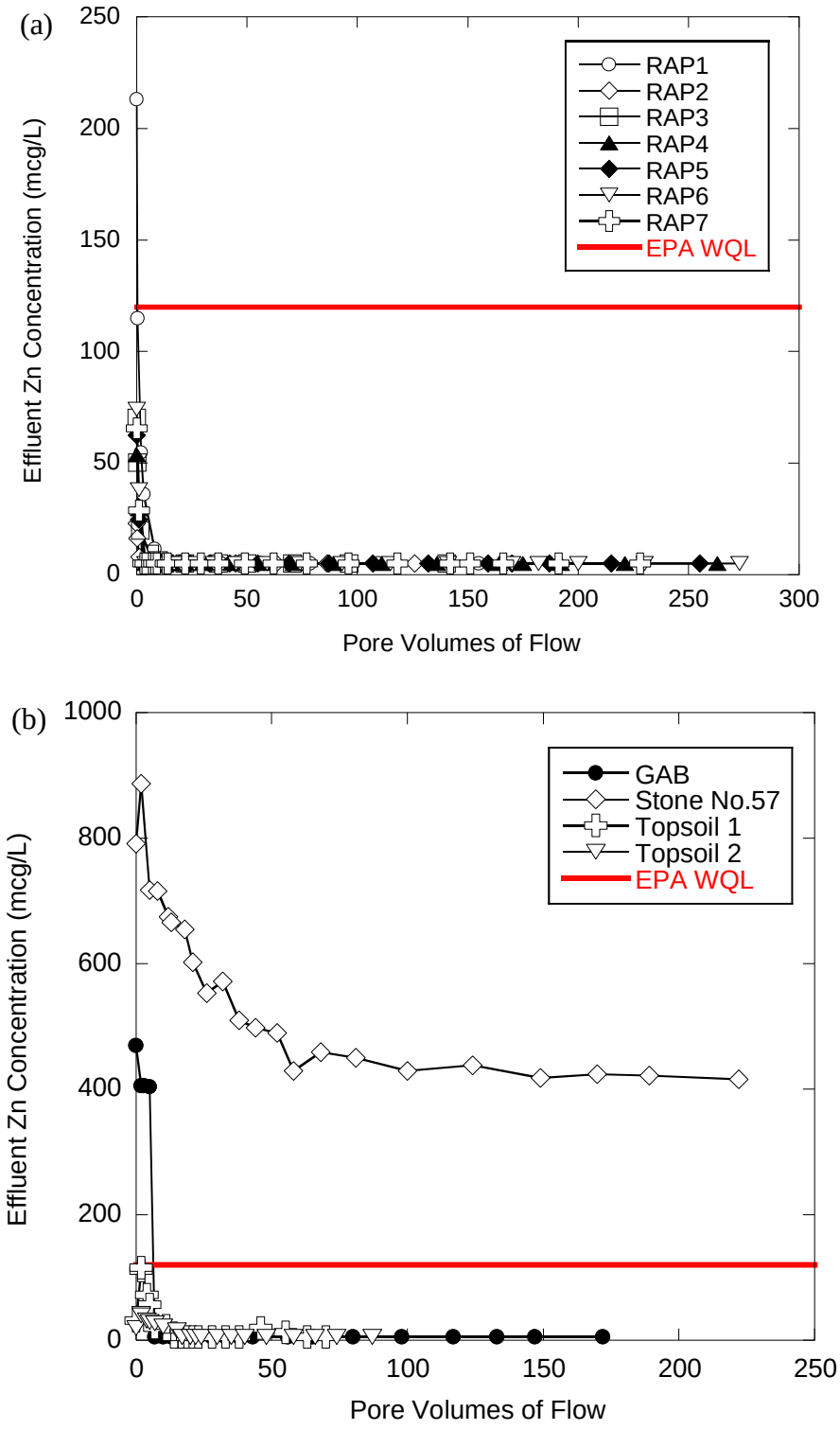

Figure 3.12. CLT elution curves for Zn pertaining to a) RAP and b) control materials.

concentrations occur mainly during the first pore volume of flow. The exception to this trend is Mn in leachates of four RAPs (RAP4, RAP5, RAP6, and RAP7) that has a slightly delayed response – the concentrations spike at four pore volumes of flow. The first-flush elution pattern occurs due to release of metals from the water-soluble fraction and sites with low adsorption energies (Bin-Shafique et al., 2002; Morar et al., 2012). Most of the metals are washed out from the surface of RAP particles into the aqueous solution until the concentration difference between the metal source and the aqueous solution is reduced (Ogunro and Inyang, 2003). Moreover, RAP is dominated by sand-sized and gravel-sized particles that do not have a large reactive surface area and colloid-like behavior thus have a limited cation exchange capacity (Sparks, 2010; Brady and Weil, 2010), which leads to high initial effluent concentrations of metals (Bin-Shafique et al., 2006). The first-flush leaching for several metals in RAP leachates was recognized by other researchers as well (Brantley and Townsend, 1999; Legret et al., 2005; Kang et al., 2011).

Of the metals analyzed, only aqueous Cu and Zn concentrations for RAP4 and RAP1, respectively, exceed the EPA WQLs. RAP4 has the maximum Cu concentration of 16.1 μg/L during the first PVF, but it falls below 5 μg/L at 2 PVF, which is significantly under the regulatory limit of 13 μg/L. The peak concentration of Zn leached from RAP1 is nearly two times higher than the water quality limit (213 μg/L versus 120 μg/L, Table 3.3). However, this concentration is reduced to ~EPA WQL (115 μg/L) at 0.5 PVF and continues decreasing with an increase in the PVF. At 16 PVF, leached Zn concentration is below the MDL. Similar findings were

reported by Legret et al. (2005) for Cu and Zn leaching from RAP during column leach experiments.

Amphoteric leaching behavior of Cu and Zn, where concentrations increase at extreme acidic and extreme alkaline conditions, was recognized by other researchers who conducted studies on different geomaterials (Edil et al., 2010; Lim et al., 2004). Zn is the least mobile for pH values between 9 and 10 (Stumm and Morgan, 1996; Lim et al., 2004). In other words, as pH approaches this range, the abundance of leached Zn decreases, which is generally confirmed for RAP in this study. On average, RAP1 has the lowest effluent pH (7.34) while RAP2 has the highest pH (8.50). Subsequently, RAP1 leaches the greatest quantity of Zn, whereas RAP2 leaches the lowest quantity of Zn (213 μg/L versus 23 μg/L). Many researchers recognized dissolution and/or desorption of Zn as favorable at lower pH (Edil et al., 1992; Kirby and Rimstidt, 1994; Fleming et al., 1996; Sauer et al., 2005; Edil et al., 2010).

As for Cu, its solubility is expected to decrease significantly with increasing pH (Ricou et al., 1999; Yan et al., 2001; Goswami and Mahanta, 2007; Liu et al., 2008). However, no relationship is observed when peak CLT Cu concentrations are plotted against effluent pH (data not shown here). Possible explanations may be a minimal change in the pH that may not accurately represent the effect of pH on leaching behavior of Cu and a dynamic flow in CLTs that could inhibit the amphoteric pattern that would likely be evident for a wider pH range (Cetin et al., 2012).

Leaching of Al for RAP2 and RAP3 above the MDL occurs at ~35 PVF when pH increases from 8.29 to 8.50 and from 7.84 to 8.10, respectively, a lagged-response leaching pattern. It is speculated that the elevated aqueous Al concentration is triggered by the increase in pH (data not shown here) thus alluding to an amphoteric leaching pattern of Al (Langmuir, 1997; Kenkel, 2003). A comparable type of the elution curve for Al was observed by Edil et al. (2010), who conducted column leach tests on different roadway materials. On the other hand, Al leaching from RAP1 follows a first-flush pattern with the highest amount of Al being leached during the first PVF, which then sharply decreases with an increase in the pore volume of flow to below the MDL. This might be due to high water-soluble concentration of Al (Kang et al., 2011). RAP1 also contains a two times larger quantity of Al than RAP2 and RAP3, as determined by the total elemental analyses (12,138 mg/L versus 5660-5942 mg/L, Table 3.1), which could have contributed to the much higher initial effluent concentration of Al for RAP1 than for RAP2 and RAP3 (Dayioglu, 2016). Moreover, the stabilized effluent pH of RAP1 is neutral (pH ~ 6.90), which allows Al to remain insoluble and most likely in the form of aluminum hydroxide [$Al(OH)_3$] (Stumm and Morgan, 1996; Bin-Shafique et al., 2002; Gitari et al., 2009).

Early peak concentrations of Ba are detected for the effluents from all RAP materials except for RAP3. The release of Ba into the effluents from the remaining six RAPs peak at PVFs between 3 and 9. The concentration of RAP7 spiked at 3 PVF when the effluent pH is raised from 7.03 to 7.44 and reaches a peak at 8 PVF and pH of 7.56. From this point onward, Ba remains soluble at a steady level, but does not appear to be strongly affected by pH. This is comparable to the findings of Edil et al.

(2010), who reported leaching of Ba from roadway materials as "amphoteric-like, but less pH-dependent." By contrast, effluent Ba concentrations for RAP3 have a strong positive correlation with the effluent pH (data not show here). Even though the concentration of Ba herein is expected to decrease or at least reach a plateau due to the precipitation of barium carbonate ($BaCO_3$) and barium sulfate ($BaSO_4$) (Moffett et al., 2007; Edil et al., 2010), the mobility of Ba clearly increases with the increasing pH. In addition to low concentrations of leached Ca (Figure 3.5a) and high concentrations of leached Ba (Figure 3.8a), RAP3 is rich in Ca (Table 3.1), which altogether may indicate the presence of $CaCO_3$ precipitate that does not impede the availability of Ba (Moffett et al., 2007; Edil et al., 2010; Dayioglu, 2016; Cappuyns, 2017).

Leaching of B from all seven RAPs exhibits the first-flush leaching with peak concentrations within the first PVF (Figure 3.7a). Alike elution curves for B were observed by Bin-Shafique et al. (2002), Edil et al. (2010), and Cetin et al. (2012), who conducted column leaching experiments on different geomaterials. Similarly, early peak concentrations are evident for Ni (Figure 3.11a). The first-flush elution curves are noticed for four RAPs (RAP1, RAP4, RAP5, and RAP6), while no Ni is detectable throughout the test for the remaining three RAPs (RAP2, RAP3, and RAP7). These results agree with the previous column leaching studies conducted on roadway materials by Bin-Shafique et al. (2002) and Edil et al. (2010). The leaching amounts of Ni and B do not correlate with the chemical compositions of RAPs (Tables 3.1 and 3.3).

By comparison, the control materials do not leach Al, Cd, Pb, and V throughout the test. For example, although the effluent pH from Stone No. 57 is acidic thus favorable for dissolution of metals, Stone No. 57 does not release any Al into the solution likely due to the low content of Al itself (Table 3.1). For the topsoil leachates, the pH remains between 6.5 and 7, which is recognized as the insoluble range for Al (Stumm and Morgan, 1996; Sparks, 2003; Lim et al., 2004). Furthermore, the first-flush leaching pattern of all metals is evident for the reference materials. The exception is leaching of Mn from both topsoils, which appears to be highly soluble and generally independent of pH.

Unlike the leachates from RAP, the leachates from the reference materials have considerable contents of As. The concentrations of As for GAB effluent slightly exceed the EPA WQL (348 μg/L versus 340 μg/L). Alkaline pH such as that of GAB effluent (pH 8.82) favors high concentrations of As typically in a form of negatively charged oxyanionic As, whereas low pH such as that of Stone No. 57 (pH 5.66) is likely to contribute to lower adsorption affinity and increase protonation of oxyanionic As species (Dijkstra et al., 2002).

Stone No. 57 leaches high concentrations of Cu and Zn (67.2 μg/L and 887 μg/L, respectively), significantly above the EPA WQLs, which are also much higher than those leached by RAPs (Table 3.3). GAB also leaches much higher concentrations of Zn than RAP (470 μg/L versus 213mg/L, Table 3.3). Since both Cu and Zn are classified as amphoteric metals, their abundance is enhanced by acidic and alkaline conditions (Edil et al., 2010). As compared to the effluent pH range for RAP (6.69-8.50), Stone No.57 leachate is more acidic (4.80-5.66), while GAB leachate is

more basic (7.22-8.82). Such effluent pH values for Stone No. 57 and GAB would favor the release of Cu and Zn. Stone No. 57 also leaches Cr, which is not surprising considering its acidic effluent pH that enhances dissolution of Cr (Edil et al., 2010).

Finally, the influence of Na on the effluent pH and leaching of metals from RAP is not recognized (data not shown here). Na is a monovalent ion with a large hydrated radius and as such is easily washed out from a geomaterial (Brady and Weil, 2010). Also, the influent 0.02M NaCl readily dissociates and continually supplies the leachate with the same amount of Na. Moreover, there appears to be no effect of bitumen content on the leaching of metals. It is speculated that the type of parent rock and its adsorption capacity have a dominant role in the leaching potential of RAP (Lindgren, 1996).

3.4.3 Comparison of WLT and CLT results

The pH of RAP leachates obtained by WLTs is higher than that obtained by CLTs. WLTs yield the pH in the range of 8.30-9.34, while CLTs produce effluent pH in the range of 6.69-8.50. As a reference, lower effluent pH in CLTs than WLTs is observed for the control materials as well (pH 5.86-8.82 versus pH 6.21-9.47); however, the range does not include pH of Stone No.57 because WLTs were not performed on it.

In WLTs, the EPA WQL is exceeded for Cu leachates from two RAP materials only (RAP1 and RAP2, Table 3.2). In RAP leachates from CLTs, the peak concentration of Cu for RAP4 and the peak concentration of Zn for RAP1 are above the EPA WQLs (Table 3.3). In regard to the control materials, all aqueous concentrations from WLTs are below the EPA WQLs. However, the effluent

concentrations of As, Cu, and Zn for GAB and Stone No. 57 exceed the regulatory limits set by the EPA (Table 3.3).

In summary, WLT is a small-scale test used for a quick estimate of the metal leaching behavior and does not simulate the flow conditions likely to exist in the field (Cetin et al., 2012). CLT provides a more realistic quantitative analysis of the leaching of contaminants in the environment. WLT samples are agitated aggressively compared to the smooth fluid flow through the column set-up, which likely increases the surface contact between the leaching solution and the solid particulates and may result in higher leached metal amounts in the effluents (Cetin et al., 2012). The liquid-to-solid ratio in WLT is 20:1 and remains constant, while the liquid-to-solid ratio in CLT is 0.1:1 and varies with time. Moreover, WLT is finalized in 18 hours, whereas CLT is dynamic and data fluctuate for a longer period of time. Finally, WLT is limited by the short amount of time, which may not allow for the establishment of equilibrium between the liquid and solid phases (Cetin et al., 2012).

All of the above make the comparison between the WLT and CLT results of metal leaching somewhat challenging. Nonetheless, both tests provide an insight into the leaching potential of RAP. It may be concluded that Maryland RAPs do not release excessive amounts of toxic elements as determined through either test.

3.4.4 Modeling of Contaminant Transport in Surface Waters (UMDSurf)

UMDSurf was used to predict concentrations of Al, Cu, Ni, and Zn in surface water bodies at 20, 50, 100, 200, 500, and 1000 meters away from the point of entrance by the leachate from a RAP-amended highway shoulder backup (Figure 3.3). A maximum metal concentration obtained by the column leach test (CLT) was used as

the input concentration at t = 0 sec. The instantaneous injection (t = 10 sec) of 2.2 lb [1 kg] solute in the main channel of a stream having a cross-sectional area of 107 ft^2 [10 m^2], an average flow velocity of 3.2 ft/s [1 m/s], and a dispersion coefficient of 54 ft^2/s [5 m^2/s] was considered (De Smedt et al., 2005; van Genuchten, 2013). No radioactive decay or production was assumed to exist. The leachate exiting the RAP material was assumed to pass through the natural formation before reaching surface waters.

The selection of analyzed metals was based on the effluent concentrations from CLTs. RAP1 and RAP4 leached Zn and Cu, respectively, in the amounts that exceeded the EPA WQL. Al and Ni were also chosen because the EPA has regulations on them for protection of aquatic life and human health in fresh water. For reference purposes, the same elements were considered for control materials (GAB, Stone No. 57, Topsoil 1, and Topsoil 2). Inorganic component concentrations that were below the minimum detection limits were not analyzed here.

Figures 3.13 through 3.19 illustrate the forecasted concentrations of Al, Cu, Ni, and Zn at different horizontal distances in surface waters from the point of contact for RAP and control material leachates passing through the natural formation composed of CL or CL-ML. In surface waters, concentrations of all metals leached from RAP are significantly lower than the WQLs. Even though the initial concentrations of Zn for RAP1 and Cu for RAP4 are above the WQLs (213 μg/L versus 120 μg/L and 16.1 μg/L versus 13 μg/L, respectively), they drop to the levels below the WQLs after travelling through the natural formation. The decrease in the concentrations immediately at the entrance of leachates into the surface waters is

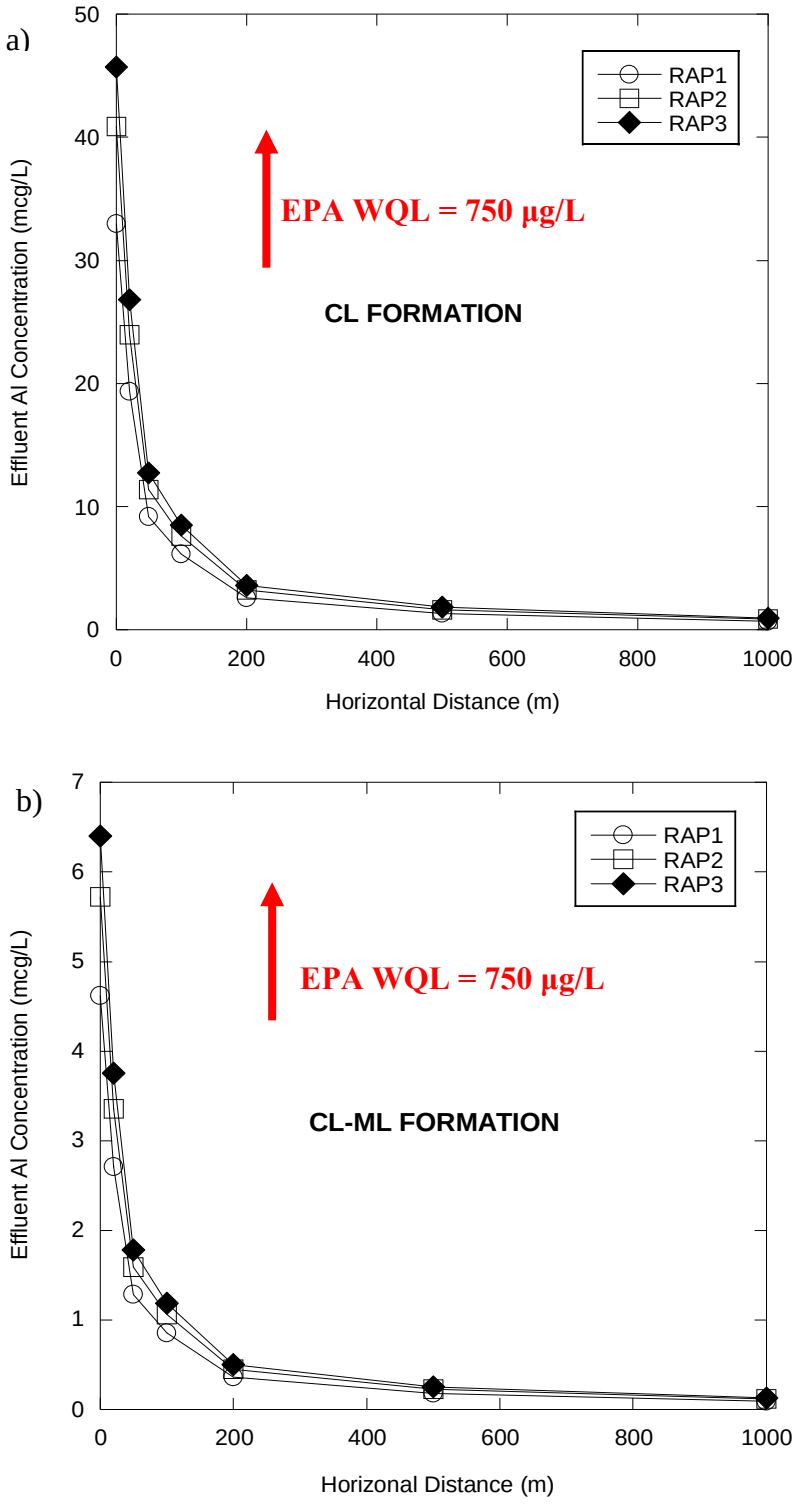

Figure 3.13. Surface water concentrations of Al for RAP with increasing horizontal distance when a) RF = 7 and b) RF = 50.

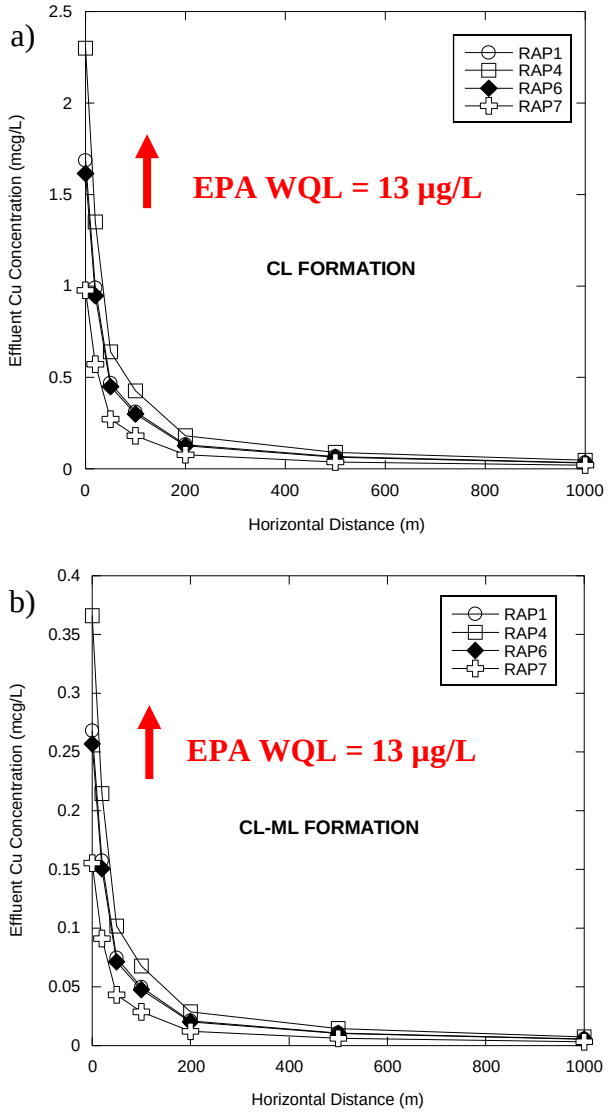

Figure 3.14. Surface water concentrations of Cu for RAP with increasing horizontal distance when a) RF = 7 and b) RF = 44.

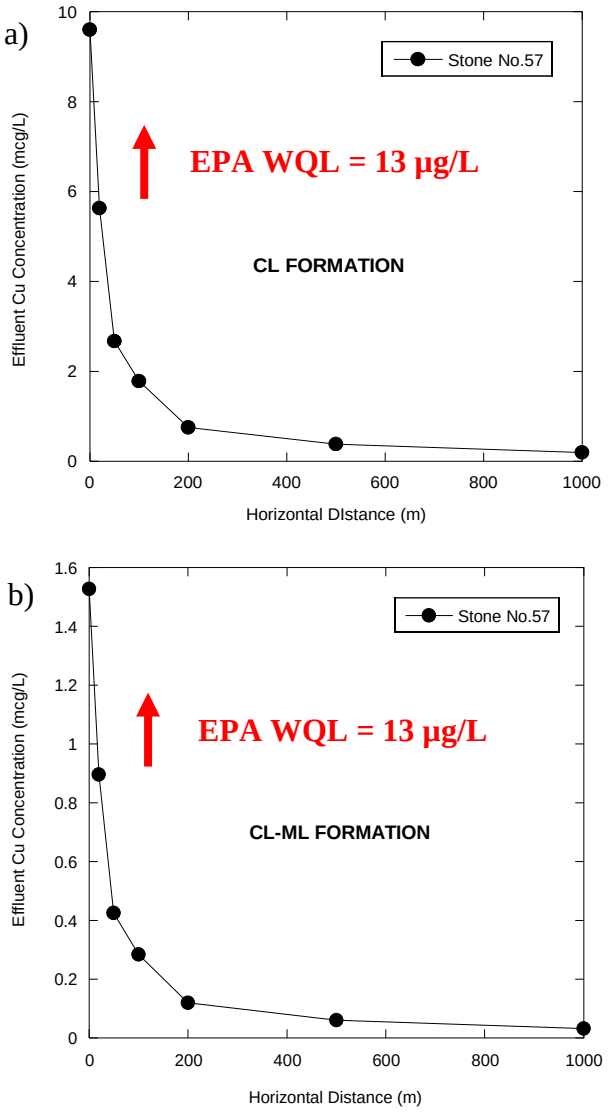

Figure 3.15. Surface water concentrations of Cu for control materials with increasing horizontal distance when a) RF = 7 and b) RF = 44.

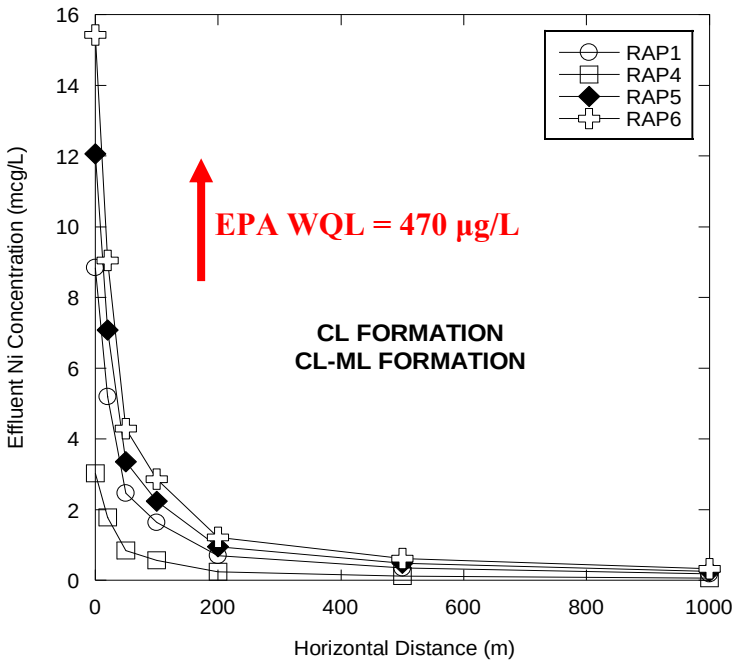

Figure 3.16. Surface water concentrations of Ni for RAP with increasing horizontal distance when RF = 7.

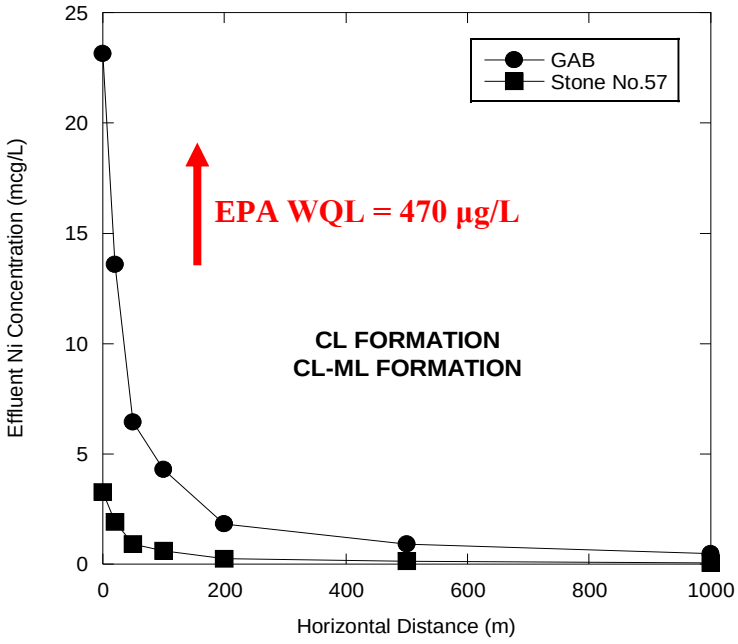

Figure 3.17. Surface water concentrations of Ni for control materials with increasing horizontal distance when RF = 7.

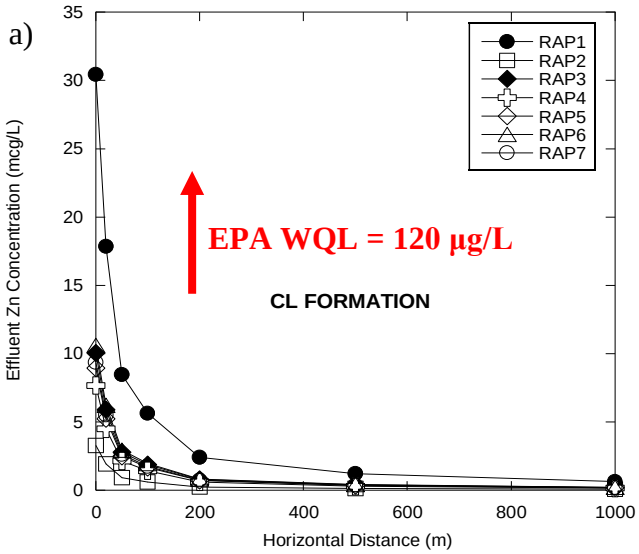

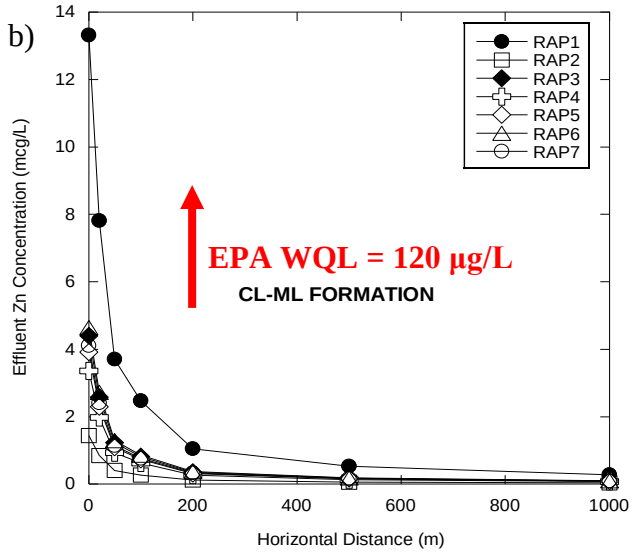

Figure 3.18. Surface water concentrations of Zn for RAP with increasing horizontal distance when a) RF = 7 and b) RF = 16.

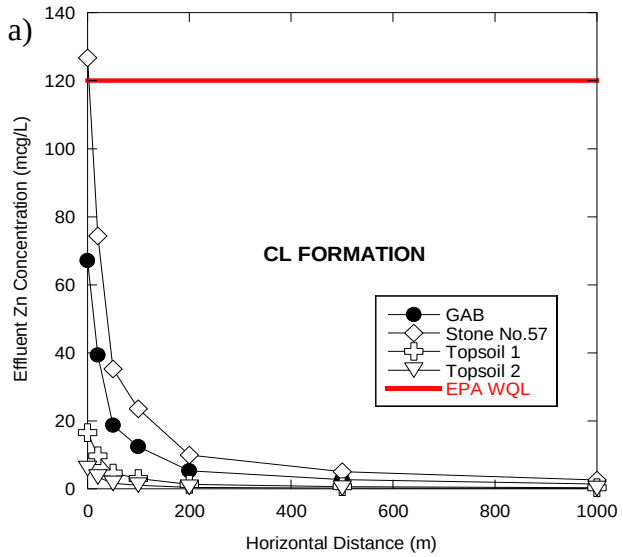

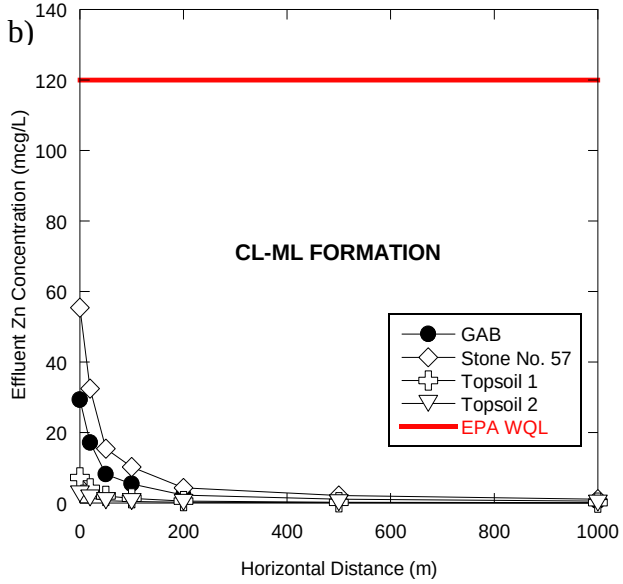

Figure 3.19. Surface water concentrations of Zn for control materials with increasing horizontal distance when a) RF = 7 and b) RF = 16.

more dramatic for the CL-ML formation than for the CL formation due to the higher pH approaching neutral levels (6.3 versus 5.9). The initial concentration of Zn leached from RAP1 drops to 30.4 μg/L and 2.3 μg/L upon exiting the CL and CL-ML formations, respectively. The CL and CL-ML soils reduce the initial Cu concentration for RAP4 leachate to 2.3 μg/L and 0.366 μg/L, respectively.

As the reference, the concentrations of all metals in the surface waters leached from the control materials are lower than the regulatory limits. The exception to this trend is Zn leached from Stone No. 57 and passed through the CL soil. Its concentration remains slightly above the WQL upon reaching the surface waters (127 μg/L versus 120 μg/L), but conforms to the regulatory limit after 3.5 m.

In all cases, the metal concentrations from RAP and control material leachates decrease even further in the surface waters with the increasing horizontal distance. Once the leachates enter the surface waters, the metal concentrations decrease by 50% at a horizontal distance of 26 m and are below the EPA WQLs. For instance, the aqueous Zn concentrations for RAP1 at the point of contact between the surface water and the natural formation composed of CL soil or CL-ML soil are 30.4 or 13.3 μg/L, respectively, and they experience a twofold decrease 26 m away from the point of contact. At a horizontal distance of 1,000 m, the concentrations of Zn are further reduced to 0.630 μg/L and 0.276 μg/L for the CL formation and the CL-ML formation, respectively.

Moreover, the rate of decrease in the metal concentration increases if the initial concentration is higher. For example, Figure 3.13 shows that the initial concentration of Al is higher for RAP3 than for RAP1 and RAP2 and, therefore,

decreases at a greater rate, as indicated by a steeper slope. It should also be remarked that the percolation of the leachate from the highway shoulder backup and the absorption of metals by the natural soil deposit is a reasonable assumption because there is no intent of constructing a highway shoulder backup in Maryland from RAP that would be in a direct contact with a surface water body.

3.5 CONCLUSIONS

A laboratory study consisting of water leach tests (WLTs) and column leach tests (CLTs) was conducted to investigate the leaching characteristics of recycled asphalt pavement (RAP) used as a highway shoulder backup material. Metal concentrations for RAP leachates obtained by CLTs were utilized in a numerical model, named UMDSurf, to simulate the effect of natural formation and distance on surface water contamination. The same testing program was performed on the control soils, i.e., graded aggregate base, Stone No. 57, and two topsoils. The following observations were made:

1) Water leach tests carried out on RAP yielded effluent pH in the range of 8.30-9.34. Metal concentrations in the RAP leachates were either below the minimum detection limits or below the EPA water quality limits (WQLs) for protection of aquatic life and human health in fresh water, with an exception of the effluent Cu concentrations for RAP1 and RAP2 that slightly exceeded the regulatory limit of 13 μg/L. In comparison, effluent pH for the control materials varied between 6.21 and 9.47, and all of effluent metal concentrations from the control materials were below the EPA WQLs.

2) Column leach tests conducted on RAP produced leachates with a pH range of 6.69-8.50. Peak effluent concentrations of As, Cd, Cr, Pb, and Zn were below the minimum detection limits for all RAP materials. Only Cu concentrations in RAP4 leachate and Zn concentrations in RAP1 leachate exceeded the EPA WQLs. However, these concentrations of Zn and Cu decreased to below the standard limits at 2 PVF and 0.5 PVF, respectively. Amphoteric pattern for Zn leached from RAP was generally recognized; as effluent pH approached a range of 9-10, the availability of Zn in the solution was curtailed.
3) Leaching of B, Cu, Mn, Ni, and Zn for all RAP materials exhibited a first-flush pattern followed by stabilized concentrations. Peak concentrations occurred mainly during the first pore volume of flow. Leaching of Mn from four RAP materials (RAP4, RAP5, RAP6, and RAP7) slightly deviated from this norm; the elution curves displayed a delayed response – the concentrations spiked at four pore volumes of flow.
4) CLT effluent pH for the control materials varied between 4.80 and 8.82. Solutions leached from Stone No. 57 and Topsoil 1 had pH below 6.5 thus did not conform to the EPA WQL. Aqueous metal concentrations of Al, Cd, Pb, and V were not detected for any of the reference materials. GAB leached As and Zn in the amounts that exceeded the EPA WQLs (348/340 μg/L versus 470/120 μg/L). Stone No. 57 leachate contained elevated concentrations of Cu and Zn with respect to the regulatory limits (67.2/13 μg/L versus 887/120 μg/L). It is speculated that basic and acidic conditions of GAB and Stone No. 57, respectively, favored the release of these metals.

5) WLT and CLT results could not be compared due to differences in liquid-to-solid ratios (20:1 for WLT versus 0.1:1 for CLT), test durations (18 hours for WLT versus two months for CLT), and test conditions (static for WLT versus dynamic for CLT). Nonetheless, both tests provided an insight into the leaching potential of RAP. RAP did not release excessive amounts of toxic metals in either case.
6) The results of chemical transport model showed that the metal concentrations in surface waters decrease to levels below the EPA WQLs after travelling through the natural formation. The aqueous concentrations of Zn for RAP1 and Cu for RAP4 that were initially above the WQLs conformed to the regulatory limits upon reaching the surface waters. The decrease in the metal concentrations was more striking in the case of the CL formation than the CL-ML formation due to its near neutral pH thus the greater metal retardation capability.
7) The numerical model also showed that the concentrations of metals in surface waters decreased even further as the horizontal distance away from the natural formation increased. At 26 m away from the point of contact between the natural formation and the surface waters, the inorganic component concentrations leached from RAP-based highway shoulder backups decreased by the additional 50% and continued to decrease with the increasing horizontal distance.

4 SUMMARY AND RECOMMENDATIONS

4.1 SUMMARY AND CONCLUSIONS

Although recycled asphalt pavement (RAP) is generally recognized as a construction and debris waste material that does not pose a significant threat to human health and the environment, there was a need to more adequately assess its hydraulic and environmental characteristics for the use in Maryland highway shoulder backups. A battery of laboratory hydraulic conductivity tests were conducted on seven recycled asphalt materials using a bubble-tube constant head permeameter. To address the potential leaching of metals from RAP, a series of batch water leach tests (WLT) and column leach tests (CLT) were performed. The contaminant transport in surface waters like rivers and streams as a function of distance was numerically simulated via UMDSurf.

Graded aggregate base (GAB), Stone No. 57, and two topsoils (Topsoil 1 and Topsoil 2, herein) were selected as control materials due to their common applications in Maryland State highway shoulder practices. Their hydraulic and metal leaching properties were determined in the same manner as for the RAP materials. The overall conclusions are summarized below.

1) The hydraulic conductivity of RAP ranged from 6.89×10^{-3} cm/s to 1.14×10^{-1} cm/s, with an average of 4.08×10^{-2} cm/s, which is significantly higher than the hydraulic conductivity of the topsoils, 7.16×10^{-5} cm/s and 6.23×10^{-4} cm/s, and lower than that of Stone No. 57, 2.4×10^{0} cm/s. Therefore, Maryland RAPs can be classified as free-draining materials since their hydraulic conductivity coefficients were above 10^{-4} cm/s. There

was a general increase in the hydraulic conductivity of RAP with an increase in the fines content and sand-to-gravel ratio and a decrease in the coefficient of uniformity.

2) A higher free lime content (CaO) within RAP yielded a lower dry density and a higher hydraulic conductivity coefficient. There was an indication that more bitumen coating on RAP aggregate caused an overall increase in the hydraulic conductivity, but the bitumen percent range was too narrow to allow for clear conclusions. Varying the percent of bitumen for a single RAP material may provide a better insight into the effect of hydrophobic bitumen on hydraulic conductivity.
3) RAP had a potential to leach Cu and Zn, but the elevated concentrations of these two metals measured in CLTs were temporary and decreased rapidly. Leaching of Zn followed an amphoteric pattern; its availability in the leachates decreased as pH approached a range of 9-10. On the other hand, GAB and Stone No. 57 released greater concentrations of Cu, Zn, and As than RAP. This leaching was likely favored due to more extreme effluent pH conditions. It should be noted, however, that only one type of GAB were utilized in this study and the same leaching potential may not be observed for other GAB materials.
4) In surface waters, the concentrations of metals leached from RAP were below the EPA water quality limits (WQLs) for protection of aquatic life and human health in freshwaters. The transport of metals was significantly retarded by the natural formation located between the RAP-amended

highway shoulder backup and the body of surface water. The metal concentrations were further reduced by ~50% at locations in the surface waters 26-m away from the natural formation. The same trend was observed for the reference materials, except for Zn concentration from Stone No. 57 leachate passed through the CL formation; it reached the satisfactory concentration set by the EPA after 3.5 m in the surface waters.

4.2 RECOMMENDATIONS FOR FUTURE RESEARCH

Field hydraulic conductivity studies on sections of RAP-based highway shoulder backups are suggested. The ability to measure a two-dimensional flow in situ may result in hydraulic conductivity coefficients different than those obtained in the laboratory. Additionally, subjecting RAP to various degrees of compaction in the field may affect interlocking of particles hence hydraulic conductivity of RAP.

Even though Maryland RAPs can be deemed as environmentally sound materials for the construction of highway shoulder backups, the effect of aging on hydraulic and environmental suitability of RAPs was not considered in the current study. Moreover, the influent solution for the column leach tests did not simulate the runoff from highway travel lanes and highway shoulders, but rather precipitates typical for Maryland regions. In order to model the highway runoff as the additional source of pollution, it is recommended that the influent solution in a future study is spiked with different metals.

Due to a low percent of bitumen and a large percent of aggregate contained within RAP, it is believed that the type of stone material plays the major role in the leaching of metals due to different adsorption potentials (Lindgren, 1996).

Accordingly, the parent rock of the RAP material should be identified in a future study.

Despite the small content of asphalt binder within RAP, the potential of RAP to leach polycyclic aromatic hydrocarbons should be considered and compared to the new asphalt samples. Finally, performing field leaching tests using lysimeters are proposed for a future study because characteristics of the environment where leaching takes place affect the rate and extent to which inorganic components are released from RAP.

APPENDICES

APPENDIX A: HYDRAULIC BEHAVIOR OF RECYCLED ASPHALT PAVEMENT

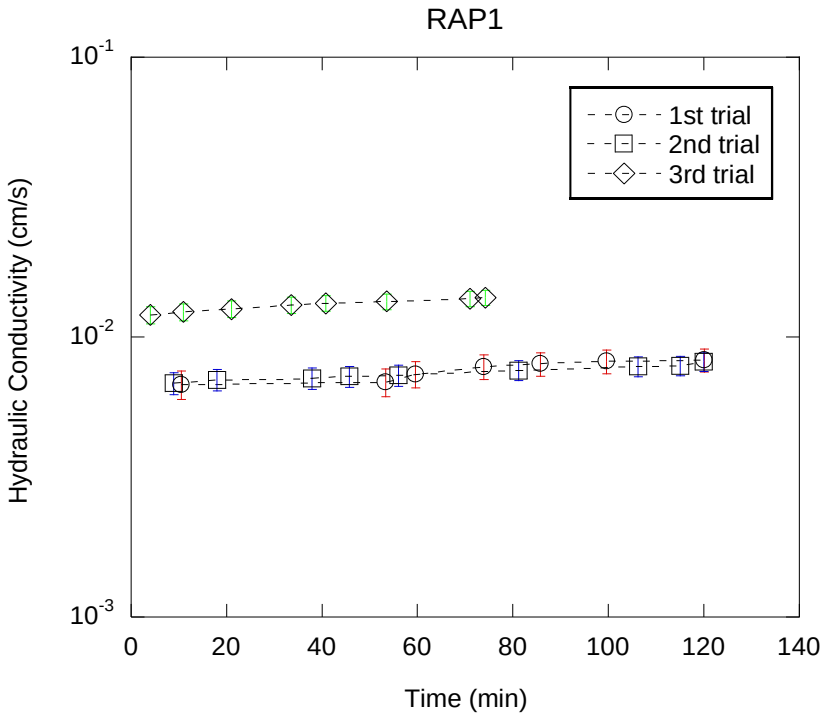

Figure A.1. Hydraulic conductivity as a function of time for RAP1.

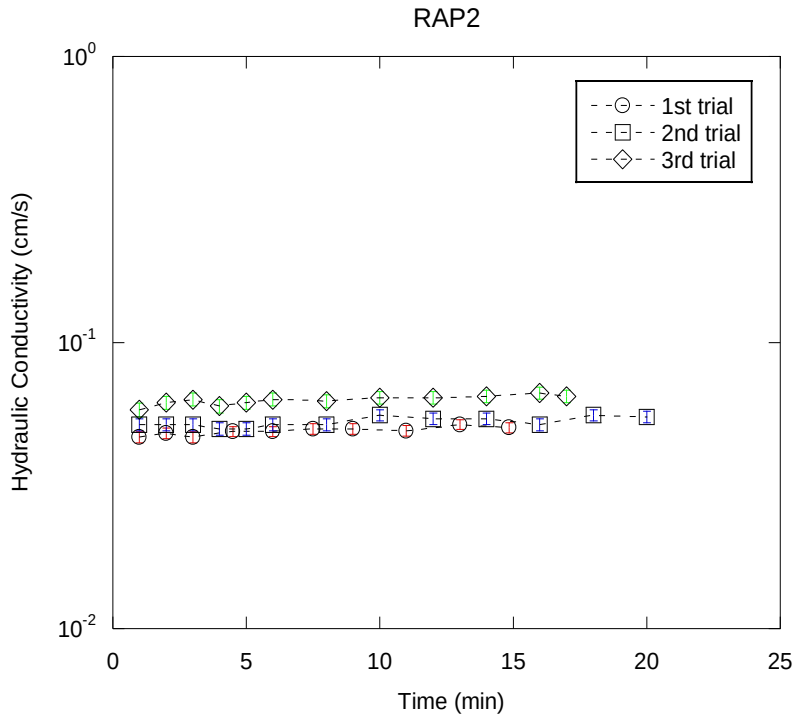

Figure A.2. Hydraulic conductivity as a function of time for RAP2.

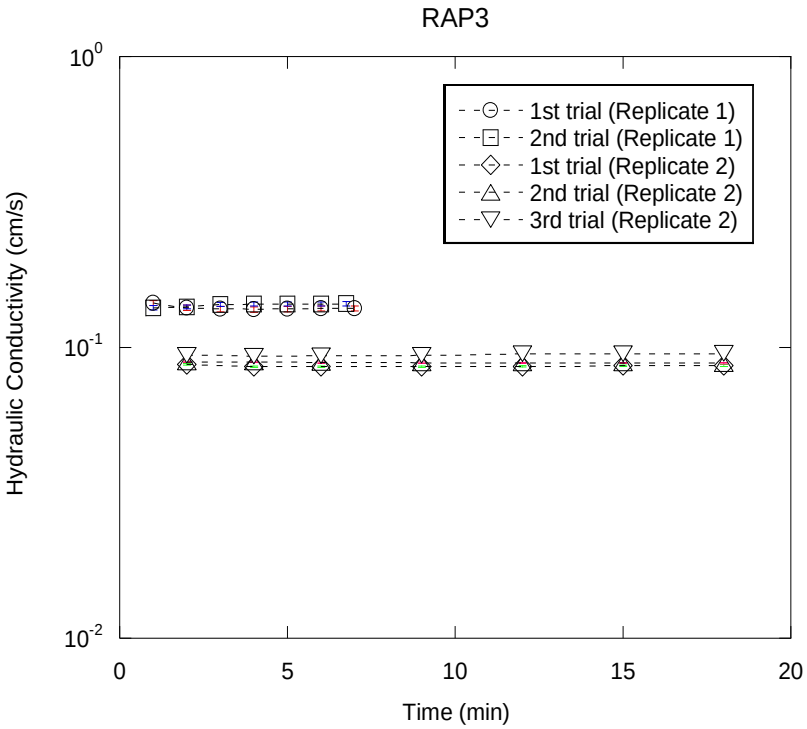

Figure A.3. Hydraulic conductivity as a function of time for RAP3.

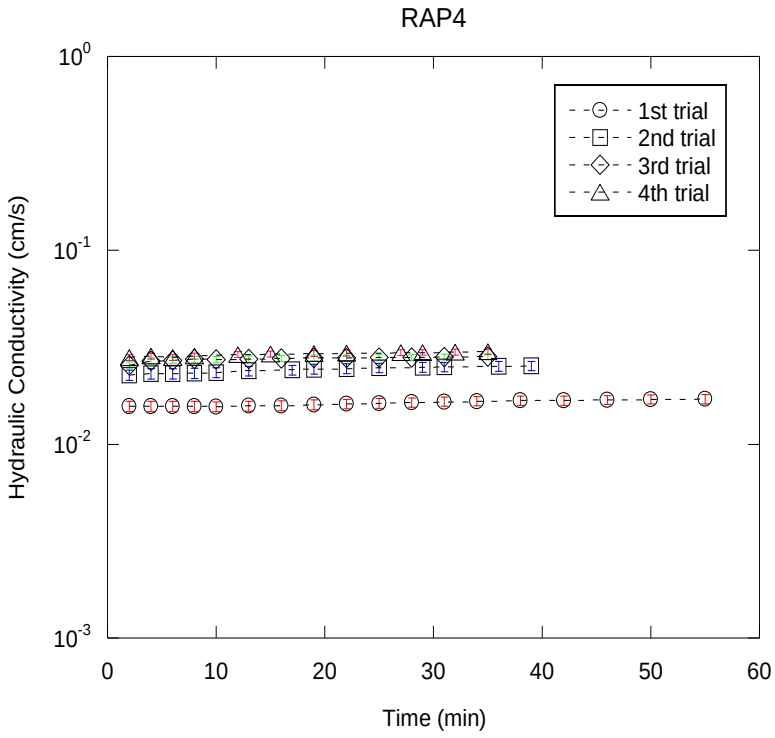

Figure A.4. Hydraulic conductivity as a function of time for RAP4.

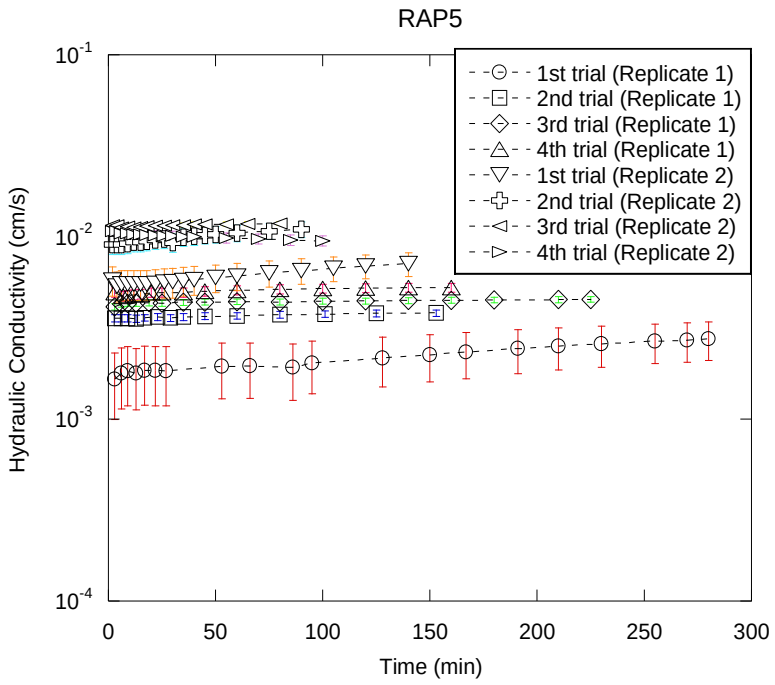

Figure A.5. Hydraulic conductivity as a function of time for RAP5.

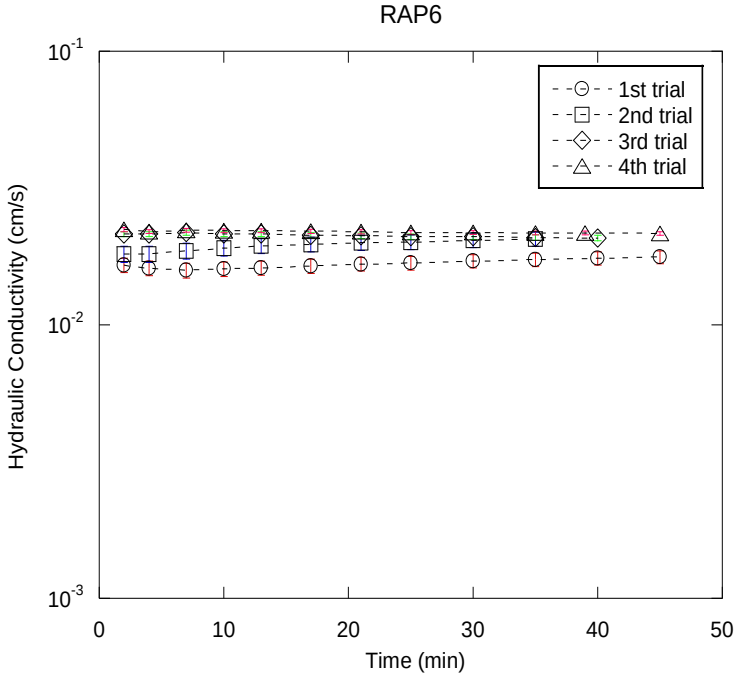

Figure A.6. Hydraulic conductivity as a function of time for RAP6.

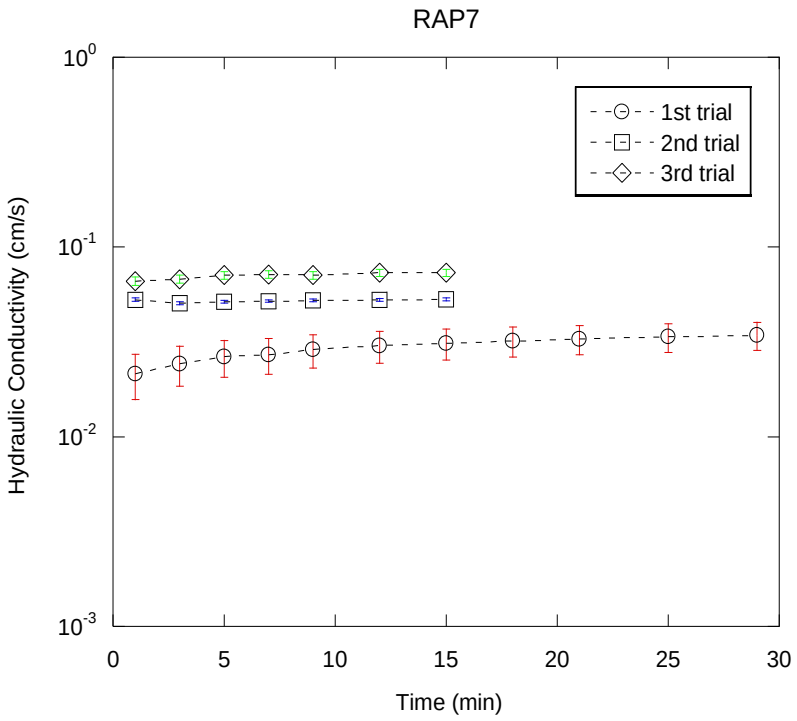

Figure A.7. Hydraulic conductivity as a function of time for RAP7.

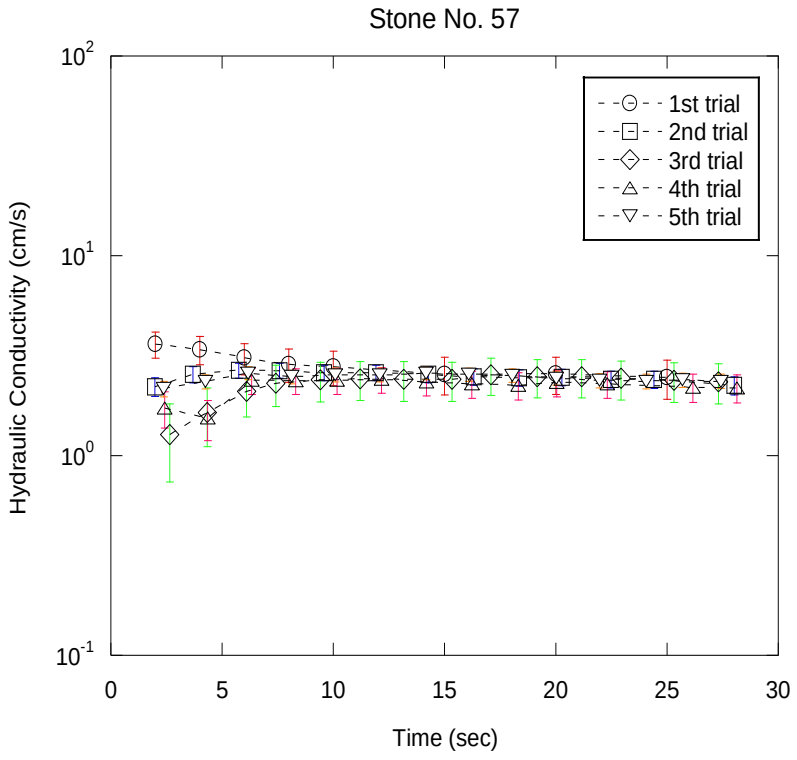

Figure A.8. Hydraulic conductivity as a function of time for Stone No.57.

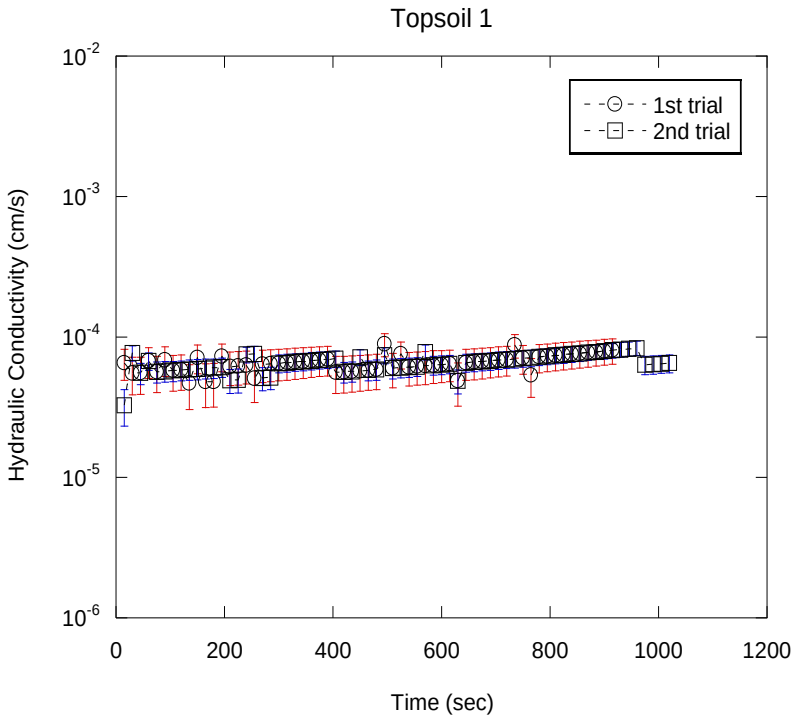

Figure A.9. Hydraulic conductivity as a function of time for Topsoil 1.

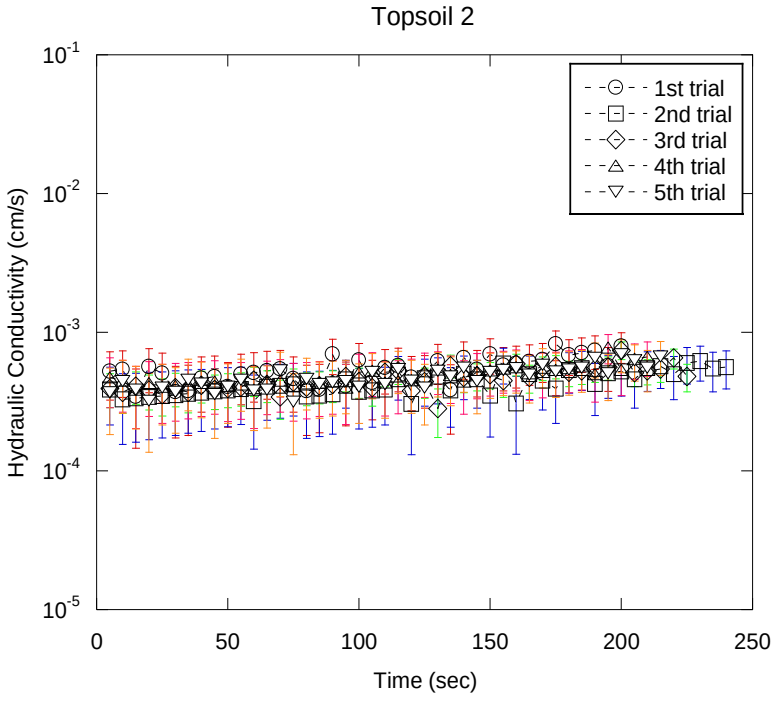

Figure A.10. Hydraulic conductivity as a function of time for Topsoil 2.

References

Aydilek, A. H., Haider, I., Cetin, A., Kaya, Z., & Hatipoglu, M. (2015). Development of Design Guidelines for Proper Selection of Graded Aggregate Base in Maryland State Highways (Report No. MD-15-SP109B4G-1).

American Association of State Highway and Transportation Officials. (2010). "AASHTO T 164: Quantitative Extraction of Asphalt Binder from Hot Mix Asphalt," *Standards Specifications for Transportation Materials and Methods of Sampling and Testing*, 30th ed., AASHTO, Washington, DC.

American Association of State Highway and Transportation Officials. (2010). "AASHTO T 308: Determining the Asphalt Binder Content of Hot Mix Asphalt (HMA) by the Ignition Method," *Standards Specifications for Transportation Materials and Methods of Sampling and Testing*, 30th Ed., AASHTO, Washington, DC.

Alyamani, M. S. and Sen, Z. (1993). Determination of Hydraulic Conductivity from Complete Grain-Size Distribution Curves, *Groundwater*, 31(4), 551-555.

Apul, D. S., Gardner, K. H., Eighmy, T. T., Fällman, A., & Comans, R. N. (2005). Simultaneous Application of Dissolution/Precipitation and Surface Complexation/Surface Precipitation Modeling to Contaminant Leaching. *Environmental Science & Technology*, 39(15), 5736-5741. doi:10.1021/es0486521

Arulrajah, A., Piratheepan, J., Disfani, M. M., & Bo, M. W. (2013). Geotechnical and Geoenvironmental Properties of Recycled Construction and Demolition

Materials in Pavement Subbase Applications. *Journal of Materials in Civil Engineering*, 25(8), 1077-1088. doi:10.1061/(asce)mt.1943-5533.0000652

Asphalt Specific Gravity. (2012). Retrieved from: http://www.pavementinteractive.org/asphalt-specific-gravity/

ASTM D698-12e2 Standard Test Methods for Laboratory Compaction Characteristics of Soil Using Standard Effort (12 400 ft-lbf/ft^3 (600 kN-m/m^3)), ASTM International, West Conshohocken, PA, 2012, https://doi.org/10.1520/D0698-12E02

ASTM C702/C702M-11 Standard Practice for Reducing Samples of Aggregate to Testing Size, ASTM International, West Conshohocken, PA, 2011, https://doi.org/10.1520/C0702_C0702M-11

ASTM D1557-12e1 Standard Test Methods for Laboratory Compaction Characteristics of Soil Using Modified Effort (56,000 ft-lbf/ft^3 (2,700 kN-m/m^3)), ASTM International, West Conshohocken, PA, 2012, https://doi.org/10.1520/D1557-12E01

ASTM D2434-68(2000) Standard Test Method for Permeability of Granular Soils (Constant Head), ASTM International, West Conshohocken, PA, 2000, https://doi.org/10.1520/D2434-68R00

ASTM D3987-12 Standard Practice for Shake Extraction of Solid Waste with Water, ASTM International, West Conshohocken, PA, 2012, https://doi.org/10.1520/D3987-12

ASTM D4318-17 Standard Test Methods for Liquid Limit, Plastic Limit, and Plasticity Index of Soils, ASTM International, West Conshohocken, PA, 2017, https://doi.org/10.1520/D4318-17

ASTM D5856-15 Standard Test Method for Measurement of Hydraulic Conductivity of Porous Material Using a Rigid-Wall, Compaction-Mold Permeameter, ASTM International, West Conshohocken, PA, 2015, https://doi.org/10.1520/D5856-15

Berthelot, C., Podborochynski, D., Marjerison, B., and Gerbrandt, R. (2009). Saskatchewan field case study of triaxial frequency sweep characterization to predict failure of a granular base across increasing fines content and traffic speed applications, *Journal of Transportation Engineering*, ASCE, 135(11), 907-914.

S. Bin, L. Zhibin, C. Yi, and Z. Xiaoping. (2007). Micropore structure of aggregates in stabilized soils. *Journal of Materials in Civil Engineering*, 19, 99-105.

Bin-Shafique, M. S., Benson, C. H., and Edil, T. B. (2002). Leaching of heavy metals from fly ash stabilized soils used in highway pavements. *Geo Engineering Report No. 02-14,* Geo Engineering Program, University of Wisconsin-Madison, Madison, WI.

Bin-Shafique, S, Edil, T B., Benson, C H., and Hwang, K. (2006). Concentrations from Water Leach and Column Leach Tests on Fly Ash Stabilized Soils,*Environmental Engineering Science*. 23 (1). 53-67.

Bouchedid, M.B. and Humphrey, D.N. (2005). Permeability of base material for Maine roads, *Journal of the Transportation Research Board*, 1936, 142-149.

Brady, N. C., and Weil, R. R. (2010). *The Nature and Properties of Soils* (14th ed.). Upper Saddle River, NJ: Pearson/Prentice Hall.

Brandt, H. (1981). Alteration of soil parameters by stabilization with lime, *Proceedings of the 10th International Conference on Soil Mechanics and Foundation Engineering*, Stockholm, 3, pp. 587–594.

Brantley, A.S., and T.G. Townsend. (1999). Leaching of pollutants from reclaimed asphalt pavement. *Environ. Eng. Sci*, 16, 105–116. doi:10.1089/ees.1999.16.105

Broms, B. B., and Boman, P. (1979b). Lime columns - A new foundation method. ASCE, *Journal of the Geotechnical Engineering Division*, 105(4), 539-556.

Cardoso, R., Silva, R. V., De Brito, J., & Dhir, R. (2016). Use of recycled aggregates from construction and demolition waste in geotechnical applications: A literature review. *Waste Management*, 49, 131-145. doi:10.1016/j.wasman.2015.12.021

Cappuyns, V. (2017). Barium (Ba) leaching from soils and certified reference materials, *Applied Geochemistry*, article in press. doi.org/10.1016/j.apgeochem.2017.05.002

Carrier, W. D. (2003). "Goodbye, Hazen; Hello, Kozeny-Carman," *Journal of Geotechnical and Geoenvironmental Engineering*, 129, 1054–1056

Casagrande, A. and Fadum, R. E. (1940), Notes on soil testing for engineering purposes, *Harvard Univ. Grad. School of Engineering Publ*. 268, 74 p.

Cetin, B., Aydilek, A. H., and Li, L. (2012). Experimental and numerical analysis of metal leaching from fly ash-amended highway bases. *Waste Management*, 32(5), 965-978. doi:10.1016/j.wasman.2011.12.012

Copeland, A. (2011). "Reclaimed asphalt pavement in asphalt mixtures: State of the practice", *Report No. FHWA-HRT-11-021*, Federal Highway Administration, Washington, DC.

Côté, J., and Konrad, J. M. (2003). Assessment of the hydraulic characteristics of unsaturated base-course materials: a practical method for pavement engineers. *Canadian Geotechnical Journal*, 40(1), 121-136.

Cuisinier, O., Auriol, J., Le Borgne, T., and Deneele, D. (2011). Microstructure and hydraulic conductivity of a compacted lime-treated soil. *Engineering Geology*, 123(3), 187-193. doi:10.1016/j.enggeo.2011.07.010

Dayioglu, A. Y. (2016). *Geotechnical and Environmental Impacts of Steel Slag in Highway Embankments* (Unpublished doctoral dissertation). University of Maryland, College Park.

De Smedt, F., Brevis, W., and Debels, P. (2005). Analytical solution for solute transport resulting from instantaneous injection in streams with transient storage. *Journal of Hydrology*, 315(1-4), 25-39. doi:10.1016/j.jhydrol.2005.04.002

Dijkstra, J. J., Van der Sloot, H. A., and Comans, R. N. J. (2002). Process identification and model development of contaminant transport in MSWI bottom ash. *Waste Management*, 22(5), 531.

Dijkstra, J. J., Meeussen, J. C., and Comans, R. N. (2004). Leaching of Heavy Metals from Contaminated Soils: An Experimental and Modeling Study. *Environmental Science & Technology*, 38(16), 4390-4395. doi:10.1021/es049885v

Disfani, M. M., Arulrajah, A., Bo, M. W., and Hankour, R. (2011). Recycled crushed glass in road work applications. *Waste Management*, 31(11), 2341–2351.

Edil, T. B., Sandstorm, L. K. and Berthouex, P. M., (1992). Interaction of Inorganic Leachate with Compacted Pozzolanic Fly Ash, *Journal of Geotechnical Engineering, ASCE, New York*, 118 (9), 1410-1430.

Edil, T. B., Benson, C. H., O'Donnell, J. B., and Komonweeraket, K. (2010). *Evaluation of the environmental performance of CCPS in roadway applications* (Publication No. 52). 2010, WI: Recycled Materials Resource Center.

Federal Highway Administration, (2012). "User guidelines for byproducts and secondary use materials in pavement construction," *FHWA Report FHWA-RD-97-148*, McLean, Virginia.

Fleming, L. N., Abinteh, H. N., and Inyang, H. I. (1996). Leachant pH effects on the leachability of metals from fly ash, *Journal of Soil Contamination*, 5(1), 53-59.

Gambrell, R. P., Wiesepape, J. B., Patrick, W. H., and Duff, M. C. (1991). The effects of pH, redox, and salinity on metal release from a contaminated sediment. Water, Air, & Soil Pollution, 57(1), 359-367.Gelhar, L. W., Welty, C., and

Rehfeldt, K. R. (1992). A Critical Review of Data on Field-Scale Dispersion in Aquifers, *Water Resources Research*, Vol. 28, pp. 1955-1974.

Gitari, W. M., Fatoba, O. O., Petrik, L. F., & Vadapalli, V. R. (2009). Leaching characteristics of selected South African fly ashes: Effect of pH on the release of major and trace species. *Journal of Environmental Science and Health, Part A*, 44(2), 206-220. doi:10.1080/10934520802539897

Goswami, R. K., and Mahanta, C. (2007). Leaching characteristics of residual lateritic soils stabilized with fly ash and lime for geotechnical applications. *Waste Management*, 27(4), 466-481. doi:10.1016/j.wasman.2006.07.006

Gupta, S.C., D.H. Kang, and A.Z. Ranaivoson. (2009). Hydraulic and mechanical properties of recycled materials, *Local Road Research Board*, MnDOT 2009(32), Minnesota Dep. of Transportation, St. Paul.

Haider, I. (2013). *Geomechanical and hydraulic behavior of Maryland Graded Aggregate Base Materials* (Master's thesis, University of Maryland, College Park). University of Maryland, College Park.

Hewitt, C.N. and Rashed, M.B. (1990). An integrated budget for selected pollutants for a major rural highway, *Sci. Total. Environ.*, 93, 375–384.

Holtz, R. D., and Kovacs, W. D. (1981). *An introduction to geotechnical engineering.* Englewood Cliffs, NJ: Prentice-Hall.

Holtz, R. D., Kovacs, W. D., and Sheahan, T. C. (2011). *An introduction to geotechnical engineering* (2nd ed.). Upper Saddle River, NJ: Pearson.

Kang, D., Gupta, S. C., Ranaivoson, A. Z., Siekmeier, J., & Roberson, R. (2011). Recycled Materials as Substitutes for Virgin Aggregates in Road

Construction: I. Hydraulic and Mechanical Characteristics. *Soil Science Society of America Journal*, 75(4), 1265-1275. doi:10.2136/sssaj2010.0295

Kang, D., Gupta, S. C., Bloom, P. R., Ranaivoson, A. Z., Roberson, R., & Siekmeier, J. (2011). Recycled Materials as Substitutes for Virgin Aggregates in Road Construction: II. Inorganic Contaminant Leaching. *Soil Science Society of America Journal*, 75(4), 1276-1284. doi:10.2136/sssaj2010.0296

Kenkel, J. (2003). *Analytical chemistry for technicians* (3rd ed.). Boca Raton, FL: Lewis.

Keller, G. (2013). "Information summary asphalt grindings / RAP (recycled asphalt pavement)" United States Department of Agriculture, Forest Service, Workshop at the Tahoe Regional Planning Agency office, Stateline, NV, June 13-14, 2013.

Kirby, C. S. and Rimstidt, J. D. (1994). Interaction of Municipal Solid Waste Ash with Water. *Environmental Science and Technology*, 28, 443-451.

Koch, S., Huntington, G., and K. Ksaibati. (2011). Performance of reclaimed asphalt pavement on unpaved roads, *FHWA report number FHWA-WY-11/03F*, Dept. of Civil Engineering, University of Wyoming. Laramie, Wyoming.

Kosson, D. S., Van Der Sloot, H. A., Sanchez, F., and Garrabrants, A. C. (2002). An integrated framework for evaluating leaching in waste management and utilization of secondary materials. *Environmental Engineering Science*, 19(3), 159-204.

Langmuir, D. (1997). *Aqueous Environmental Geochemistry*, Prentice-Hall, Inc., New Jersey.

Lee, J., Edil, T., Tinjum, J., & Benson, C. (2010). Quantitative Assessment of Environmental and Economic Benefits of Recycled Materials in Highway Construction. *Transportation Research Record: Journal of the Transportation Research Board*, 2158, 138-142. doi:10.3141/2158-17

Legret, M. and Pagotto, C. (2003). A preliminary assessment of the distribution of trace elements emitted by road traffic, *First International Symposium on Environment and Transport*, Avignon, France, Proceedings no 93, Inrets ed., Arcueil, France, pp.67–74.

Legret, M., Odie, L., Demare, D., & Jullien, A. (2005). Leaching of heavy metals and polycyclic aromatic hydrocarbons from reclaimed asphalt pavement. *Water Research*, 39(15), 3675-3685. doi:10.1016/j.watres.2005.06.017

Lim, T. T., Tay, J. H., Tan, L. C., Choa, V., and Teh, C. I. (2004). Changes in mobility and speciation of heavy metals in clay-amended incinerator fly ash. *Environmental Geology*, 47(1), 1-10.

Lindgren, A. (1996). Asphalt wear and pollution transport. *Science of The Total Environment*, 189-190, 281-286. doi:10.1016/0048-9697(96)05220-5

Little, D. N. (1999). Evaluation of Structural Properties of Lime Stabilized Soils and Aggregates. Retrieved from http://www.lime.org/documents/publications/free_downloads/soils-aggregates-vol1.pdf

Liu, Y., Li, Y., Li, X., and Jiang, Y. (2008). Leaching behavior of heavy metals and PAHs from MSWI bottom ash in a long-term static immersing experiment. *Waste Management*, 28(7), 1126-1136. doi:10.1016/j.wasman.2007.05.014

Liu, Y. Y., Zhao, Y. S., Dong, J., Liu, P., Zhu, Z. G., and Sun, Y. (2008). pH buffering capacity of geological media on landfill leachate. *Huan jing ke xue= Huanjing kexue*, *29*(7), 1948-1954.

Locander, R. (2009). *Analysis of using reclaimed asphalt pavement (rap) as a base course material* (Rep. No. CDOT-2009-5). Denver, CO: Colorado Department of Transportation.

Mallela, J., Quintus, H. V., and Smith, K. (2004). *Consideration of lime-stabilized layers in mechanistic-empirical pavement design.* The National Lime Association.

McCallister, L.D. (1990). *The effects of leaching on lime-stabilized expansive clays*. Doctoral thesis, The University of Texas at Arlington, TX.

McDaniel, R., Kowalski, K. and Shah, A., (2012). "Evaluation of reclaimed asphalt pavement for surface mixtures," *Publication FHWA/IN/JTRP-2012/03*, Joint Transportation Research Program, Indiana Department of Transportation and Purdue University, West Lafayette, Indiana, 2012.

McLaughlin, M., Andrew, S., Smart, M., and Smolders, E. (1998). Effects of sulfate on cadmium uptake by Swiss chard: I. Effects of complexation and calcium competition in nutrient solutions. Plant and Soil, 202(2), 211-216.

Mokwa, R. L., and Peebles, C. S. (2005). *Evaluation of the Engineering Characteristics of Rap/Aggregate Blends.* (Rep. No. FHWA/MT-05-008/8117-24). FHWA.

Morar, D.L. (2008). *Leaching of metals from fly ash-amended permeable reactive barriers.* Master's Thesis, University of Maryland, College Park.

Morar, D., Aydilek, A.H., Seagren, E.A., and Demirkan, M.M. (2012). Metal Leaching from Fly Ash- Sand Reactive Barriers, *Journal of Environmental Engineering*, doi:10.1061/(ASCE)E.E. 1943-7870.0000531.

Morse, A., A.M. Jackson, and R. Davio. (2001). Environmental characterization of traditional construction and maintenance materials, *Proc. of an Int. Conf. on Beneficial Use of Recycled Materials in Transportation Applications*, pp. 311-321, Arlington, VA.

MSMT 321 Moisture-Density Relations of Plain and Stabilized Dense Graded Aggregate, Office of Materials Technology, State Highway Administration, Maryland Department of Transportation, 2011.

Muschack, W. (1990). Pollution of street runoff by traffic and local conditions, *Sci. Total Environ.*, 93, 419–431.

National Asphalt Pavement Association. (2017). *Recycling*, NAPA, Lanham, MD.

New York Department of Transportation, (2002), "Item 203.24000015 – shoulder backup material," EI 02-027, State of New York, retrieved from https://www.dot.ny.gov/spec-repository-us/203.24000015.pdf

Nokkaew, K., Tinjum, J. M., and Benson, C. H. (2012). Hydraulic Properties of Recycled Asphalt Pavement and Recycled Concrete Aggregate. *GeoCongress 2012*. doi:10.1061/9780784412121.152

Nokkaew, K. (2014). *Hydraulic properties of recycled asphalt pavement aggregates and effect of soil suction on resilient modulus for pavement design*. Doctoral Dissertation, Dept. of Civil Engineering, University of Wisconsin-Madison, WI.

Ogata, A. and Banks, R. B. (1961). A Solution of the Differential Equation of Longitudinal Dispersion in Porous Media. *US Geological Survey Profl. Paper 411-A*, US Geological Survey, Washington D. C.

Ogunro, V.O. and Inyang, H.I. (2003). Relating batch and column diffusion coefficients for leachable contaminants in particulate waste materials. *Journal of Environmental Engineering*, ASCE, 129(10), 930-942.

Okafor, F. O. (2010). Performance of Recycled Asphalt Pavement as Coarse Aggregate in Concrete. *Leonardo Electronic Journal of Practices and Technologies*, (17), 47-58.

Onur, E. M. (2014). *Predicting the hydraulic conductivity of sandy soils from grain size distributions* (Master's thesis, Kent State University, 2014). Kent State University.

Periodic table. (2017). Retrieved from LennTech: http://www.lenntech.com/periodic/periodic-chart.htm

Public Health Statement. (2017, March 23). Retrieved from Agency for Toxic Substances and Disease Registry: https://www.atsdr.cdc.gov/substances/index.asp

Rahman, M. A., Imteaz, M. A., Arulrajah, A., Piratheepan, J., and Disfani, M. M. (2015). Recycled construction and demolition materials in permeable pavement systems: geotechnical and hydraulic characteristics. *Journal of Cleaner Production*, 90, 183-194. doi:10.1016/j.jclepro.2014.11.042

Rathje, E. M., Rauch, A. F., Trejo, D., Folliard, K. J., Viyanant, C., Esfellar, M., Jain, A., and Ogalla, M. (2006). *Evaluation of Crushed Concrete and Recycled Asphalt Pavement as Backfill for Mechanically Stabilized Earth Walls.* (Rep. No. FHWA/TX-06/0-4177-3).

Ricou, P., Lecuyer, I., and Cloirec, P. L. (1999). Removal of Cu^{+2}, Zn^{+2}, and Pb^{+2} by adsorption onto fly ash and fly ash/lime mixing. *Wat. Sci. Tech.*, 39 (10-11), 239-247.

Sauer, J. J., Benson, C. H., and Edil, T. B. (2005). "Leaching of heavy metals from organic soils stabilized with high carbon fly ash." Geo Engineering Report No. 05- 01, Geo Engineering Program, University of Wisconsin-Madison, Madison, WI.

Sauer, J. J., Benson, C. H., Aydilek, A. H., and Edil, T. B. (2012). Trace Elements Leaching from Organic Soils Stabilized with High Carbon Fly Ash. *Journal of Geotechnical and Geoenvironmental Engineering*, 138(8), 968-980. doi:10.1061/(asce)gt.1943-5606.0000653

Shedivy, R.F., Meier, A., Edil, T.B., Tinjum, J.M., and Benson, C.H. (2012). *Leaching Characteristics of Recycled Asphalt Pavement Used as Unbound Road Base*. University of Wisconsin-Madison, WI.

Snyder, M. B. and Bruinsma, J. E. (1996). Review of Studies Concerning Effects of Unbound Crushed Concrete Bases on PCC Pavement Drainage, *Transportation Research Record*, No. 1519, pp. 51-58.

Solomon, F. (2009). Impacts of Copper on Aquatic Ecosystems and Human Health. *MINING.com*.

Sparks, D. L. (2003). *Environmental soil chemistry* (2nd ed.). San Diego, CA: Academic Press.

Stumm, W., and Morgan, J. J. (1996). *Aquatic chemistry: chemical equilibria and rates in natural waters* (3rd ed.). New York, NY: Wiley.

Svensson, A. (2014). *Estimation of Hydraulic Conductivity from Grain Size Analyses*, Master's Thesis, Chalmers University of Technology, Goteborg, Sweden.

Theis, T. M. and Wirth, J. L. (1977). Sorptive Behavior of Trace metals on Fly Ash in Aqueous Systems. *Environmental Science and Technology*, 11(12), 1096-1100.

Townsend, D.C. and Kylm, T.W. (1966). Durability of lime-stabilized soils. *Highway Research Board Bulletin*, 139: 25-41.

Trzebiatowski, B. and Benson, C. (2005). Saturated Hydraulic Conductivity of Compacted Recycled Asphalt Pavement. *Geotechnical Testing Journal*, 28(5), 514-519. doi:10.1520/gtj12698

Van Genuchten, M. T. (1981). Analytical Solutions for Chemical Transport with Simultaneous Adsorption, Zero-order Production, and First-order Decay, *Journal of Hydrology*, Vol. 49, pp. 213-233.

Van Genuchten, M. T., Leij, F. J., Skaggs, T. H., Toride, N., Bradford, S. A., and Pontedeiro, E. M. (2013). Exact Analytical Solutions for Contaminant Transport in Rivers. 1. The equilibrium advection dispersion equation, *Journal of Hydrology and Hydromechanics*, 61(2), 146-160. doi:10.2478/johh-2013-0020

Van Genuchten, M. T., Leij, F. J., Skaggs, T. H., Toride, N., Bradford, S. A., and Pontedeiro, E. M. (2013). Exact Analytical Solutions for Contaminant Transport in Rivers. 2. Transient storage and decay chain solutions. *Journal of Hydrology and Hydromechanics*, 61(3), 250-259. doi:10.2478/johh-2013-0032

Viyanant, C. (2006). *Potential use of recycled asphalt pavement and crushed concrete as backfill for mechanically stabilized earth walls* (Doctoral dissertation, University of Texas at Austin, 2006). Austin, TX: University of Texas at Austin.

Wartman, J., Grubb, D. G., and Nasim, A. S. M. (2004). Select engineering characteristics of crushed glass. *J. Mater. Civ. Eng*., 16(6), 526–539.

Whiteoak, D. (1990). *The shell bitumen handbook*. Surrey: Shell bitumen.

Xiao,Y., Tutumluer, E., Qian, Y. (2012). Gradation effects influencing mechanical properties of aggregate base and granular subbase in Minnesota, *Transportation Research Board Meeting*, Washington D.C.

Yan, R., Gauthier, D., and Flamant, G., (2001). Volatility and chemistry of trace elements in a coal combustor, *Fuel* 80, 2217 – 2226.